Fakultät für Medizin

Institut für Neurowissenschaften

The role of Orai2 in calcium homeostasis and regulation of mGluR1-dependent synaptic transmission in cerebellar Purkinje neurons

Arjan Dijke

Vollständiger Abdruck der von der Fakultät für Medizin der Technischen Universität München zur Erlangung des akademischen Grades eines

Doctor of Philosophy (Ph.D.)

genehmigten Dissertation.

Vorsitzender: Prof. Dr. Claus Zimmer

Betreuerin: Priv.-Doz. Dr. Jana Hartmann

Prüfer der Dissertation:

Prof. Dr. Arthur Konnerth

Prof. Dr. Alexander Dietrich

Die Dissertation wurde am 19.09.2018 bei der Fakultät für Medizin der Technischen Universität München eingereicht und durch die Fakultät für Medizin am 26.09.2018 angenommen.

Summary

The metabotropic glutamate receptor type 1 (mGluR1) is highly expressed in Purkinje neurons (PNs) of the mammalian cerebellum, and mGluR1-dependent synaptic signalling is crucial for cerebellar function, e.g. motor learning and motor coordination. At parallel fiber-PN synapses, activation of mGluR1 evokes a complex synaptic response consisting of a slow excitatory postsynaptic potential (sEPSP) involving the *transient receptor potential canonical* (TRPC) channel subunit TRPC3 and inositol trisphosphate receptor- (IP_3R)-dependent calcium release from endoplasmic reticulum (ER) calcium stores. In many non-excitable cell types it has been demonstrated that the depletion of ER calcium stores activates store-operated calcium entry (SOCE) that is based on the interaction between the ER calcium sensor *stromal interaction molecule* 1 (STIM1), the calcium-permeable ion channel Orai1 and (in certain cell types) TRPC channels in the plasma membrane (PM). Less is known about SOCE or other mechanisms of calcium homeostasis in neurons. In addition, the mechanism of TRPC3 activation downstream of mGluR1 is unknown. In cerebellar PNs, it was earlier demonstrated that STIM1 controls both the calcium content of ER calcium stores and the TRPC3-mediated sEPSP. However, both types of mGluR1-dependent responses are transiently rescued in the absence of STIM1 in PN-specific STIM1 knockout ($STIM1^{pko}$) mice by calcium influx through voltage-gated calcium channels (VGCCs). The aim of the work for this thesis was to elucidate how the activation of TRPC3 is regulated by calcium and how it relates to calcium homeostasis in cerebellar PNs.

Using whole-cell patch-clamp recordings in combination with confocal calcium imaging in acute cerebellar slices from $STIM1^{pko}$ mice I first showed that the depolarization-induced effect on TRPC3 activability outlasts the transient increase of the intracellular calcium concentration by minutes, is not sensitive to the antagonist of Sarco/endoplasmic reticulum calcium-ATPase (SERCA) CPA and the “slow” calcium chelator EGTA but was abolished by intracellular perfusion with the “fast” calcium buffer BAPTA. Thus, TRPC3 is not regulated by direct

binding of calcium ions but by PM-delimited nanodomain coupling to a STIM1-controlled calcium conductance such as Orai1. However, in many neuronal cell types in the brain including PNs the homolog of Orai1, Orai2, is more abundant than Orai1. The significance of this specific expression pattern for neuronal function is not known.

Immunostaining confirmed the presence of Orai2 protein in the somatodendritic compartment of PNs. Streptavidin-staining of biocytin-filled PNs in cerebellar slices demonstrate normal morphology of somata, dendrites and spines in mice with a genomic deletion of Orai2 ($Orai2^{-/-}$) mice. However, the importance of Orai2 expression in PNs for cerebellar function is emphasized by a deficit in motor coordination on in mice with an Orai2 deficiency restricted to PNs ($Orai2^{pko}$ mice). In PNs lacking Orai2 calcium release signals in response to local application of the mGluR1-specific agonist dihydroxyphenylglycine (DHPG), repetitive parallel fiber stimulation, IP_3 uncaging, and local application of the ryanodine receptor (RyR) agonist caffeine were largely abolished. Moreover, agonist and synaptic stimulation of mGluR1 revealed that TRPC3 activation is practically eliminated in the absence of Orai2 while the AMPAR-dependent fast synaptic transmission remains unaltered in $Orai2^{-/-}$ mice. Similarly to $STIM1^{pko}$ mice, mGluR1-dependent responses were rescued transiently by VGCC-mediated calcium influx, either evoked by somatic depolarization or climbing fiber activation. Again, this rescue was not sensitive to CPA or EGTA but to BAPTA.

However, stronger depolarization and larger calcium influx was required to restore mGluR1 responsiveness in all tested cells. These data point to a very selective and specific role of Orai2 in PNs and very likely neurons in general. It is the ion channel that is primarily responsible for the refilling of ER calcium stores at resting membrane potential. Furthermore, this thesis demonstrates for the first time a novel role for an Orai protein beyond calcium store replenishment: By enabling the coupling between mGluR1 and TRPC3 it is directly involved in synaptic transmission, neuronal activity and sensorimotor integration in the cerebellum.

List of Abbreviations

4AP	4-Aminopyridine
ACPD	1-Amino-1,3-dicarboxycyclopentane
ACSF	Artificial cerebral spinal fluid
AMPAr	α-amino-3-hydroxy-5-methyl-4-isoxazolepropionic acid receptor
BAPTA	1,2-bis(o-aminophenoxy)ethane-N,N,N′,N′-tetraacetic acid
CaMKII	Calcium/calmodulin-dependent protein kinase II
CF	Climbing fiber
CNQX	Cyanquixaline (6-cyano-7-nitroquinoxaline-2,3-dione)
CPA	Cyclopiazonic acid
DAG	Diacylglycerol
DHPG	(S)-3,5-Dihydroxyphenylglycine
DMSO	Dimethyl sulfoxide
EGTA	Ethylene glycol-bis(β-aminoethyl ether)-N,N,N',N'-tetraacetic acid
EPSC	Excitatory postsynaptic current
EPSP	Excitatory postsynaptic potential
ER	Endoplasmic reticulum
GABA	Gamma-aminobutyric Acid
GPCR	G Protein-coupled receptor
I_{CRAC}	Calcium release-activated calcium current
IP3	Inositol trisphosphate
IP3R	Inositol trisphosphate receptor
IPI	Interpulse interval
mGluR1	Metabotropic glutamate receptor 1
NMDA	N-methyl-d-aspartate
OAG	1-oleoyl-2-acetyl-sn-glycerol
OGB-1	Oregon Bapta Green 1
$Orai1^{PKO}$	Orai1 Purkinje neuron-specific knockout
$Orai2^{PKO}$	Orai2 Purkinje neuron-specific knockout

PBS	Phosphate buffered saline
PFA	Paraformaldehyde
PhoDAG	Photo-activatable diacylglycerol
PIP2	Phosphatidylinositol 4,5-bisphosphate
PKC	Protein kinase C
PLCβ	Phospholipase C beta
PLD	Phospholipase D
PM	Plasma membrane
PN	Purkinje neuron
PPF	Paired-pulse facilitation
qPCR	Quantitative polymerase chain reaction
RyR	Ryanodine receptor
SCA	Spino-cerebellar ataxia
SERCA	Sarco/endoplasmic reticulum calcium-ATPase
SOCE	Store-operated calcium entry
STIM	Stromal interaction molecule
$STIM1^{PKO}$	STIM1 Purkinje neuron-specific knockout
TRP	Transient receptor potential
TRPC	Transient receptor potential canonical
VGCC	Voltage-gated calcium channels
ΔF/F	Delta F over F (relative fluorescence change)

Table of Content

Chapter 1 Introduction

1.1 The Cerebellum

The cerebellum (small brain, Latin) is a brain structure that is present in all vertebrates, albeit in different forms and levels of complexity (Voogd et al. 1998). It lies on the posterior side inside the skull and is mostly covered by the cerebral hemispheres. Recently a number of reports provide experimental proof of non-motor roles of the cerebellum, for example Wagner and colleagues (Wagner et al. 2017) (for an overview of non-motor roles of the cerebellum the reader is directed to a review of Strick (Strick, 2009)). Nonetheless, the bulk of literature touching upon functions of the cerebellum describes motor functions. Among the best described motor processes mediated by the cerebellum are oculomotor coordination (Baier et al. 2009), motor control of speech (Ackermann, 2008) (Riecker et al. 2005), grip force (Fellows et al. 2001), voluntary limb movement (Goodkin et al. 1993) and the timing of motor behavior (Bastian et al. 1996). For an extensive review on the functions of the cerebellum during the behaviors mentioned please consult a consensus review published in Cerebellum in 2015 (Manto et al. 2015). Considering the scope of this work, if suffices to say the cerebellum is heavily involved in the modulation of motor movement.

The cerebellum consists of the cerebellar cortex and the deep cerebellar nuclei in the white matter. The cerebellar cortex is organized in three layers. Starting from the surface of the cerebellum, the first layer is the molecular layer, which contains the dendritic trees of the Purkinje neurons (PNs) which is the major cell type of the cerebellum. In addition to that interneurons such as basket and stellate cells and processes of specialized cerebellar astrocytes, namely the Bergmann glia cells, are located in the molecular layer. The second layer is the PN layer, which is the thinnest layer and consists of the PN somata and the somata of the Bergmann glia cells on top of them. Finally, the innermost layer of the cerebellar cortex consists mainly of granular cells and is therefore called the granular layer.

1.2 Purkinje Neurons

The PN is unique in a number of ways. First of all, it is one of the largest neurons of the brain. Not only is the soma large compared to other neurons, but also the extended dendritic tree and its numerous spines. Second, the dendritic tree is spread out in an almost flat, two-dimensional plane. Lastly, a PN receives numerous inhibitory inputs on their somata and dendritic tree. One input into the cerebellum is transmitted via mossy fibers. Mossy fibers are the axons from a number of sources, notably from inside the cerebellum as feedback signal from the deep cerebellar nuclei. Sources from outside the cerebellum are pontine nuclei relaying input from the cerebral cortex via the pontocerebellar pathway, the vestibular nerve and nuclei, the spinal cord and the reticular formation. The mossy fibers terminate on granular cells, which then project onto the PNs. The second synaptic input coming into the cerebellum is the climbing fiber (CF), which rises from the inferior olive and forms synapses on PNs. Both these cerebellar inputs are excitatory; released glutamate activates PNs, which project to deep cerebellar nuclei that send projections to other parts of the brain.

PNs themselves are Gamma-aminobutyric Acid (GABA)-ergic and are surrounded by a strong inhibitory network formed by interneurons located in the molecular and PN layer. A schematic overview of connectivity within the cerebellum is presented in Figure 1. Both parallel fibers and CF are glutamatergic. *In vivo*, parallel fibers drive spiking activity in PNs by evoking simple spikes. PNs are innervated by hundreds of thousands of parallel fibers, but usually receive input from only one CF. *In vivo* CF discharge at a frequency of 1Hz, which causes semi global depolarization of the dendritic trees of PNs (Ito, 2006).

Signaling downstream of the cerebellum originates almost exclusively from the deep cerebellar nuclei. The largest efferent pathway is the superior cerebellar peduncle, which is formed by a large white matter tract passing through the brain stem. An important motor related fiber tract runs from the cerebellum into the ventrolateral nucleus of the thalamus, which in turn projects to the primary motor cortex of the cerebral cortex. Other major brain areas that are targeted by the cerebellum are for example the hypothalamus, amygdala, hippocampus,

vestibular nuclei. Additionally, a number of nuclei in the pontine reticular formation are connected by efferent fibers from the cerebellum (Zhang et al. 2016).

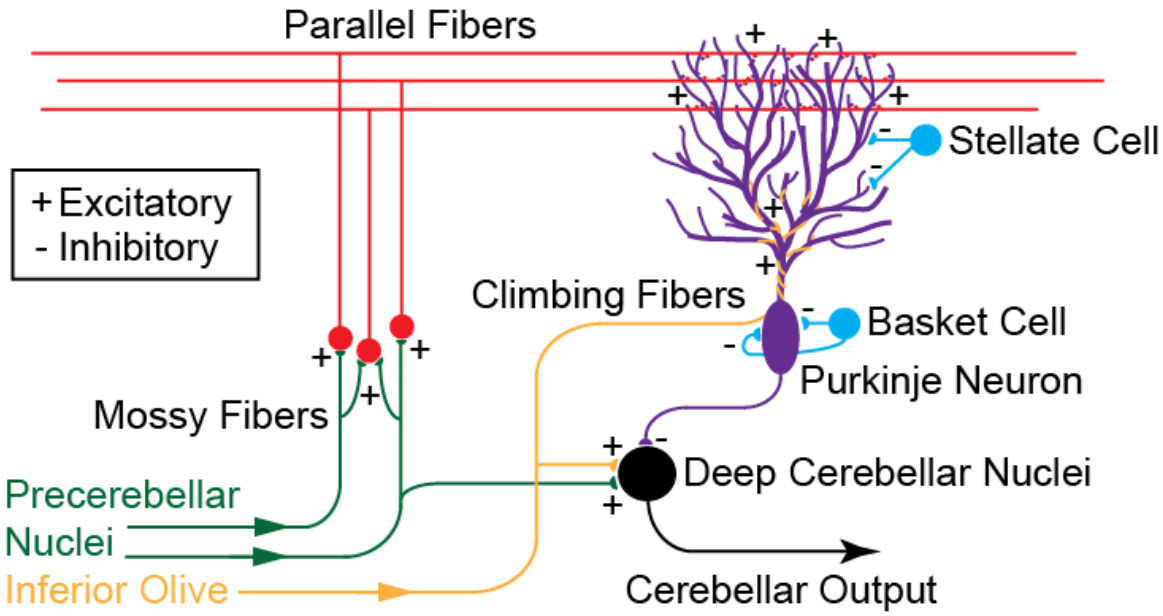

Figure 1 *Schematic representation of cerebellar connectivity*

With the prevalent role the cerebellum takes during motor behavior, cerebellar dysfunction is likely to result in some form of ataxia. Typical symptoms of cerebellar ataxias are dyssynergia, dysmetria, dysdiadochokinesia, and dysarthria (Diener et. al, 1992). By now, numerous types of cerebellar degeneration are known to cause different types of ataxia (Manto et. al, 2009). Typical classification of ataxias can be made based on whether they are episodic or hereditary; one class of hereditary ataxias is formed by a group of diseases that originates in the cerebellum or spinal cord, namely the spino-cerebellar ataxias (SCAs). The known SCAs can genetically be divided in three groups: 1. Expanded CAG (also called polyQ) regions, 2. Repeat expansions in non-protein coding regions and 3. single basepair mutations such as deletion, insertion, missense and duplication. One common feature between all SCAs is the pattern of neurodegeneration in the cerebellum, but also often involving the brainstem (Paulson, 2009). Although it is thought that in the case of polyQ mutations transcription factors are affected,

much is unknown about the molecular causes of SCAs. Recently, three publications linked SCA1, 2 and 3 to a disturbance of metabotropic glutamate receptor 1 (mGluR1) (Konno et al. 2014; Meera et al. 2017; Shuvaev et al. 2017) (references referring to SCA1, 2 and 3, respectively). This protein has a large role in PN functioning, as I will describe in the following section.

1.3 Metabotropic glutamate receptors

Glutamate is the predominant neurotransmitter used by excitatory synapses in the mammalian brain (Hayashi, 1952). For a long time it was thought that glutamate could only exert functions on neurons via ionotropic glutamate receptors such as NMDA (N-methyl-d-aspartate), AMPA (a-amino-3-hydroxy-5-methyl-4-isoazolepropionic acid) and kainate receptors (Hermans et al., 2001). In 1985, however, a study showed that glutamate can stimulate the intracellular production of Inositol trisphosphate (IP_3) (Sladeczek et al., 1985), a finding that was confirmed in the following years. Thus, a distinct class of glutamate receptors, the metabotropic glutamate receptors, was identified. The first cloning of the now termed mGluR was done in 1991 and mGluR1a was described (Masu et al. 1991). Five years later, all now known eight mGluR subtypes were described and classified based on pharmacology and their downstream intracellular pathways (Conn et al., 1997). The mGluR family belongs to the vast group of proteins called G protein-coupled receptors (GPCRs) because the first event after glutamate binding to mGluRs is the activation of a heterotrimeric G protein.

mGluRs are expressed throughout the brain, mGluR1 being the most abundant member of the family in the brain (Lein et al. 2007). Together with mGluR5, mGluR1 forms a subfamily called ‘group I’ metabotropic glutamate receptors. Upon binding of glutamate, these receptors activate phospholipase C (PLC) via a Gq heterotrimeric G protein. The other two subfamilies are formed by class II and class III, which both inhibit adenylyl cyclase, which lowers cyclic AMP. Of all brain regions, the highest expression of mGluR1 is found in the cerebellum, where mGluR1 is perisynaptically located at postsynaptic sites of parallel fibers (Hartmann et al. 2015).

1.4 Function of mGluR1 in the cerebellum

The function of mGluR1 in cerebellar PNs is highly related to the overall function of the cerebellum such as fine tuning of movements and motor learning (Eccles, 1967). Impairment of mGluR1 in patients with Hodgkin's disease leads to paraneoplastic cerebellar ataxia due to the production of autoantibodies against mGluR1 (Sillevis Smitt et al. 2000). Consistent with that a knockout mouse line lacking mGluR1 showed strong signs of ataxia (Aiba, 1994) This phenotype could be rescued with PN-specific expression of mGluR1 on the genetic background of the general mGluR1 knockout (Ichise et al. 2000). This unequivocally proves the importance of mGluR1 in PNs for cerebellar function. In line with this another study showed that adult mice in which mGluR1 is conditionally deleted in PNs only start showing ataxic behavior (Nakao et al. 2007). Additionally, mice lacking mGluR1 show impaired long term depression (LTD). Eyeblink conditioning proved not to be possible in these mice, indicating a role of mGluR1-mediated plasticity during cerebellar motor learning (Aiba, 1994).

1.5 Downstream pathways of mGluR1 in cerebellar PNs

For many years synaptic transmission and postsynaptic signaling in PNs have been studied in acute cerebellar slices. In sagittal slices the dendritic tree of PNs lies in the plane of the slice and parallel fibers run perpendicularly to the plane of the slice. Excitatory postsynaptic potentials (EPSP) resulting from the electrical stimulation of the parallel and CF, respectively, were first identified in 1990 by the mentor of this thesis, Arthur Konnerth (Konnerth et al. 1990). At parallel fiber synapses, AMPA receptors are activated with single shock stimuli (Konnerth et al. 1990; Llano et al. 1991b), The activation of mGluR1, in contrast, requires repetitive stimulation (Batchelor et al. 1993; Batchelor et al. 1994; Batchelor et al. 1997; Takechi et al. 1998) most likely due to the perisynaptic location of mGluR1 (Nusser et al. 1994). Thus, only high levels of glutamate in the synaptic cleft will ensure an effective activation of the receptors. Whole-cell patch-clamp recordings from PNs filled with calcium-sensitive fluorescence dyes in conjunction with confocal fluorescence imaging revealed that activation of mGluR1 in PNs is fol-

lowed by two types of responses: a highly localized dendritic calcium transient that is independent of membrane potential changes (Llano et al. 1991a; Finch et al. 1998; Takechi et al. 1998) (Figure 2) and a slow EPSP (Batchelor et al. 1993; Batchelor et al. 1994; Batchelor et al. 1997) ("Slow" relates to the much faster AMPA receptor-dependent EPSP.)

As mentioned before, the first step in the cascade of events following binding of glutamate to mGluR1 is the activation of a G_q protein. Of all members of the G_q subclass of G proteins, G_{11} and G_q are the major isoforms in the adult brain (Wilkie et al. 1991; Mailleux et al., 1992) and are found at parallel fiber synapses of PNs (Tanaka et al. 2000).Although an *in vitro* assay showed that both G_q protein subtypes ($G\alpha_q$ and $G\alpha_{11}$) couple to mGluR1 with equal effectiveness (Hartmann et al., 2004), $G\alpha_q$ knockout mice failed to show a mGluR1-mediated calcium transient. In mice that lack $G\alpha_{11}$, on the other hand, mGluR1-mediated calcium responses were similar to those recorded in wild type mice. Since the expression of $G\alpha_q$ is about ten times higher than that of $G\alpha_{11}$ (Hartmann et al, 2004) an expression level-dependent effect of $G\alpha_q$ actions is a valid explanation for this major difference. Thus, $G\alpha_q$ contributes mostly to the mGluR1-mediated activation of PLC. The main PLC subtypes in the cerebellum are Phospholipase C beta (PLCβ)1, 3 and 4. Upon knockdown of PLCβ4, CF elimination is strongly impaired, although this phenomenon was mainly seen in the rostral part of the cerebellum. The latter observation can be explained by the regional relative expression of PLCβ4, which is higher expressed in the rostral cerebellum. In other parts of the cerebellum, PLCβ3 is the dominant type (Kano et al. 1998). The PLC cleaves Phosphatidylinositol 4,5-bisphosphate (PIP_2) in the PM and thereby produces DAG and IP_3 that is released into the cytosol. IP3 binds to its own receptor in the membrane of the endoplasmic reticulum (ER) and releases calcium ions from this intracellular calcium store into the cytosol. This gives rise to the mGluR1-dependent dendritic calcium transient.

The most abundant IP_3 receptor in PNs is IP_3R1 (Sharp et al. 1999); IP_3R2 is expressed in lower amounts and IP_3R3 is not present. Interestingly enough, within the native environment of the PN, IP_3Rs sensitivity is low compared to *in*

vitro conditions. Compared to astrocytes, hepatocytes, exocrine cells and vascular endothelium, IP_3Rs in PNs require 10-20 times higher cytosolic IP_3 concentrations to release calcium from the ER. When isolated from PNs, however, the sensitivity of IP_3Rs is similar to that of IP_3Rs from other cell types. This discrepancy can be attributed to a number of proteins that bind to IP_3Rs in PNs and modulate its function (Hartmann et al. 2011). The consequence of these characteristics is that calcium release following IP_3 production is strongly space limited (Hartmann et al., 2011). The ER store itself can be challenged by both IP_3R activation, as well as activation of RyRs, which appear to share a common calcium pool with IP_3 receptors (Khodakhah et al. 1997).

The mGluR1-dependent slow depolarization was observed both following parallel fiber (Batchelor et al. 1993, Batchelor et al. 1997) and CF activation (Dzubay et al., 2002). However, the bulk of literature describing mGluR1-mediated synaptic transmission results from studying parallel fiber synapses. The onset of the slow current starts around 100ms after repetitive parallel fiber stimulation (Bachelor et al. 1997); this delay indicates recruitment of an internal signaling pathway. When measured in the voltage clamp mode the ionic properties of the mGluR1-dependent slow excitatory postsynaptic currents (sEPSCs) are similar to those permeating through the canonical *transient receptor potential* (TRPC) channels. Indeed, it was initially suggested that TRPC1 is the responsible ion channel (Kim et al. 2003). However, later experiments in our own group in TRPC3-deficient knockout mice demonstrated that TRPC3, rather than TRPC1, is underlying the slow depolarization following mGluR1 activation in PNs (Hartmann et al. 2008) (Figure 2).

1.6 The TRPC subfamily of cation channels

Transient receptor potential (trp) channels were first found in 1977 in photoreceptors of a *Drosophila* (Minke et al. 1977) mutant that exhibited a transient receptor potential during continuous illumination. To date 28 *trp* genes grouped into six families are identified. The family with the closest relation to the original TRP channel in *Drosophila* is the TRPC family of “classical” or “canonical” TRP chan-

nels (Moran et al. 2004). All seven members of the TRPC family (TRPC1-7) have six transmembrane domains with a pore forming region between the fifth and sixth domain. TRPC subunits form homo- or heterotetramers with diverse preferences (Clapham et al. 2001).

TRPC3 is the most abundantly expressed TRPC channel in PNs (Hartmann et al, 2008). Mutant mice lacking TRPC3 show impaired motor behavior indicating an important role of TRPC3 for cerebellar function most likely based on its mediation of slow mGluR1-dependent synaptic transmission at parallel fiber synapses (Hartmann et al. 2008) (Fig. 2). Interestingly, in a spontaneous mouse mutant it was found that a point mutation in the *trpc3* gene that results in increased TRPC3 activation following mGluR agonist application is underlying the ataxic phenotype which the mouse line owes its name (moonwalker, *mwk*) (Becker et al. 2009). TRPC3 expression is upregulated during dendritic development (Huang et al. 2007), and the gain of function mwk mutation leads to impaired dendritic outgrowth in PNs (Becker et al. 2009). This indicates that TRPC3 has more functions in PNs in addition to synaptic transmission.

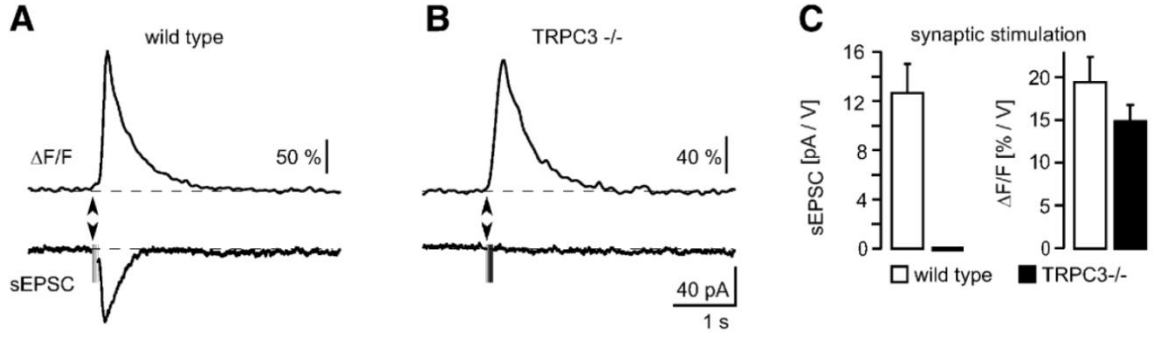

Figure 2 Identification of TRPC3 as the ion channel responsible for the slow depolarization following mGluR1 activation in cerebellar PNs*. Left: in wild type mice, activating mGluR1 in PNs via parallel fiber stimulation activates calcium release from stores (top) and a slow depolarization (bottom). Middle: Although the calcium release signal is preserved (top), the mGluR1-mediated slow current is abolished in TRPC3$^{-/-}$ PNs (bottom). Right: summary of experiments. Adjusted from Hartmann (Hartmann et al. 2008)*

1.7 TRPC3 activation mechanisms

With few exceptions (Stroh et al. 2012) TRPC channels are activated downstream of G_q coupled receptors (Clapham et al. 2001). However, the gating mechanism of TRPC channels is unknown. Findings about the molecules involved downstream of the metabotropic receptors are contradictory and difficult to pinpoint (Hartmann et al. 2015).

The molecular mechanisms underlying TRPC3 activation in PNs are only partially resolved and largely unclear. Reproducibility of findings regarding TRPC activation in their native environment such as the PN is a general problem because most of them result from studies on heterologous expression systems or cultured cell lines.

Of the two G_q proteins found in PNs, $G\alpha_q$ seems to be crucial for TRPC3 activation, while $G\alpha_{11}$ deletion did not influence the success rate of activating TRPC3 (Hartmann et al. 2004). The role of PLCβ for the generation of the slow mGluR1-mediated depolarization was described in the late 90s (Sugiyama et al. 1999) with the use of a transgenic PLCβ4 knockout mouse that lacked the mGluR1-dependent slow EPSPs in the anterior cerebellum where PLCβ4 is the predominant PLC subtype. Others (including our own group) could not confirm this observation using PLC antagonist U73122 (Hirono et al. 1998) (Canepari et al. 2001) (Henning, unpublished). U73122, however, might not be a suitable drug for the use in neurons since it inhibits also certain potassium channels (Klose et al, 2008). A more recent study proposed PLD, rather than PLC, as an activator of TRPC3 (Glitsch, 2010). The same group later also showed that TRPC3 activation is independent of kinase regulation (Nelson et al. 2012). Indirect evidence for a possible involvement of the PLC in TRPC3 activation is the inhibition of TRPC3 by PIP2 depletion in HEK 293 cells (Imai et al. 2012). This experiment shows that depletion of the substrate of PLC renders the protein unable to activate TRPC3.

Besides IP_3, there is a second product of PIP_2 hydrolysis by the PLC, DAG. TRPC3, together with TRPC6 and TRPC7 belongs to the so-called DAG-activated subfamily of TRPCs. The DAG-sensitivity of TRPC3 was first reported in CHO-K1 cells (Hofmann et al., 1999). However, attempts to activate TRPC3 in

PNs in cerebellar slices using the DAG-analog oleyl-acetylglycerol (OAG) and an inhibitor of the DAG-kinase in our own group failed (Henning, Hartmann and Konnerth, unpublished).

1.8 STIM1, calcium homeostasis and TRPC3 activation

The quest for TRPC3 activation mechanisms was given new impulse when it was discovered that in transfected HEK293 cells TRPC3 can be gated by direct molecular interaction with STIM1 (Zeng et al., 2008).

The gene coding for STIM1 was initially identified in a genetic screen for B-lymphocyte activating molecules (Parker et al. 1997). Later STIM1 was found to be involved in a process called capacitive calcium entry, (CCE) or store-operated calcium entry (SOCE). These terms refer to the mechanism of the replenishment of the ER intracellular calcium store that is critical for calcium homeostasis (Putney, 1986). STIM1 and its homolog STIM2 have a single transmembrane domain and reside in the ER membrane, where they function as intraluminal calcium sensors. When the ER calcium store is depleted, calcium ions unbind from the N-terminal EF-hand calcium-binding domain (Roos et al, 2005). STIM1 molecules then form clusters that are translocated to ER-PM junctions where they open Orai channels (Muik et al. 2008). These calcium permeable channels are responsible for the earlier identified calcium release-activated calcium current (I_{CRAC}; (Hoth et al., 1992) that is required for the refilling of ER calcium stores in non-excitable cells. Because of the reported interaction between STIM1 and TRPC channels (Zheng et al., 2011) and because TRPC3 in cerebellar PNs is activated concomitantly with IP_3 receptor-mediated release of calcium ions from the ER STIM1 appeared to be a good candidate for the missing link between Gq activation and opening of TRPC3.

In cerebellar PNs, the function of STIM1 was assessed in two studies. In 2015, our lab published a study that describes the role of STIM1 in PNs at resting membrane potential (Hartmann et al. 2014). The PN-specific deletion of STIM1 in conditional knockout ($STIM1^{pko}$) mice did not affect fast synaptic transmission mediated by AMPA receptors. However, $STIM1^{pko}$ mice showed virtually no

mGluR1-mediated response to synaptic or agonist stimulation. Calcium stores were unresponsive to IP_3 and caffeine, and spontaneous store refilling at resting membrane potential was impaired in $STIM1^{pko}$ mice. The slow mGluR1-mediated current through TRPC3 was absent in $STIM1^{pko}$ mice, too. Motor control in $STIM1^{pko}$ mice was impaired, similarly to TRPC3-deficient knockout mice (Hartmann et al., 2008), but less than in general mGluR1-knockout mice (Aiba et al., 1994). A crucial finding in this study was the observation that depolarization restores responsiveness of dendritic ER calcium stores to IP_3. Apparently, ER Calcium stores are refilled following calcium influx through VGCCs. Surprisingly, immediately after a transient depolarization the activation of TRPC3 was possible in $STIM1^{pko}$ mice (Figure 3). This shows that STIM1 is not directly activating TRPC3 in PNs, but plays an intermediate role that most likely involves calcium.

Later it was shown by others (Ryu et al. 2017) that STIM1 regulates cytosolic calcium clearance in PN somata during action potential firing. In the absence of STIM1 in $STIM1^{pko}$ mice the delay in calcium clearance results in a reduction of neuronal excitability and disruption of cerebellar memory consolidation. However, the experiments in this study were not performed in voltage clamp, allowing the cell to be spontaneously active. Membrane depolarization causes calcium influx over the PM, thereby possibly obscuring any effects that STIM1 can have on calcium homeostasis.

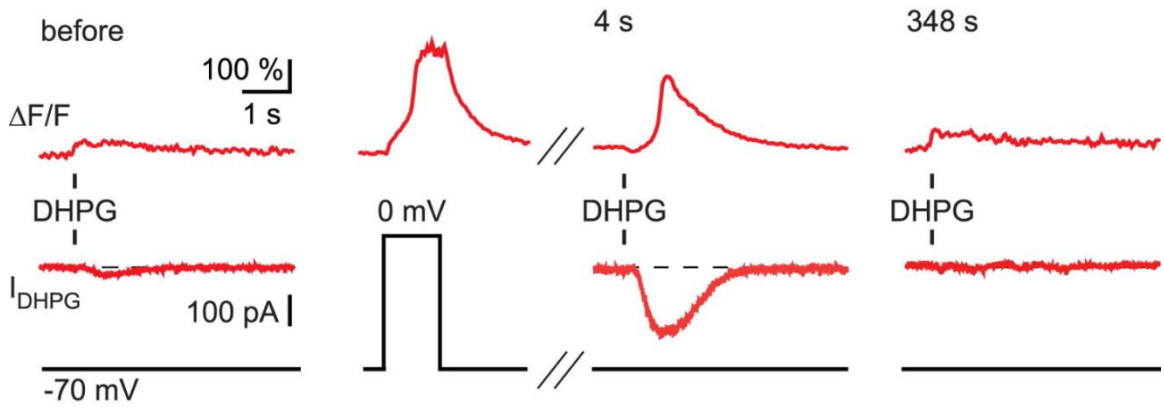

Figure 3 Rescue of the mGluR1-mediated response in STIM1 knock down PNs by transient depolarization. *Left: PNs lack mGluR1 responsiveness. Middle: transient depolarization (bottom trace) evokes a short calcium transient mediated by calcium influx over the PM (top trace). The depolarization restores mGluR1 responsiveness and allows calcium release from stores as well as TRPC3 activation. Right: After almost 6 minutes the respond is back to baseline (adjusted from Hartmann et al. 2014).*

1.9 Orai channels

The finding that TRPC3 in cerebellar PNs is regulated by STIM1-dependent, voltage-independent calcium influx through the PM gave rise to the hypothesis that it is regulated by an Orai channel. Orai proteins were previously found to be the pore forming subunits of I_{CRAC} channels (Feske et al. 2006) (Zhang et al. 2006). There are three Orai subtypes, namely Orai1, 2 and 3, that exhibit a high degree of homology (Hogan et al. 2015). Single Orai subunits contain four transmembrane domains, and both their N- and C-terminals are located on the cytosolic side (Vig et al. 2006).The Orai-STIM interaction and the mechanism of store-refilling is best known for the STIM1-Orai1 complex in non-excitable cells. Upon store depletion, STIM1 and Orai1 redistribute and colocalize at so-called ER-PM junctions. The initial clustering of STIM in so called puncta is independent of Orais (Hogan et al. 2015). Seconds to minutes after store refilling, both STIM and Orai return to their native state.

A previous expression analysis done in our laboratory had revealed that In PNs Orai2 is more abundant than Orai1 and Orai3 (Hartmann et al. 2014). Alt-

hough the homologs of STIM1 and Orai1, STIM2 (Liou et al. 2005; Williams et al. 2001) and Orai2/3 (Feske et al. 2006; Mercer et al. 2006; Vig et al. 2006), respectively, were discovered at the same time, much less is known about their cellular functions. Experiments from our lab indicate a lack of function of STIM2 in PNs (Ryan Alexander, unpublished data). So far, it has been revealed that Orai2 and Orai3 also show SOCC characteristics (DeHaven et al. 2007; Hoth et al. 2013; Mercer et al. 2006).

1.10 STIM, Orais and calcium homeostasis in neurons

The involvement of STIM and Orai in neurons is being investigated for about a decade. Although capacitative calcium entry was already found in neurons (Kraft, 2015), with the identification of STIM and Orai proteins neuronal calcium homeostasis could be studied on a more detailed level. All STIM and Orai variants can be found in the brain (Wissenbach et al. 2007), with STIM1 showing the highest expression in the cerebellum (Klejman et al. 2009; Hartmann et al., 2015; Figure 4). Interestingly, in other brain areas like the hippocampus and the cortex STIM2 is the predominant STIM homolog (Lein et al. 2007). Kleijman et al. demonstrated activation of STIM1 and Orai1 following calcium store depletion in cultured neurons from cortex, hippocampus and PNs from cerebellum. This indicates a similar role for STIMs and Orais in neurons and non-excitable cells. Other studies have found divergent roles for STIM1, it was reported that upon activation of STIM1 by store depletion, L-Type voltage gated calcium channels are inhibited by STIM1 (Park et al. 2010). Thus, STIM1 seems to regulate ER and cytosolic calcium concentrations in more intricate ways as initially thought.

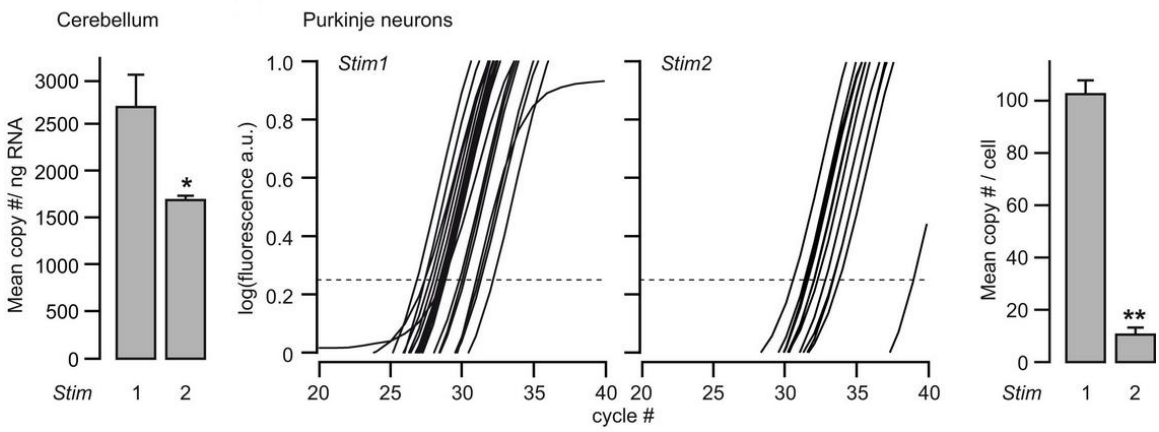

Figure 4 Abundance of STIM1 and STIM2 in cerebellum *Left: Quantification of STIM1 and 2 in whole cerebellum tissue. Middle: fluorescent traces obtained during single (Purkinje) cell quantitative PCR for STIM1 and STIM2. Right: quantification of the single cell qPCR experiment (adjusted from Hartmann et al. 2014).*

Because STIM proteins in non-excitatory cells have been found to interact with Orai channels, it seems likely that functions of STIM1 in neurons also depend on Orai. Evidence of STIM-Orai interactions in neurons have been slowly accumulating during recent years. In Drosophila neurons, STIM and Orai are required for store operated calcium entry (Venkiteswaran et al. 2009). Impairment of store operated calcium entry by reducing STIM or Orai expressing causes flight defects, demonstrating that not only STIM, but also Orai are required in Drosophila neurons. In mammalian neurons, evidence for STIM-Orai-mediated calcium influx was found in a growing number of neuronal structures (Xia et al. 2014) (LaLonde et al. 2014)

Besides the evidence of interaction between STIM and Orai, store operated calcium entry in neurons have been linked to normal physiological functions. SOCE was found in sensory neurons and acts during axonal trauma (during for instance spine damage) to maintain calcium homeostasis; SOCE depends in these neurons on Orai1 and STIM1 (Gemes et al. 2011). On the other hand, hippocampal neurons who suffer from ischemia after neuronal injury increased their STIM and ORAI expression, and inhibiting expression with short interference RNA increased the chance of neuronal survival and improved neurological function of rats (Zhang et al. 2014). Injection of STIM1 sRNA caused impairment of

mGluR1-mediated store depletion in hippocampal neurons, demonstrating a link between STIM1 and mGluR1 activation (Ng et al., 2011). Later findings linked mGluR1-dependent signaling to STIM1 (Hou et al. 2015) (Hartmann et al. 2014). Sun and colleagues showed that loss of mushroom spines in Alzheimer's disease (AD) is prevented by overexpression of STIM2, and STIM2 itself is downregulated in older AD brains. STIM and Orai are involved in more pathologies, as will be described in the next paragraph (Sun et al. 2014).

1.11 Medical implications

STIM and Orai-mediated store operated calcium entry has been linked to a number of diseases. Pathological dysregulation of calcium homeostasis, such as found in epilepsy, can be countered by pharmacologically inhibiting store operated calcium entry in epileptic rats (Steinbeck et al. 2011) and after traumatic neuronal injury (Hou et al. 2015). In cell culture, mice medium spiny neurons who overexpress a mutant Huntington protein fragment show increased store operated calcium entry, which can be treated by short interference RNA against STIM1 or Orai1 (Vigont et al. 2015).

Another brain disease in which STIM and Orai might be involved is Alzheimer's disease (AD). Although the causes of AD are still unknown, one of the causes could be an overall imbalance in calcium signaling and homeostasis, a hypothesis called the 'calcium hypotheses'. In short, the hypothesis states that disruption of calcium signaling and homeostasis via abnormal functioning of calcium handling proteins (such as ion channels) could underlie the pathogenesis of AD. Experimental proof of AB peptides interacting with calcium-regulating proteins is becoming more abundant (Popugaeva et al. 2015). Indeed, several reports link STIM and/or Orai and AD.

In primary cortical neurons from an Alzheimer mouse model, attenuated store operated calcium entry was linked with γ-secretase STIM1 cleavage and spine instability, and could be rescued by γ-secretase inhibition or STIM1 overexpression (Tong et al. 2016). A later study linked STIM1 to Alzheimer's albeit via a different mutation (Ryazantseva et al. 2017). The STIM1-Orai complex is

furthermore involved in axon growth via calcium regulation in cultured embryonic dorsal root ganglions (Mitchell et al. 2012) (Shim et al., 2013).

1.12 Aim of the study

The aim of this study is to elucidate the STIM1-dependent activation mechanism of TRPC3. Initially, I used STIM1 deficient mice and describe novel conditions under which TRPC3 is activated. I proceeded to search for missing links in the molecular mechanisms that underlie TRPC3 activation in PNs. During these inquiries, I successfully applied a novel, light-activated molecular tool, namely Photo-activatable diacylglycerol (PhoDAG). Finally, I identify Orai2 as the STIM1-activated calcium channel, which is critically involved in TRPC3 activation and calcium homeostasis in PNs, and which is crucial for cerebellar motor behavior.

The significance of this work applies to many disciplines. First, I am the first to describe a role of Orai2 channels for the activation of TRPC3. Second, this work is the first that links Orai2 to ataxic behavior, which could contribute to our current understanding of cerebellar ataxias. Finally, my work demonstrates a major contribution of SOCE to neuronal function.

Chapter 2 Material and Methods

2.1 Animals

All experiments were carried out in accordance with institutional animal welfare guidelines of the government of Bavaria, Germany.

STIM1 cell type specific knockout (STIM1^{PKO}) mice (Hartmann et al. 2014) were generated by crossing mice in which exon 6 of STIM1 was flanked by *LoxP* sites (Baba et al. 2008) with mice that express the *Cre* recombinase under the control of the GluD2 promoter (Yamasaki et al. 2011). The resulting mice have a deletion of STIM1 specifically in PNs.

Generation of TRPC3 knockout (TRPC3$^{-/-}$) mice used during our experiments were described before (Hartmann et al. 2008).

CamKII$^{-/-}$ mice: Mice carrying a *loxP* sequence on the first and second exon of *camk2a* (Jackson laboratories, catalogue number #006575) (Hinds et al. 2003) were crossed with mice that express *Cre* under the control of the GluD2 promoter (Yamasaki et al. 2011). In the resulting offspring α- Calcium/calmodulin-dependent protein kinase II (CaMKIIa) is deleted exclusively in PNs.

Orai2 general knockout (Orai2$^{-/-}$) mice were a generous gift of the lab of Stefan Feske and the generation of these mice has been recently published (Vaeth et al. 2017).

Orai2^{PKO} mice: Mice carrying a floxed exon 2 of the *Orai2* gene were generously provided by the group of Marc Freichel. These mice were bred with mice expressing *Cre* under the control of the GluD2 promotor (Yamasaki et al. 2011). The resulting mice carry an Orai2 deletion in PNs specifically.

Orai1^{PKO} mice: Mice carrying a floxed exon 2 on the Orai1 gene were provided by Prakriya and colleagues (Somasundaram et al. 2014). These mice were bred with mice expressing *Cre* under the control of the GluD2 promotor (Yamasaki et al. 2011). In the resulting offspring *Orai1* is deleted in exclusively in PNs.

Control mice were mice with floxed alleles that did not express *Cre* in the case of STIM1^{PKO}, Orai2^{PKO} and Orai1^{PKO} mice. Black6 mice were used as control for

Orai2$^{-/-}$ and CaMKII$^{-/-}$ mice. The mice were reared in a 12 hours light/dark cycle and kept with food and water *ad libitum*.

2.2 Electrophysiological solutions and pharmacological agents

All substances reported except standard salts for solutions will be reported with the name and in brackets the (online catalogue number, and company) of purchase.

For slice preparation and perfusion of slices during experiments artificial cerebrospinal fluid (ACSF) containing (in mM) 125 NaCl, 4.5 KCl, 2 $CaCl_2$, 1 $MgCl_2$, 1.25 NaH_2PO_4, 26 $NaHCO_3$, and 20 glucose with an osmolality of ~ 315 mosm. ACSF was freshly prepared at the beginning of an experimental day. The internal solution (IS) for patch-clamping was prepared on a weekly basis as a stock solution and stored at -20°C. Before usage the IS stock was melted and diluted (80:20 IS/H_2O) to the final concentration. This allowed us to later mix the internal solutions with pharmacological agents or calcium indicators. In almost all experiments for instance, the calcium indicator Oregon Bapta Green 1 (OGB-1) was added. The final composition (unless stated otherwise) was in mM: 148 potassium-gluconate, 10 HEPES, 10 NaCl, 0.5 $MgCl_2$, 4 Mg-ATP, 0.4 Na_3-GTP, and 0.1 Oregon Green BAPTA-1 (06807, Molecular Probes). The pH was adjusted to 7.3 with 3M KOH and the osmolarity was tested to be approximately 310 mosm. During all experiments, 10 µM bicuculine (14340, Sigma) was added to block GABAergic transmission by GABA-A receptors. In experiments with 200Hz electric stimulation of parallel fibers, α-amino-3-hydroxy-5-methyl-4-isoxazolepropionic acid receptor (AMPAR)-mediated synaptic transmission was partially blocked with 10 µM Cyanquixaline (6-cyano-7-nitroquinoxaline-2,3-dione) (CNQX) (C239, Sigma). For depletion of intracellular stores the SERCA blocker 30µM cyclopiazonic acid (CPA) (C1530, Sigma) was used. Direct activation of mGluR1 was achieved by local pressure ejection (10psi; 100ms) of 200µM of the group 1 agonist (S)-3,5-dihydroxyphenylglycine (DHPG) (0805, Tocris).

IP_3 uncaging experiments were performed with internal solution containing 400 µM NPE-IP_3 (I23580, Invitrogen). Uncaging of IP_3 was done by a 10ms light

pulse delivered from an ultraviolet laser (Coherent Cube; 375 nm, 15 mW at the laser head) and was directed to the surface of the slice with the use of a tapered lensed optical fiber (Nanonics; working distance 6 ± 1 µm, spot diameter 6 ± 1 µm). The success of uncaging was assessed by the large, out-of-range flash artifact followed by a slower fluorescent signal that represented IP_3-mediated calcium release from stores. PhoDAG (PhoDAG-11) was kindly provided by the group of Dirk Trauner (Ludwig-Maximilian University). PhoDAG was diluted in Dimethyl sulfoxide (DMSO) and BSA. The external solution was such that the final concentration of DMSO and BSA did not exceed 0.1%. The final concentration of PhoDAG was 200 µM. Calphostin (C6303, Sigma) was diluted in DMSO to a final working concentration of 1 µM; the final concentration of DMSO was 0.1%. 1-oleoyl-2-acetyl-sn-glycerol (OAG) (O6754 Sigma) was diluted in DMSO to a final working concentration of 100 µM. GSK1702934A (10-1445, Focus Biomolecules) was diluted in external solution to a working concentration of 10 µM.

2.3 Preparation of brain slices

Acute slices from the cerebellar vermis were prepared in accordance with the animal care and use guidelines of the government of Bavaria, Germany.

The mice were anesthetized using CO_2 and decapitated. Starting from caudal at the level of the cervical medulla to rostral ending at bregma 1mm bilateral incisions and a frontal incision of the cranium were performed. The epicranium was removed and the cerebellum and part of the cerebrum were laid open. After two paramedian sagittal cuts at the level of the cerebellar hemispheres, one horizontal cut at the base of the skull (basis crania interna) and a horizontal cut through the cerebrum (bregma ~ -1mm) the cerebellar vermis was rapidly dissected and placed in ice-cold ACSF (0°C – 2°C) bubbled with 95% O2 and 5% CO_2. Using cyanoacrylate based superglue (UHU Sekundenkleber, Bühl) one lateral side of the tissue block was glued to a stage, placed into a slicing chamber and subsequently submerged in ice-cold oxygenated ACSF. Parasagittal slices of the cerebellar vermis with a thickness of 300µm were cut using a vibratome slicer (Leica VT1200S). In order to increase the quality of the slices the

built-in Vibrocheck function of the slicer was used in order to minimize vertical vibrations of the blade. The cut slices were transferred to an oxygenated storage chamber and kept for 30 to 45 minutes at 34°C (Edwards et al. 1989). Slices were left to rest at least 1 hour before the start of the experiment. Finally the slices were stored in ACSF at room temperature for up to 8 hours. For experimental recordings one slice was transferred to a recording chamber and mechanically fixed at the bottom of the recording chamber with a grid of nylon threads glued to a U-shaped platinum frame. During the entire experiment the slice was continuously perfused (perfusion rate 2 – 2.5 ml/min) with ACSF containing 10 µm bicuculine in order to block $GABA_A$ receptors. All experiments were performed at room temperature. PNs near the surface of the slice were identified based on their location in the PN layer and their morphology (size and shape of the somata).

2.4 Electrophysiology

Recordings were obtained with an EPC-9 amplifier (HEKA; Germany) and 'Pulse' software (HEKA; Germany) was used for data acquisition. Patch pipettes (3–4MΩ) were pulled on a Narishige puller (model PC-10) from borosilicate glass (Hilgenberg). During the recordings, the slices were continuously perfused with ACSF at room temperature. The liquid junction potential for the used IS and ACSF was calculated to be 14.5 mV and was left uncorrected. Following gigaseal formation the fast capacitance was corrected for and the whole-cell configuration was attained with application of short negative pressure pulses to the pipette. After break in, the slow membrane capacitance was compensated for. Data were sampled at 20 kHz and filtered with a 10 kHz Bessel filter. Afferent stimulation was performed using a patch pipette filled with 1 M NaCl (1 MΩ resistance). The stimulation pipette was placed on top of the molecular layer, right on top of the target dendrite. Stimuli were applied by a triggered isolated pulse stimulator (Model 2100; A-M Systems) with varying pulse duration and pulse number, depending on the experiment.

2.5 Live cell calcium imaging

A multipoint confocal microscope using dual spinning disc technology (QLC 100; VTi), attached to an upright microscope (E600FN; Nikon) and equipped with a 40× objective (NIR Apo, NA 0.8; Nikon) was used to acquire fluorescence images from dendritic fields in parallel to the patch clamp recordings. Spinning disk microscopy has the advantage of a confocal system, i.e. out-of-focus light is filtered out in order to increase the signal to noise ratio.

Excitation was generated by a Sapphire laser (Coherent; USA) with a wavelength of 488 nm and adjustable output power of up to 75 mW. Full-frame 80x80 pixel images were recorded at 40 Hz with a CCD camera (NeuroCCD, RedShirt imaging, USA). Synchronization of the spinning disc with the CCD camera was achieved by utilization of a function generator (TG1010A; TTi). Data acquisition and conversion to text files was done via in house written software in LabView. As region of interest (ROI) a circle of six pixels diameter placed on the first responding dendritic region was chosen; as background, a larger dark area close to the region of interest was chosen. Fluorescence recordings were corrected for ambient light by subtracting a single image without laser illumination from all images recorded with laser illumination. Then the recordings were background-corrected by subtracting the averaged brightness values of the pixels in the background ROI from all images in the recording. Finally, relative fluorescence changes were calculated as $\Delta F/F\ [\%] = (F-F_0)/F_0 \times 100$ with F being the brightness values on the CCD pixels at each particular time point of the recording and F_0 being the baseline brightness. A custom-made macro in Igor Pro (Wavemetrics, USA) was used to calculate $\Delta F/F$ for ROIs by averaging the relative fluorescence changes of all pixels contained in this ROI. The 'baseline' calcium levels (F_0) before stimulation were determined by averaging the first 40 frames of the recording.

False color images were made by loading the CCD camera recording as a TIFF stack in 16 bit mode into Image J. Then a maximum-intensity projection of the stack was made and the resulting image was converted to black-and-white as a dendritic overlay template. A "baseline image" was obtained by maximum-

intensity projecting the last 20 images (e.g. 0.5 seconds) before stimulation. Analogously, the “peak image” was the result of maximum-intensity projection of 20 images recorded during the peak of the calcium response. The ‘baseline’ is subtracted from the ‘peak’ using the image calculator option in ImageJ and the resulting image is converted to the’16 color’ mode using the appropriate lookup table. Finally, the false color spot is excised from the image and placed in the the dendritic template image at the identical location using Adobe Photoshop (USA).

2.6 Fluorescent immunostaining

Mice of designated genotype were deeply anesthetized with isoflurane. The chest was opened by cutting through the ribcase and exposing the heart. A needle was inserted into the left atrium and a small cut was made in the right ventricle. After a flush of phosphate buffered saline (PBS), the mouse was perfused with cold 4% paraformaldehyde (PFA). After a clear discoloration of the liver, indicating successful perfusion, the brain was removed and stored at 4°C in 4% PFA. Longer storage was done at 4°C in PBS. After storage, 50 µm broad cerebellar sections were made using a Vibrotome (Leica, VT1200S). Slices were immediately after slicing used for immunostaining. Slices were permeabilized 3% normal calf serum and 0.3% Triton X-100 overnight at 4°C. Slices were incubated with one of three primary antibodies: Orai1 (Abcam, ab59330), Orai2 (Abcam, ab180146), Orai3 (Abcam, ab15558) diluted 1:100 overnight at 4°C, and were co-immunostained with calbindin (ab82812, abcam) 1:1000. Slices were washed five times 5 min. in PBS on a shaker and incubated with secondary antibodies (for Orais: 488, rabbit, Thermo Fisher; for calbinding: 564, goat, Thermo Fisher) for 1 hour at room temperature. Slices were washed five times in PBS and mounted (Vectashield, Vector Labs). Slices were scanned with a scanning confocal microscope (FV, 3000, Olympus) and images were acquired using FluoView (Olympus). More precisely, the images were 1024 by 1024 pixels; stacks were composed of single images taken at a vertical distance of 1 µm, and each image was scanned only once. Laser strength and photomultiplier tube (PMT) gain was determined in wild type slices for 20x and 60x separately and

applied for all other genotypes. Maximum-intensity projections of all images in a stack were done using Image J. Further post processing involved balancing out colors linearly in 16bit mode; the resulting intensity values were applied to all other slices.

2.7 Biocytin-Streptavidin immunostaining

Cerebellar slices were prepared as described in section 3.3. Next, cells were whole-cell patch-clamped and loaded with standard internal solution supplemented with 20 mg/ml biocytin (B2461, Merck) as mentioned in section 3.2. Perfusion was allowed for approximately half an hour, after which the patch pipette was gently removed from the cell at the lowest speed possible in order to let the PM reseal. Then the slices were immediately placed in 4% PFA and remained there overnight at 4°C. The following day the slices were transferred to a PBS solution containing 1% Normal Goat Serum, 1% Triton X-100 and GFP-conjugated streptavidin (1:200) (Molecular Probes, S11223) and were incubated overnight at 4°C. Next, the slices were washed five times in PBS and mounted (Vectashield, Vector Labs). Slices were scanned with a scanning confocal microscope (FV, 3000, Olympus) and images were acquired using FluoView (Olympus). More precisely, the images are 4096 by 4096 pixels taken with a 20x objective; stacks were composed of images taken at 1 µm vertical distance, and each image was scanned twice and averaged. Magnified images are 4096 by 4096 pixel images taken with a 60x objective at a vertical distance of 0.2 µm. Each image was averaged by scanning each section four times. Maximum-intensity projection of stack was done using Image J. Further post processing involved balancing out colors linearly in 16bit mode.

2.8 Quantitative single cell RT-PCR

For cell harvesting, we applied a similar procedure described originally by Durand et al. (Durand et al., 2006). Slices were placed into the recording chamber, similarly to electrophysiology experiments. PNs were identified visually using an upright microscope (Nikon Eclipse, E600FN; Nikon, Japan). Pipettes used for

targeted harvesting were made from borosilicate glass (2.0/0.3 mm; Hilgenberg) using a Narishige PC-10 pipette puller similarly to patch pipettes but with a much larger tip diameter (ca. 5 µm). The pipette solution consisted of 4 µl H_2O and 1 µl M-MLV Reverse Transcriptase 5x Reaction Buffer ("First Strand Buffer" – FSB; Promega, USA). The tip of the pipette was placed under visual control tightly to the soma of the selected PN. Gentle suction was applied through a mouthpiece connected to the pipette. After complete incorporation of the soma, the negative pressure was released to minimize the collection of extracellular solution. The content of the pipette was pressure-ejected into an Eppendorf tube (0.5 ml) and immediately frozen in liquid nitrogen and later stored at -80°C.

The Reverse Transcription (RT) was performed as follows: The harvested material was complemented with the "Master Mix 1" (1µl "Nonidet P-40", 1% (Roche); 1µl "Primer random p(dN)6", 5mM (Roche); 1µl dNTPs, 10mM each (Promega), 1 µl FSB and 1 µl "RNasin Plus" (Promega)). The mixture was incubated at 70°C for 5 min and subsequently at 0°C for 5min. After that 10 µl of "Master Mix 2" (2µl FSB, 6,5µl H2O and 1,5µl M-MLV Reverse Transcriptase (Promega)) were added to each tube which was then incubated for 1-2h at 37°C. The resulting cDNA was isolated and purified with the use of silica matrix and subsequently stored at -80°C until quantitative RT-PCR. Rapid-cycle PCR reactions were optimized and performed in 20µl reactions in glass capillaries according to the manufacturer's instructions using the LightCycler FastStart DNA Master SYBR Green I kit (Roche).

Samples were quantified by using 'Lightcycler' software. Raw fluorescence data was plotted against cycle number, and a cut off value ('Crossing Point', CP) was determined as the cycle number in which the fluorescence for each sample rises above the noise band for the first time and the exponential phase of cDNA amplification is entered. Relative expression was determined by $2^{-Cp(Orai2)} / 2^{-Cp(GAPDH)}$.

2.9 Quantitative tissue RT-PCR

To analyze the tissue expression of Orai2 in the cerebellum, a small block of tissue (maximum a cube of 3 by 3 by 3 mm or 30 mg) was cut from the cerebellar vermis and stored in RNAlater (Qiagen) at 4°C for maximum one week. RNA was extracted using the RNeasy Mini Kit (Qiagen). RNA content was measured using a Nanodrop device. Next, RNA was transcribed to cDNA using Omniscript RT-Kit (Qiagen). After that, cDNA was diluted to 8 mg/ml and quantitative polymerase chain reaction (qPCR) was performed in 20µl reactions in glass capillaries according to the manufacturer's instructions using the LightCycler FastStart DNA Master SYBR Green I kit (Roche). cDNA samples were quantified similar as described in section 2.8.

2.10 Behavior tests

Elevated beam test: Mice were handled in the experimental room for 3 days at the same time of the day as the later experiment. On the experiment day, the mice were placed in the experimental room half an hour before experimental onset. At the start of the experiment, the mice were placed on a cylindrical plastic beam (0.8 cm diameter) close to one of the 2 platforms at the extreme ends of the beam. The native house of the mice was placed on the platform were the mouse was placed close to, to motivate the mouse to walk. After the mouse entered the house, the mouse was placed on approximately the middle of the beam and imaged using a handicam while it walked towards the house. Mouse placement was repeated five times. Mice that were unable to walk were excluded. Data was analyzed with Windows Movie Maker to count paw slips with single frame precision.

Rotarod: Rotarod experiments were performed on a Rotarod (model 47600, Ugo Basile) with a preprogrammed speed increase, which went from 4 to 40 rpm in 5 minutes. Mice were placed 30 minutes before experiment onset in the experimental room with the rotarod running at stationary speed of 4 rpm. On the first day, mice were placed on the rotarod and the acceleration started when the mice stayed on the rotarod revolting with constant speed for 20 seconds.

Time recording began at the start of acceleration and was stopped when the mice fell off or when it began to cling to the rod and rotate with it (an event that happened very seldom). The trial was repeated twice every day with a one hour interval at at the same time of the day every day for four days.

2.11 Analysis

For electrophysiology and calcium imaging, raw traces were loaded into IGOR PRO (Wavemetrics, USA) and processed using in-house written macros. Outcome values were entered in Excel (Microsoft, USA). Statistics were performed with GraphPad (GraphPad Software, San Diego) and Excel. Normality of data was assessed observing frequency distributions of the data, rather than normality tests, which do not perform well with very small or very large data sets. Statistical significance is indicated as * ($p<0.05$) or ** ($p<0.001$).

For morphological measurements (Fig. 17) ImageJ was used to determine dendritic area and somata size.

Chapter 3 Results

3.1 Calcium dependence of the STIM1-mediated regulation of TRPC3 downstream of mGluR1

In order to characterize the nature of the STIM1-dependent regulation of the TRPC3-mediated current I first studied the time-dependence of its rescue by depolarization in STIM1^{pko} mice (Fig. 1). From earlier work (Hartmann et al. 2014) it was known that the effect of the depolarizing pulse is transient and that PNs in STIM1^{pko} mice are mostly unresponsive to DHPG again when DHPG is applied after more than five minutes without depolarization.

3.1.1 Long lasting effects of transient depolarization in STIM1^{PKO} mice

First, I looked into the speed with which calcium influx rescues TRPC3 activation. In acute cerebellar slices from STIM1^{pko} mice PNs were whole-cell patch-clamped and perfused intracellularly with Oregon Green Bapta 1 (OGB-1; 100 µM). The group I mGluR-specific agonist dihydroxyphenylglycine (DHPG) was applied under control conditions and either 0.5 s or four seconds after a transient depolarization to 0 mV for 1s. As reported by Hartmann et al., PNs in STIM1^{pko} mice at resting membrane potential do not respond to DHPG. However, depolarizing the cells restored both the DHPG-evoked calcium transient and the TRPC3-mediated inward current, irrespective whether DHPG (200 mM, 10 ms) was applied 4s or 0.5s after the depolarization (Fig. 1A). However, there was no significant difference in the amplitudes of the calcium transient and inward current when responses from experiments with a 0.5s interval or a 4s interval, respectively, were compared (mean ΔF/F; 0.5s: 173 ± 14%, 4s: 167 ± 16%, p = 0.73; mean I_{DHPG} amplitude; 0.5s: 114 ± 14 pA, 4s: 149 ± 24 pA, p=0.06) (Fig. 1B). In conclusion, the effect of the depolarization is fast and there is no decline of the responsiveness to DHPG within the 4s time window that was used as a standard interval in earlier experiments (Hartmann et al. 2014).

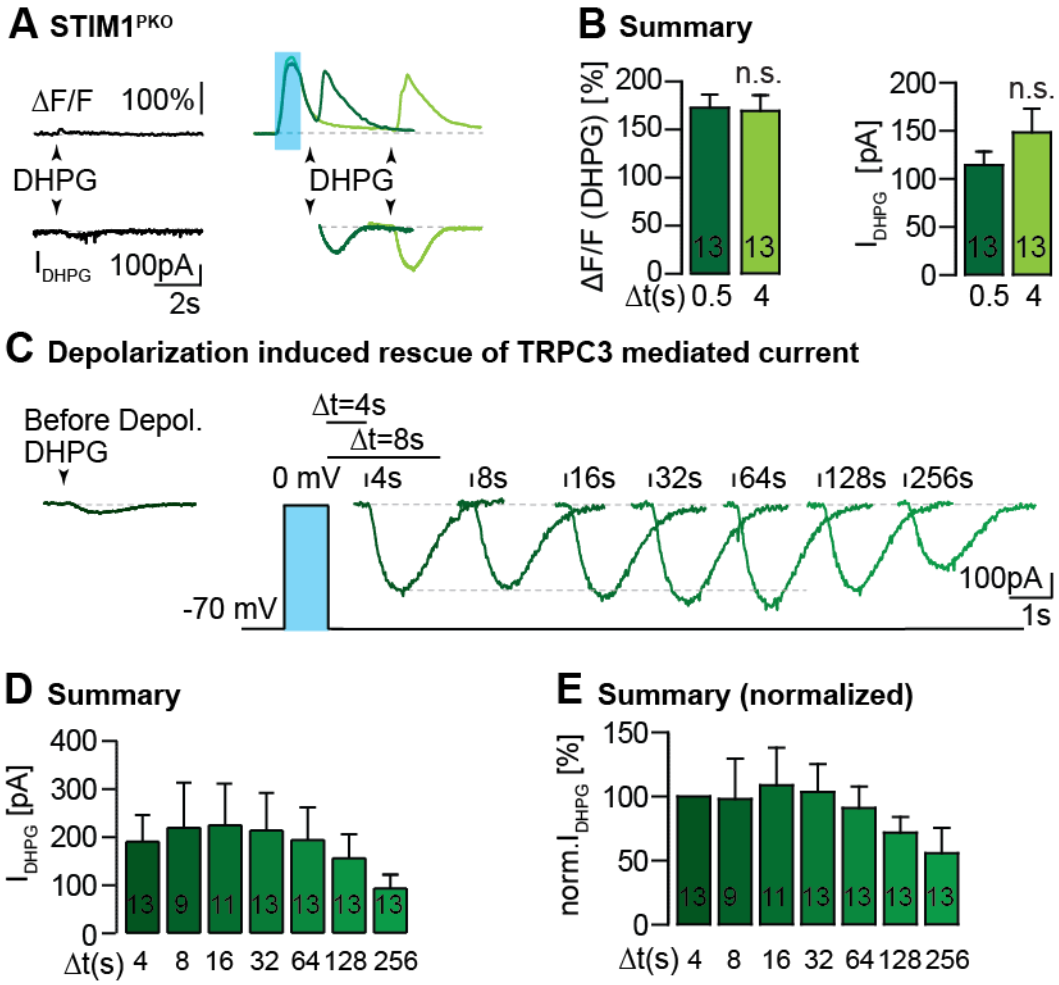

Figure 1 Transient depolarization allows reactivation of mGluR1 for minutes after calcium influx. A *DHPG application (10ms, 200µM) before (left) and after (Right) transient depolarization (1s, 0 mV) (blue bar). DHPG was applied 0.5s (dark green) or 4s (light green) after depolarization and indicated by vertical bars. Top traces show OGB-1 fluorescence recordings in dendritic subregions, bottom traces indicate current measurements via whole-cell somatic patch-clamp in voltage mode.* ***B*** *Summary: Mean ΔF/F amplitudes(left) and inward currents (I_{DHPG};right) following DHPG application taken from the experiment shown in* ***A****.* ***C*** *Similar experiment as shown in A, but with longer periods between depolarization and DHPG application. Vertical black lines indicate point of DHPG application with the time between depolarization and DHPG application indicated behind it. All applications were performed in one cell.* ***D*** *Summary: mean inward current amplitudes following DHPG application (I_{DHPG}) as shown in* ***C****.* ***E*** *Summary of the inward current in* ***C*** *normalized against the 4s value.*

In order to elucidate the temporal characteristics of the transient restoration of responsiveness to DHPG by depolarization I applied DHPG at various intervals that were multiples of the standard 4s interval. In Fig. 1C subsequently recorded inward currents from one cell stimulated with DHPG at 4s and up to 256s after the depolarizing pulse are plotted. The amplitude of the TRPC3-mediated currents decline only after 4 min (Fig. 1D, 4s 191 ± 55 pA, 8s 201 ± 86 pA, 16s 210 ± 80 pA, 32s 202 ± 73 pA, 64s 183 ± 64 pA, 128s 148 ± 47 pA, 256s 90 ± 26 pA) but were statistically the same for all intervals. Normalizing for the response at 4s did not reveal any differences either (Fig. 1E, 8s 76 ± 14 %, 16s 82 ± 11 %, 32s 84 ± 10 %, 64s 76 ±10%, 128s 68 ± 11%, 256s 59 ± 19%) Thus, a single event of calcium influx over the PM can reliably rescue mGluR1-mediated inward current in STIM1^{pko} PNs for minutes and the effect of the depolarization regarding the rescue of mGluR1 signaling in the absence of STIM1 in STIM1^{pko} mice by far outlasts the rise in the cytosolic calcium concentration due to calcium influx through VGCCs. Direct binding of calcium ions to the TRPC3 subunits as a requirement for channel gating can therefore be excluded.

3.1.2 TRPC3 activation happens independent of intraluminal calcium concentrations

Thus, it was found that TRPC3 is activable in conditions where ER calcium stores in PNs are full: at rest when STIM1 ensures store replenishment or alternatively during or following activity when stores are full due to calcium influx through VGCCs. Next, the hypothesis that the ER calcium store regulates TRPC3 activation was tested. For this purpose we used an experimental setting similar to that shown in Fig. 1A (4s interval). After an initial test that showed restoration of DHPG responses following the depolarization the experiment in the same cells was repeated in the presence of 30 µM CPA, an antagonist of SERCA that depletes ER calcium stores of mobilizable calcium ions (de Juan-Sanz et al. 2017). Surprisingly, TRPC3 activation due to DHPG-application was observed following the depolarization in the presence of CPA when the DHPG-induced calcium signal was strongly reduced as an indication of store emptying

(Fig. 2, *right* ③). The summary shows that TRPC3 is equally activated with or without CPA (Fig.2B, middle, ① 17 ± 9 pA, ② 125 ± 40 pA ③ 155 ± 50 pA). The calcium release from stores is significantly reduced following CPA application (Fig.2B, left, ① 9 ± 9 %, ② 85 ± 37 % ③ 51 ± 15 %). Note that CPA did not influence the calcium influx following depolarization (Fig 2B, right, control: 237 ± 41 %, CPA: 221 ± 38%).

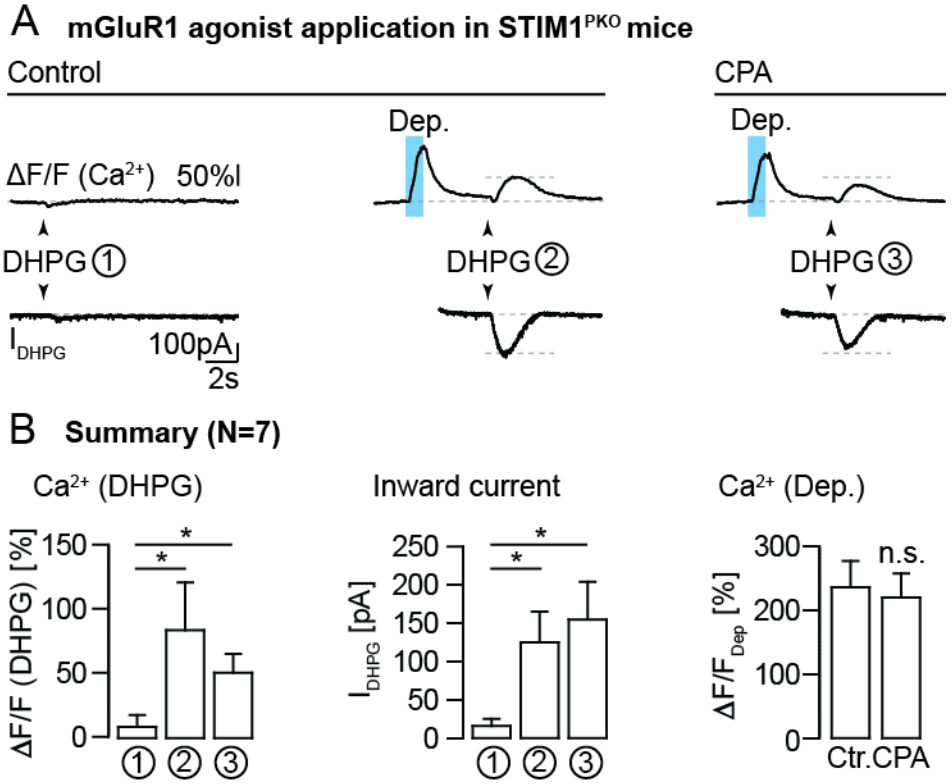

Figure 2 TRPC3 activation does not depend on calcium concentrations in the ER. A *DHPG application before (left) and after (middle) transient depolarization. Depolarization and DHPG application were repeated in the presence of CPA (30 µM) in the external medium (right). Dotted lines indicate baseline values under control conditions.* ***B*** *Summary: Mean amplitudes of relative OGB-1 fluorescence changes (ΔF/F; left) and inward currents (I_{DHPG}; middle) in response to DHPG-application for the three conditions depicted in* ***A****, and mean amplitudes of depolarization-induced calcium transients under control conditions and in the presence of CPA (right).*

The residual calcium transient in the presence of CPA occurs due to calcium influx through TRPC3 that is an unspecific cation channel that is permeable to Calcium (Clapham et al. 2001). This was proven with the use of a general TRPC3 knockout ($TRPC3^{-/-}$) mouse that completely lacks the mGluR1-dependent current but has normal IP_3R-mediated calcium release downstream of mGluR1. In acute cerebellar slices of $TRPC3^{-/-}$ mice PNs were whole-cell patch-clamped, and DHPG was applied before and after depolarization under control conditions and in the presence of CPA similarly to the experiment the $STIM1^{pko}$ mouse in Fig. 1A. It was found that in the absence of an inward current there is no DHPG-evoked calcium signal in the presence of CPA (Fig. 3). Thus, CPA effectively empties calcium stores in cerebellar PNs under these conditions. Based on these data, the hypothesis that TRPC3 activation depends on the filling state of ER calcium stores was discarded. Instead, TRPC3 appears to be regulated by the cytosolic calcium concentration.

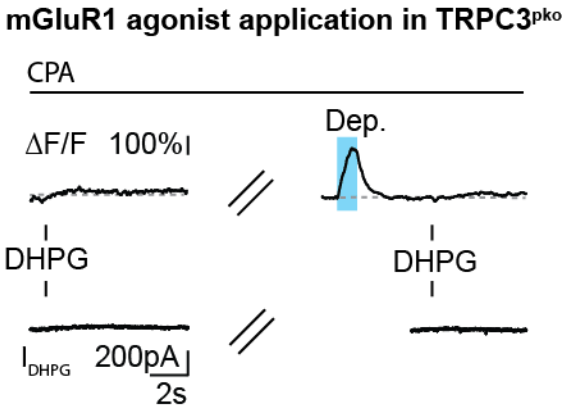

Figure 3 CPA empties calcium stores in $TRPC3^{-/-}$ mice. *Similar to Figure 2A, DHPG was applied before (left) and after (right) transient depolarization under application of CPA.*

3.1.3 TRPC3 activation is regulated by local cytosolic calcium concentrations in $STIM1^{-/-}$ mice

This hypothesis was tested in wild type mice by another variation of the experimental conditions in this protocol (① control DHPG response, ② test DHPG response after depolarization), namely by supplementing the internal solution with 20 mM ethylene glycol-bis(β-aminoethyl ether)-N,N,N',N'-tetraacetic acid (EGTA) to buffer cytosolic calcium. This prevented cytosolic calcium transients during the depolarization in 7/12 cells tested. The remaining 5 EGTA

cells that showed calcium transients were removed from the analysis. Surprisingly, despite the absence of a cytosolic VGCC-mediated calcium transient during the depolarization in the cells perfused with EGTA TRPC3 could be activated immediately thereafter as indicated by DHPG-evoked inward currents (Fi. 4A ②). However, in other experiments, when EGTA was replaced with the same concentration of 1,2-bis(*o*-aminophenoxy)ethane-*N*,*N*,*N'*,*N'*-tetraacetic acid (BAPTA) the activation of TRPC3 by DHPG-application following the depolarization was completely prevented (Fig. 4B ②). The summary in Fig. 4C shows that under EGTA conditions, TRPC3 is as strongly activated as under CPA only (Fig. 4C top, CPA 165 ± 55 pA, BAPTA 5 ± 3 pA, EGTA 128 ± 23 pA). Calcium influx via TRPC3 was buffered with either calcium chelator (Fig.4C bottom, CPA 31 ± 9 %, BAPTA 3 ± 2 %, EGTA 9 ± 6 %).

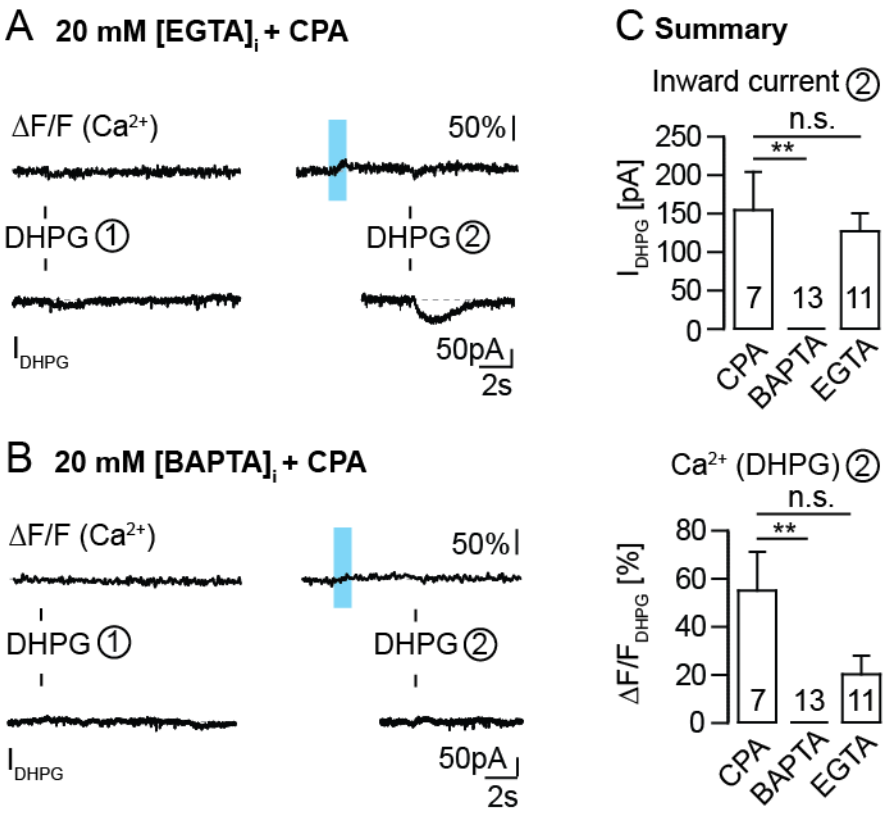

Figure 4 Fast calcium buffering prevents depolarization-induced rescue of TRPC3 activation in STIM1^{PKO} mice. A *OGB-1 fluorescence (top) and current recordings (bottom) with DHPG application before (left) and after (right) transient depolarization with 20 mM EGTA in the pipette solution intracellularly and in the extracellular presence of 30 µM CPA.* ***B*** *Analogous experiment as in A, but with 20mM BAPTA instead of EGTA.* ***C*** *Summary of the DHPG responses shown in* ***2A*** *(condition ③, CPA),* ***4A*** *(②) and* ***4B*** *(②): Mean inward current amplitudes (I_{DHPG}, top) and mean amplitudes of DHPG-evoked calcium transients ($\Delta F/F_{DHPG}$, bottom).*

The difference between the effects of both buffers reveals an important prerequisite underlying the activation mechanism of TRPC3. BAPTA and EGTA bind calcium with similar affinities, but BAPTA has nearly 100-fold faster binding kinetics than EGTA (Naraghi et al. 1997). EGTA buffers global calcium signals (hence the absence of a calcium transient following depolarization). BAPTA, however, captures calcium ions much nearer to the source (here VGCCs in the PM).

This differential sensitivity of processes dependent on calcium influx to BAPTA and EGTA has been interpreted as being due to a close physical distance between the channels and the respective calcium sensor (“nanodomain coupling”, Eggermann et al. 2012). The conclusion from the experiments described above is that the activation of TRPC3 downstream of mGluR1 in the absence of STIM1 depends on a calcium binding component that is located within nanometer range to the mouth of VGCCs in the PM.

3.1.4 TRPC3 activation depends on cytosolic calcium in wild type mice

From earlier work in our group it was known that at resting membrane potential TRPC3 depends on STIM1 (Hartmann et al. 2014) but activates normally in the presence of CPA when ER calcium stores are empty and STIM1 expression is unaltered (Henning, unpublished). In order to clarify whether the activability of TRPC3 depends on cytosolic calcium also at rest, I conducted whole-cell patch-clamp experiments in acute cerebellar slices from wild type mice.

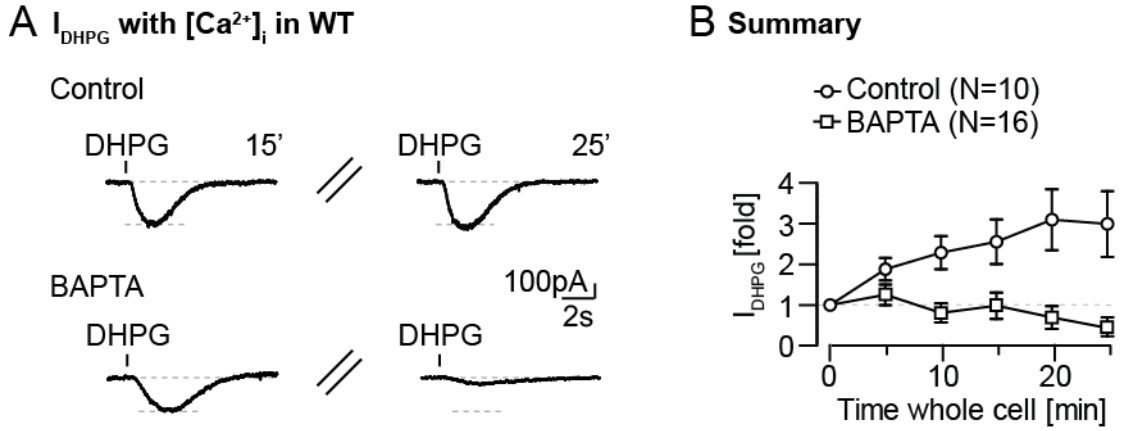

Figure 5 Fast calcium buffering prevents TRPC3 activation in WT mice. A *Top: Somatic voltage-clamp recordings with DHPG application 15 minutes (left) and 25 minutes (right) after the whole-cell configuration was established with standard intracellular solution in the pipette. Bottom: Analogous experiment with an intracellular solution substituted with 30 mM BAPTA.* ***B*** *Summary: Mean I_{DHPG} amplitudes for all experiments as shown in A for control (circles) and BAPTA containing (squares) internal solutions.*

Once the whole-cell configuration was attained by rupturing the membrane patch under the pipette tip DHPG was repeatedly applied at regular time intervals (5 min). The pipette contained either the regular internal solution or the solution that was complemented with BAPTA. Under both conditions inward currents are reliably evoked up to 15 min after the beginning of the perfusion of the cells with the respective pipette solutions (Fig. 5A, top). In control experiments the amplitude of the DHPG-evoked inward currents initially increases (E53: 0‘ 100 ± 0 pA, 5‘ 173 ± 2 pA, 10‘ 204 ± 27 pA, 15‘ 222 ± 30 pA, 20‘ 261 ± 38 pA, 25‘ 249 ± 42 pA). A possible explanation for that is an increase of the driving forces for cation currents as the liquid cytosol is increasingly exchanged with the pipette solution. The amplitude then remains stable throughout the experiment (Fig. 5B). In the cells filled with BAPTA-containing solution, in contrast, TPRC3-mediated currents do not increase initially and started to decline after 20 min into the experiment and practically disappeared after 25 min. (BAPTA: 0‘ 100 ± 0, 5’ 125 ± 25 pA, 10‘ 81 ± 24 pA, 15‘ 98 ± 32 pA, 20‘ 70 ± 28 pA, 25‘ 44 ± 20 pA) (Fig. 5A,

bottom). The observation that TRPC3 cannot be activated when all necessary molecular components are in place but cytosolic calcium is buffered led to the conclusion that permissive cytosolic calcium levels are required for TRPC3 activation.

3.1.5 Physiological calcium influx over the PM is sufficient to reactivate mGluR1 responses

Calcium influx through the PM seems crucial for TRPC3 activation in PNs (Fig. 1, 2). I wondered how relevant these findings are considering the physiological connections excitatory fibers make with cerebellar PNs. Cerebellar PNs receive massive excitatory input from the CF at a frequency of 1 Hz *in vivo* (Ito, 2006) leading to semi global calcium influx in large parts of the dendritic tree (Otsu et al. 2014). Could activation of the CF lead to store refilling and TRPC3 rescue in STIM1^{pko} PNs? With an extracellular voltage pulse CF can reliably be activated in cerebellar slices (Konnerth et al. 1990). Successful activation of CF was assessed by its all or nothing character, paired-pulse depression when the interstimulus interval is < 500 ms and the characteristic waveform of the resulting complex spike in the current clamp mode (data not shown). We confirmed that DHPG-evoked TRPC3-mediated currents are successfully rescued after activation of the CF (Fig. 6A). In summary, physiological depolarization resulting from synaptic activity and consecutive calcium influx through the PM can ensure activatability of TRPC3 in STIM1^{pko} PNs (Current: DHPG 117 ± 57 pA, CF+DHPG 251 ± 81 pA) (Fig. 6B).

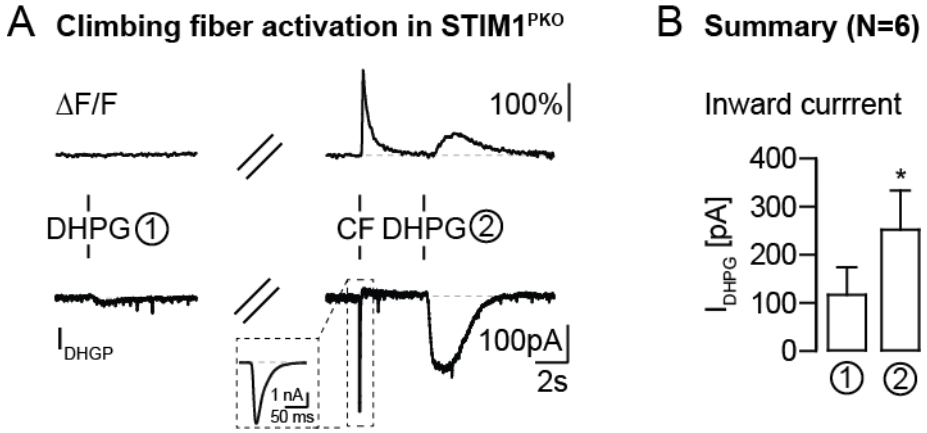

Figure 6 Rescue of mGluR1-mediated responses in STIM1PKO mice by a preceding CF activation. A *OGB-1 fluorescence (top) and whole-cell voltage-clamp recordings with DHPG applications before (left, ①) and after (right, ②) climbing CF. The inset shows the CF-mediated EPSC on a high resolution time scale.* ***B*** *Summary: Mean IDHPG amplitudes at the two time points as indicated in* ***A****.*

3.1.6 Calcium release from stores does not affect TRPC3 activation

The unknown calcium binding factor that is required for the mGluR1-dependent gating of TRPC3 during neuronal activity is located near the mouth of VGCCs. These channels, however, are closed at resting membrane potential when TRPC3 depends on STIM1 but not on the calcium concentration in the lumen of the ER. Thus, it seems justified to assume that the calcium-dependent regulator of TRPC3 could be located near to the cytosolic side of the IP_3R. Therefore, calcium ions released from the ER through IP_3Rs could be responsible for the regulation of the activability of TRPC3. In $STIM1^{pko}$ PNs the ER calcium stores at resting state (Hartmann et al. 2015). However, Hartmann et al. also reported a small increase of inward currents through TRPC3 following depolarization in PNs in wild type mice. We used this observation to test our hypothesis by exchanging the depolarization-evoked calcium influx with calcium release from stores. To force calcium from IP_3R dependent stores, in whole-cell patch-clamped PNs in cerebellar slices from wild type mice we photolytically uncaged intradendritic myo-inositol 1,4,5-triphosphate, P4(5)-1-(2-nitrophenyl)ethyl ester (NPE-caged IP_3) (400 µM) followed by puff application of DHPG to PNs.

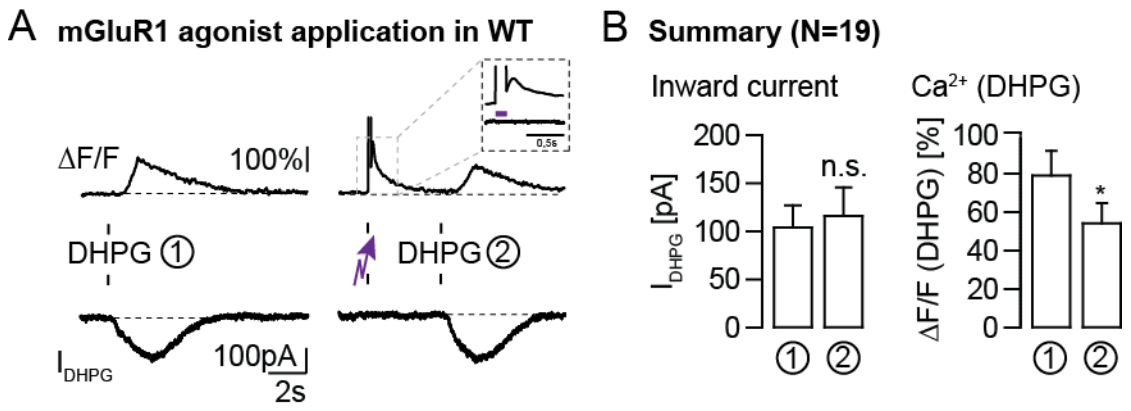

Figure 7 Calcium release from stores does not modulate TRPC3 activation. ***A*** *OGB-1 fluorescence recordings (top) and somatic voltage-clamp recordings (bottom) with DHPG application before (left, ①) and after (right, ②) IP3 uncaging (purple lightning bolt, purple bar in the inset). The inset shows the IP3 uncaging on a higher time resolution scale. For display purposes, the uncaging artifact in the ΔF/F trace is cut off.* ***B*** *Summary: Mean IDHPG amplitudes (left) and calcium signal (right) as shown in* ***A****.*

Following a short UV-illumination artefact in the fluorescence trace, a slow calcium transient could be observed (Fig. 7A, inset) indicating successful IP_3 uncaging and IP_3R-mediated calcium release from stores. The mGluR1-mediated slow calcium transient was consistently smaller after IP_3 uncaging compared to a preceding control response due to partial store depletion by IP_3 (Calcium: DHPG 79 ± 13 %, Uncage+DHPG 54 ± 11 %) (Fig. 7A, B *right*). However, we did not observe an increase in TRPC3-mediated current as was observed earlier (Current: DHPG 104 ± 23 pA, Uncage+DHPG 116 ± 30 pA) (Hartmann et al. 2014). It therefore seems unlikely that calcium release from stores modulates the strength of TRPC3 activation.

3.1.7 Summary

The findings in this chapter have broadened our understanding of the mGluR1 signaling pathway in cerebellar PNs. More precisely, I found:

- $STIM1^{PKO}$ neurons can be relieved of mGluR1 dependent signaling impairments for minutes by a single transient depolarization;
- Physiological input from the CF can rescue the mGluR1 response in $STIM1^{PKO}$ PNs;
- TRPC3 activation depends on the presence of calcium ions close to the PM;
- TRPC3 activation does not depend on the filling state of the ER calcium store;
- TRPC3 activation is likely to depend on the amount of cytosolic calcium close to the PM;
- Calcium release from store seems insufficient to modulate TRPC3 activation.

In the following section, I attempt to unravel in closer detail some of the molecular mechanisms that underlie the activation of TRPC3.

3.2 Molecular mechanisms of TRPC3 activation

After it was established that a calcium-dependent process is required to render TRPC3 activable, the next question was about the possible molecular mechanism that is involved.

3.2.1 CaMKII$^{-/-}$ mice show small alterations in mGluR1 responsiveness

TRPC3 is activated downstream of mGluR1 and G_q (Hartmann et al. 2004). Apart from the pathway downstream of mGluR1, in cell culture it was shown that calcium can modulate activation of TRPC3 channels (Zitt et al. 1997) (Shi et al. 2004) (Shi et al. 2013). In cerebellar PNs influx of calcium is not sufficient to open TRPC3 (Fig. 1, 2, 5) but permissive cytosolic calcium levels are required to allow the gating of TRPC3. The calcium-regulated enzyme calcium calmodulin-dependent kinase II (CaMKII) was demonstrated to modulate the close homologues of TRPC3, TRPC6 and TRPC7 (Shi et al. 2004) (Shi et al. 2013). We tested the hypothesis that CaMKII is involved in TRPC3 activation by testing mGluR1 activation via DHPG in PNs from CaMKII$^{-/-}$ mice. Again, as described previously, in acute cerebellar slices DHPG was locally applied to dendrites of whole-cell patch-clamped PNs filled with an OGB1-containing solution. As presented in Fig. 8A (right), CaMKII$^{-/-}$ PNs show slightly augmented TRPC3-mediated current following DHPG application compared to wild type animals (Fig. 8A, left). Strikingly, analysis of the data revealed a significant increase of the mean amplitude of TRPC3-mediated inward currents in CaMKII$^{-/-}$ mice (Fig. 8C, left), while mean amplitudes of DHPG-evoked calcium transients are not affected by the absence of CaMKII (Calcium: WT 204 ± 13 %, CamKII$^{-/-}$ 189 ± 20 %, Current: WT 189 ± 21 pA, CamKII$^{-/-}$, 411 ± 52 pA) (Fig. 8C middle left).

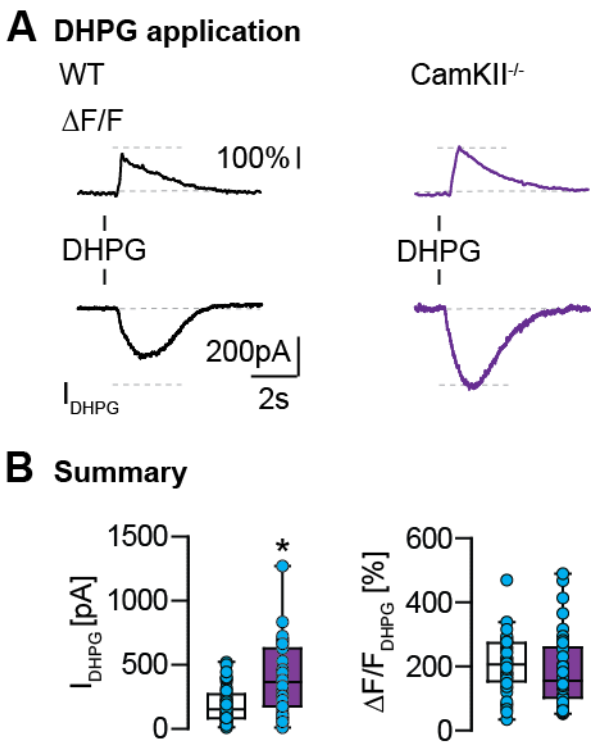

Figure 8 Increased TRPC3-mediated currents in the absence of CaMKII. A *OGB-1 fluorescence (top traces) and whole-cell voltage-clamp recordings (bottom traces) with local DHPG application to PNs in wild type (left) and CaMKII$^{-/-}$ (right) mice.* ***B*** *Summary: Box plot (Tukey's) of the IDHPG amplitudes (left) and cytosolic calcium transients (right). Blue dots indicate individual values.*

The same experiment was repeated in the presence of 30 µM CPA in the ACSF. As was demonstrated earlier (Henning unpublished, Fig. 3), under these conditions the DHPG-evoked calcium transient is entirely mediated by calcium influx through TRPC3 (Fig. 9A). This CPA-resistant calcium transient is significantly larger in CaMKII$^{-/-}$ mice than in wild type mice (Fig. 9B).This result was unexpected since Shi et al. reported that CaMKII facilitates the activation of TRPC6 (Shi et al. 2013). Based on my results in CaMKII-deficient mice I can exclude this possibility for TRPC3 in PNs.

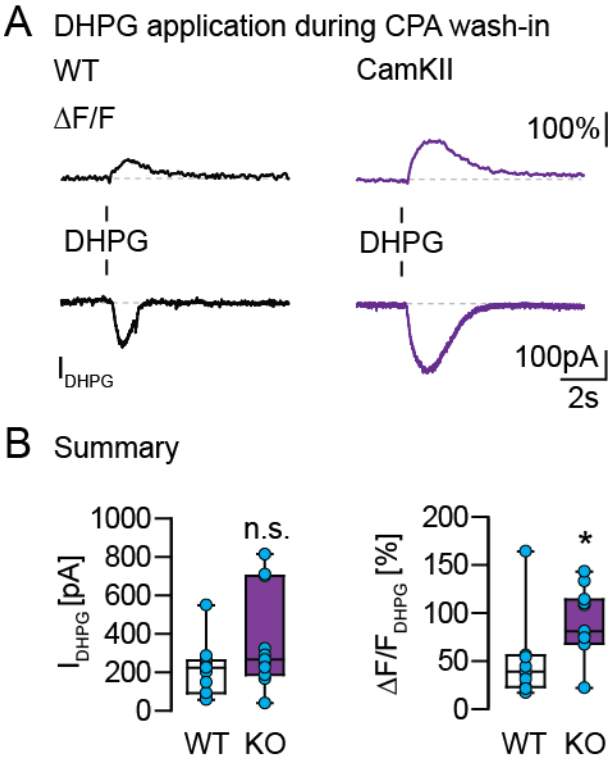

Figure 9 Increased calcium influx through TRPC3 in CaMKII$^{-/-}$ mice. A *Analogous experiment as in Figure 8A, with a bath solution containing 30 µM CPA for WT (left) and CamKII$^{-/-}$ (right).* ***B*** *Box plot (Tukey's) of IDHPG amplitudes (left) and amplitudes of cytosolic calcium transients (right). Blue dots indicate individual values.*

3.2.2 DAG and the activation of TRPC3

Similarly to TRPC6 (Clapham et al. 2001) in non-excitable cells TRPC3 has been shown to be activated by diacylglycerol (DAG), the second product of PLCβ besides IP_3 (Hofmann et al. 1999). PLCβ has been reported to be modulated by calcium (Lomasney et al. 1999) and presents itself as a likely candidate for the calcium binding TRPC3-regulator. However, the use of blockade of PLCβ with U73122 resulted in negative findings regarding TRPC3 activation (Henning, unpublished) However, a positive control that the antagonist was effective is lacking for these experiments, and therefore no clear conclusion can be drawn from them.

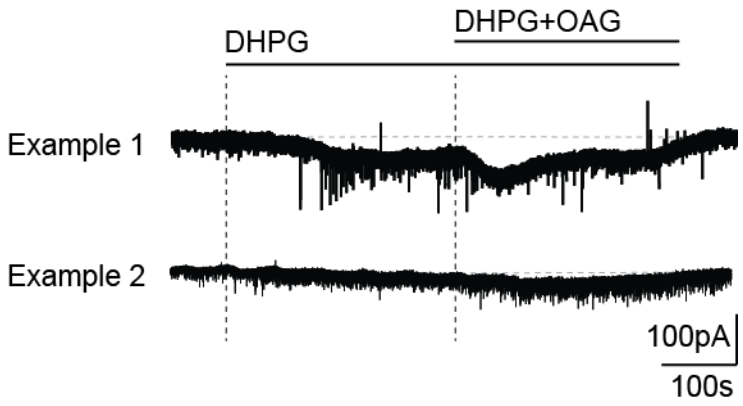

Figure 10 OAG increases DHPG-evoked inward currents in a subset of PNs. *Example traces of a cell showing a response to bath-applied OAG during (top, 'Example 1) and a cell that seemingly lacks responsiveness (bottom, 'Example 2').*

Equally impossible to interpret have been earlier experiments in our lab in which the widely used analog of DAG, oleyl-acetyl-glycerol (OAG) was applied to whole-cell patch-clamped PNs in cerebellar slices in order to examine its possible role as a direct agonist of the channel. This did not result in the activation of OAG-evoked inward currents mediated by TRPC3 (Henning, unpublished). Because OAG application itself did not yield any responses (data not shown) we decided to apply a close to subthreshold concentration of DHPG before and during the OAG application. The experiment started with perfusing the slice with a DHPG-containing solution (30µM) while membrane currents were being recorded continuously in the voltage clamp mode. In 2/5 cells a small inward current developed similarly as reported earlier for bath application of 50 µM 1-Amino-1,3-dicarboxycyclopentane (ACPD), another mGluR agonist (Hartmann et al. 2004). After 5 min OAG (100 µM) was added to the bath. In some cells this led to a further increase in the inward current that reached its maximum after approximately 1 min. following the perfusion with OAG. However, this only observed in 3/5 cells (Fig. 10). To reveal any subtle TPRC3 activating effects of OAG, we recorded current-voltage relationships (I-V curves) in control ACSF and with OAG (100 µM) in the bath. Again, the IV curves show little or no tendency towards more inward directed currents, meaning that we cannot

conclude that OAG positively modulates TRPC3 activation in our experimental setting (data not shown). Because OAG is very lipophilic it is probably captured near the surface of the slice and not reaching the dendrite of the patch-clamped PN that is most often located 20-50 µm beneath the surface of the slice. Recently, a photoactivatable DAG-analog (PhoDAG) has been developed by the group of Dirk Trauner (Frank et al. 2016). In this molecule DAG is covalently bound to a chemical group in the *trans* configuration in which it is inactive. Upon UV light illumination, the PhoDAG molecule switches from *trans* to *cis* configuration, rendering it biologically active. Green light switches the PhoDAG back in a non-active state. PhoDAG has been shown to be effective in cell cultures in a sub second time range (Frank et al. 2016; Leinders-Zufall et al. 2018). In addition, it has been shown that PhoDAG can activate TRPC channels in brain slices (Leinders-Zufall et al. 2018). With this tool we tried again to assess the role of DAG for the activation of TRPC3 in PNs. More precisely, we used a variant called PhoDAG-11. We first verified that UV light illumination did not harm nor caused current artifacts during whole cell patched wild type PCs (Fig. 11A, control). Furthermore, perfusing our vehicle solution, consisting of 0.1% DMSO, did not give rise to any unspecific currents (Fig. 11A, vehicle). We proceeded by washing in PhoDAG into the bathing solution. Upon a 5 second, local dendritic illumination with UV light we did not observe a TRPC3-mediated inward current. Instead, a long-lasting outward current was measured (Fig. 11A, PhoDAG). Under the concrete ionic conditions in the experiment and the holding potential of -70 mV of the voltage clamp this outward current must be carried by potassium ions. DAG is known to be an activator of the protein kinase C (PKC) which phosphorylates potassium channels in PNs thereby activating them (Widmer et al. 2003). The resulting outward currents might disguise TRPC3-mediated inward currents. We therefore attempted to block these PKC-mediated outward currents. Indeed, pre-incubating cerebellar slices with calphostin (1 µM), a PKC antagonist, for at least 5 min, blocked UV light-induced activation of outward currents in the presence of PhoDAG into the bath (Vehicle 6 ± 3 pA, PhoDAG 50 ± 9 pA, PhoDAG+Calphostin 3 ± 3 pA). However, no inward currents following UV-

illumination were observed (Fig.11A, calphostin). Others have used PhoDAG-1 (and -3) too, and reliably induced fast activation of TRPC2 and TRPC6 in heterologous systems, native cells and fresh mammalian tissue slices (Leinders-Zufall et al. 2018). The calphostin-experiment described above demonstrates the successful transformation of PhoDAG and its functionality as an agonist. Therefore it is justified to put up the hypothesis that TRPC3 in PNs is not activated by DAG.

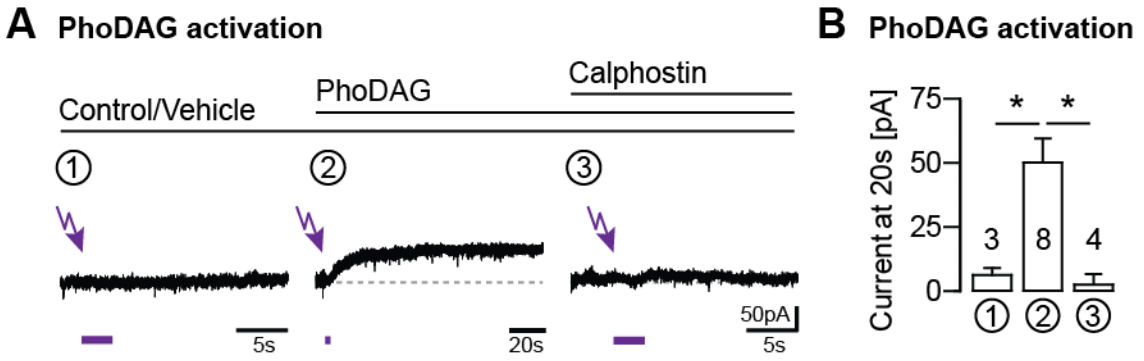

Figure 11 PhoDAG induces a PKC-dependent outward current in PN***s. A*** *Somatic whole-cell recording from a* PN *with local UV light illumination (purple arrow and bar) onto a dendritic region of a PN in the presence of vehicle (1; 0.1% DMSO), PhoDAG (2), and both PhoDAG and calphostin (3).* ***B*** *Summary: mean membrane current amplitudes after illumination.*

3.2.3 Depolarization induced TRPC3 reactivation is not mediated by TRPC3 insertion into the PM

Indu Ambudkar and her coworkers (Singh et al. 2004) showed that TRPC3 in HEK-293 cells is trafficked intracellularly in vesicles and inserted into the PM via calcium-regulated exocytosis. In PNs, exocytosis could be the process that requires calcium influx and that ensures the presence of TRPC3 in the PM. Indeed, this hypothesis could well explain our observations in STIM1^{pko} PNs, where under resting conditions the cells are not responsive to DHPG, but following calcium influx, TRPC3 is reactivated downstream of mGluR1. We wanted to know whether TRPC3 is absent from the PM during resting conditions

in STIM1^{PKO} PNs. To answer this question we relied on a newly developed direct agonist for TRPC3 and TRPC6, GSK1702934A (Doleschal et al. 2015). GSK1702934A (10 µM) was locally puff-applied (10 s) to dendrites of whole-cell patched PNs in acute cerebellar slices. As can be seen in Fig. 12A, both in STIM1^{PKO} and WT PNs, pressure ejection of GSK1702934A reliably caused a transient inward current that after decrease of local GSK concentration declined back to baseline. No significant difference between WT and STIM1^{PKO} mice was observed (mean inward current amplitudes, WT 195 ± 32 pA, Orai2$^{-/-}$ 416 ± 83 pA, STIM1^{PKO} 334 ± 71 pA, Fig. 12B, summary). Most importantly, we did not see GSK-evoked inward currents in any of the six cells tested in TRPC3$^{-/-}$ mice, which proves the specificity of the agonist (Fig. 12C, grey overlaid trace). In short, we conclude that the insertion of TPRC3 into the PM of PNs is not impaired in the absence of STIM1 in STIM1PKO mice and its reactivation does not rely on insertion of the channel into the PM.

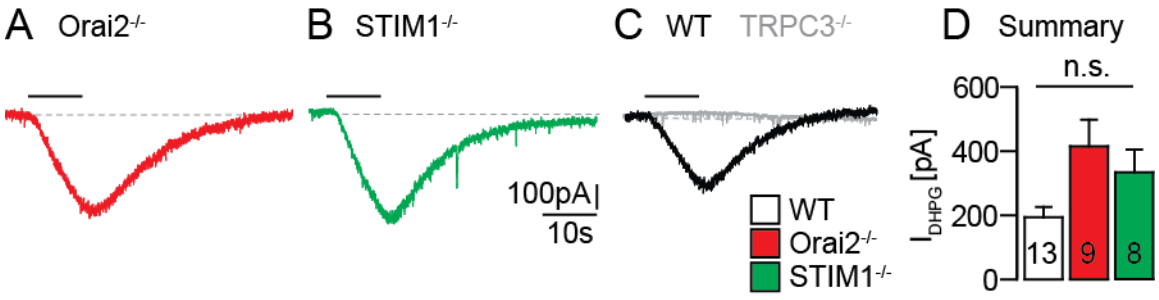

Figure 12 GSK1702934A evokes TRPC3-mediated inward currents. A, B, C *Whole-cell voltage-clamp recordings with GSK puff application on PN dendrites (black horizontal bar) in Orai2$^{-/-}$, STIM1$^{-/-}$ and WT mice, respectively. In* ***C****, the wild type trace is overlaid with an analogous experiment in TRPC3$^{-/-}$ mice (grey).* ***D*** *Summary: Mean I_{GSK} amplitudes in the genotypes indicated in* ***A****,* ***B*** *and* ***C.***

3.2.4 Summary

The experiments described in this section disproved some initial hypotheses regarding the molecular mechanism of TRPC3 activation in cerebellar PNs. In short we have shown that:

- It is unlikely that CaMKII plays a decisive role in TRPC3 activation or during calcium influx-mediated modulation of the channel;
- The DAG analog OAG as a rule did not activate TRPC3 or modulated the current though the channel in our experimental setting;
- Despite successful photoactivation of PhoDAG in fresh cerebellar tissue TRPC3 in PNs was not activated;
- Calcium influx-dependent TRPC3 insertion into the membrane as an underlying mechanism for the cellular phenotype observed in $STIM1^{PKO}$ mice can be excluded.

In the following section we decided to present data that places TPRC3 in PNs in a larger molecular network with a decisive role of one of the binding partners of STIM1, namely Orai2, for its activation.

3.3 The role of Orai2 downstream of mGluR1 in *PN* s

3.3.1 Orais are expressed in WT cerebellar PNs

Considering the role of cytosolic calcium and STIM1 in mGluR1 signaling, I continued my search of activation mechanisms of TRPC3 in cerebellar *PN*s. Gating of TRPC3 in cerebellar PNs at resting membrane potential depends on G_q activation (Hartmann et al. 2004), the presence of STIM1 and the nanodomain coupling of an unknown component (not TRPC3 itself) to a calcium-permeable channel in the PM. Orai channels are calcium-permeable channels in the PM that are opened by their interaction with STIM1 at resting membrane potential (Kraft 2015). Orai channels therefore were the most likely candidates to provide the necessary calcium needed to make the gating of TRPC3 possible. All three Orai subunits were shown to be expressed in *PN*s (Wissenbach et al. 2007). Based on mRNA levels observed during single cell qPCR measurements, Orai2 is the most abundant subtype in cerebellar *PN*s, followed by Orai1 and Orai3 (Hartmann et al. 2014). In order to demonstrate the presence of Orai proteins in *PN*s, I co-immunostained cerebellar slices for each of the three different Orai subtypes together with the *PN* marker calbindin (Fig. 13). Orai1 and 2 were detected in *PN* somata and faintly in proximal dendrites, a finding that mirrors the location of STIM1 in *PN*s (Hartmann et al. 2014).

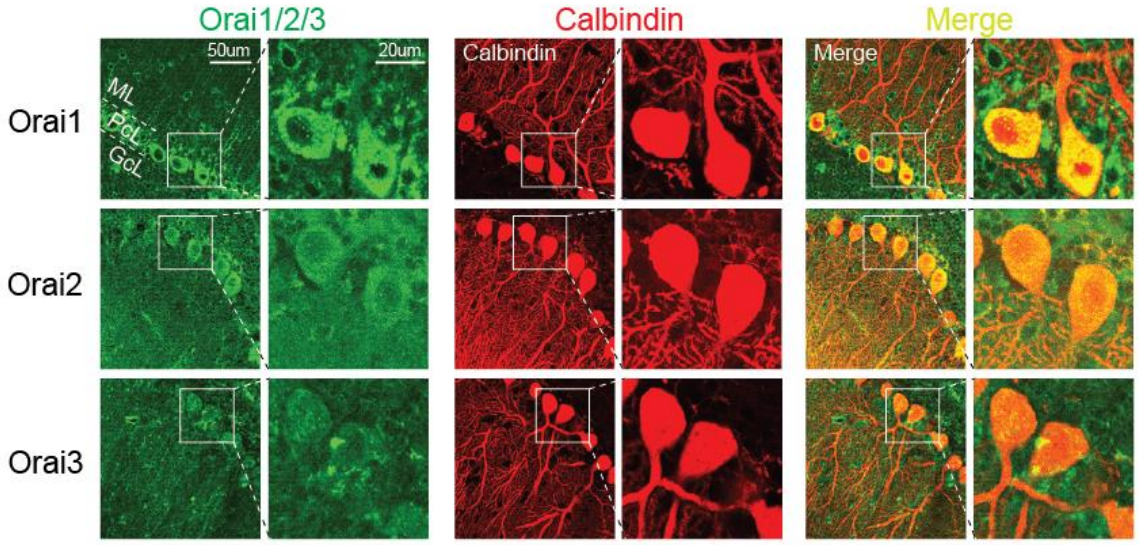

Figure 13 Presence of Orai1 and Orai2 protein in cerebellar PNs. Fixated *cerebellar slices from WT mice were stained against Orais (green) in the following order: Orai1 (top), Orai2 (middle) and Orai3 (bottom) and co-stained with the* PN *marker calbindin-D28k (red). The overlaid result is presented under 'Merge' (right) were a yellow color indicates an overlap of anti-Orai and anti-calbindin antibody binding.*

3.3.2 Orai2 is absent in Orai2$^{-/-}$ animals and does not affect dendritic morphology

To study the role of Orais on a functional level we made use of recently generated transgenic Orai2 knockout (Orai2$^{-/-}$) mice (Vaeth et al. 2017). Immunostaining against Orai2 of the cerebellar vermis tissue demonstrates that Orai2 is no longer expressed in the Orai2$^{-/-}$ mice (Fig.14). Tissue qPCR analysis of cerebellar vermis of these mice shows they virtually lack mRNA copies of *Orai2* (WT 0.01 ± 0.003, Orai2$^{-/-}$ 1.2 * 10^{-4} ± 8.4 * 10^{-5})) (Fig. 14). The mRNA copy numbers of *Stim1* and *Stim2* were not altered in the absence of Orai2. This was conformed with immunostaining for Orais in cerebellar slices from Orai2$^{-/-}$ mice, that showed intact expression of Orai1 and Orai3 and complete absence of Orai2 (Fig. 15).

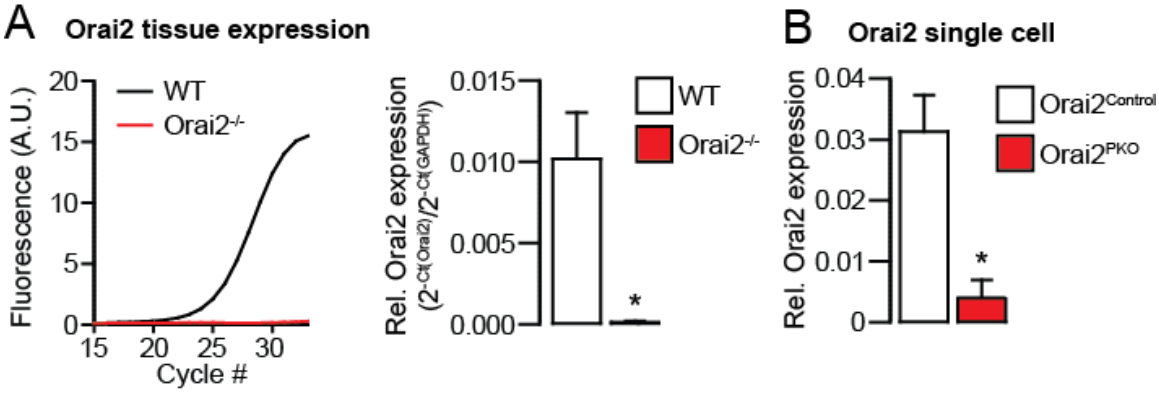

Figure 14 Tissue expression of Orai2 in WT and Orai2$^{-/-}$ animals. *Left: SYBR green fluorescence reporting the amplification of Orai2 cDNA during qPCR for WT (black) and Orai2 (red) tissue from the cerebellar vermis. Right: Summary of relative Orai2 expression normalized against the expression of the housekeeping gene gapdh (N=4 for both genotypes).*

Additionally, I analyzed the general morphology of *PN*s in wild type and Orai2$^{-/-}$ mice. PNs in acute cerebellar slices were whole-cell patch-clamped and filled with a biocytin-containing intracellular solution. Cells remained intact after gentle retrieval of the patch pipette. Slices were then fixated and streptavidin staining was performed as described in the methods section. Confocal microscope imaging stained cerebellar slices showed that deletion of Orai2 does not cause abnormal development (Fig. 16). Although it should be noted that *PN* morphology varies widely between different cells, the mean size of somata (Soma size: WT 407 ± 25 mm^2, Orai2$^{-/-}$ 392 ± 32 mm^2) as well as dendritic tree size (Dendrite size: WT 30303 ± 1745 mm^2, Orai2$^{-/-}$ 26279 ± 1406 mm^2) are similar for the two genotypes.

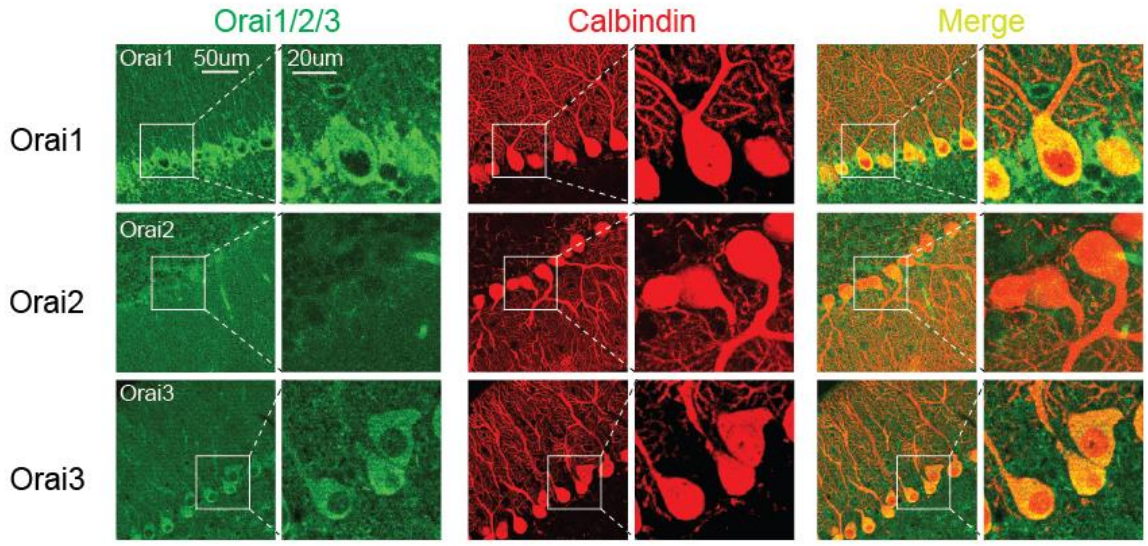

Figure 15 Orai2 protein is not detected in Orai2$^{-/-}$ mice. *Confocal images demonstrating immunostaining against Orai1 (top), Orai2 (middle) and Orai3 (bottom) on fixated cerebellar slices from an Orai2$^{-/-}$ mouse. Slices from Orai2$^{-/-}$ mice were stained against Orais (green) in the following order: and co-stained with the PN marker calbindin-D28k (red). 'Merge' represents an overlay of stainings (right) were a yellow color indicates overlap of the anti-Orai and anti-calbindin-D28k antibody binding.*

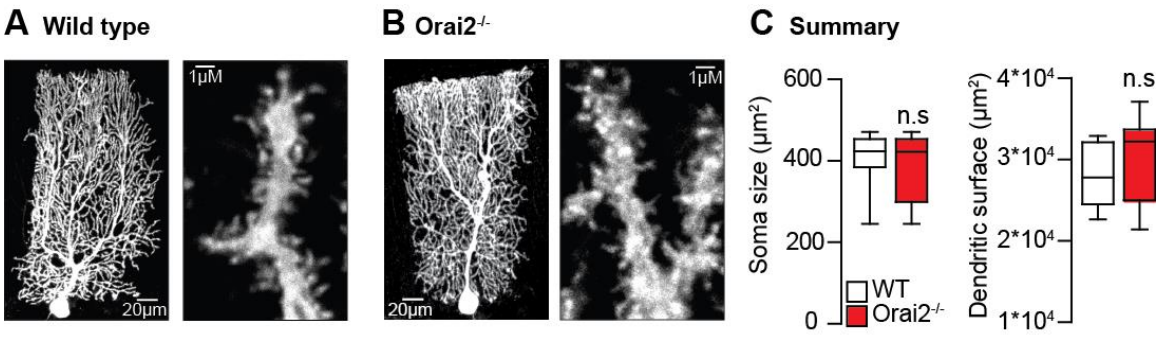

Figure 16 Deletion of Orai2 does not affect PN morphology. A *Representative overview (left) and high magnification (right) confocal images of PNs in fixated cerebellar slices from wild type mice, filled with biocytin and stained with conjugated streptavidin. Full cell images are the result of maximum intensity projections of image stacks consisting of 20-30 images captured with a slice thickness of 1 µm.* ***B*** *Analogous images to A in an Orai2$^{-/-}$ mouse.* ***C*** *Summary: Mean soma size (left) and dendritic surface area (right) in both genotypes (wild type: n = 8; Orai2$^{-/-}$: n = 8).*

3.3.3 Mice lacking Orai2 display cerebellum-mediated motor impairment

Impairments in mGluR1 signaling in PNs have been associated with motor impairment numerous times in multiple mouse models (Hartmann et al. 2011). Similar behavioral defects were found in STIM1 knockout mice (Hartmann et al. 2014) and therefore a possible motor impairment for Orai2$^{-/-}$ mice was predicted. I tested Orai2$^{-/-}$ mice on an elevated beam test, which was shown to detect even subtle PN specific impairments (Hartmann et al. 2008; Hartmann et al. 2014). I quantified the performance by the amount of paw slips the mice made while walking over a cylindrical, thin plastic beam to a ‘safe’ platform with their native house (Fig. 17A). Orai2$^{-/-}$ mice scored worse in this case compared to wild type mice (Fig.17B, *left*) by slipping with their hind paws in 13 ± 2 % of their steps (11 vs 9 mice for WT and Orai2$^{-/-}$ mice, respectively), compared to WT 5 ± 1 %, % of slips in wild type mice. Both genotypes showed equal motivation to walk over the beam and made comparable amounts of steps (WT 84 ± 5, Orai2$^{-/-}$ 68 ± 9) (Fig.17B, right). The second behavior test I performed was the Rotarod test. Wild type and Orai2$^{-/-}$ mice were placed on a rotating cylindrical beam which linearly increased its rotating speed. The test was repeated twice daily for four days; the

results are depicted in Fig 17C. Over all trails, the wild type mice were able to stay on the rotating beam longer, and over time improve their performance more compared to Orai2$^{-/-}$ mice. The final run duration was significantly different between both genotypes (73 ± 8 s for wild type and 32 ± 7 s for Orai2$^{-/-}$ mice). These data indicate that Orai2$^{-/-}$ mice suffer from motor impairments.

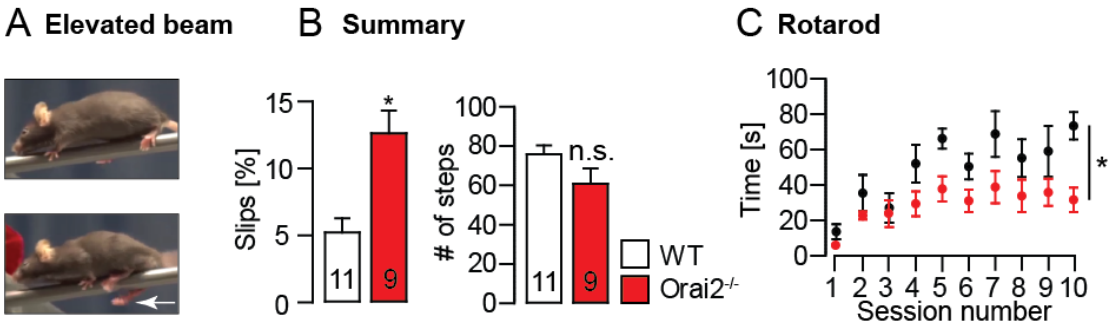

Figure 17 Orai2$^{-/-}$ mice demonstrate impaired motor coordination. A *Demonstration of the experimental setting for the elevated beam test. The share of steps with paw slips (bottom, white arrow) was used as a measure of performance.* ***B*** *Summary: mean percentage of steps with paw slips (left) and mean number of steps (right) for all mice tested.* ***C*** *Mean time spent on the accelerating rotarod for wild type (black) and Orai2$^{-/-}$ (red) mice for all ten consecutive sessions.*

It should be noted that these experiments were performed on general knockout mice, which means that Orai2 is lacking in every cell of the body. As motor behavior depends not only on the cerebellum but also other parts of the brain, and in addition also on muscles, bones and other factors, there could be confounding factors in the general Orai2 knockout mice. We therefore repeated the elevated beam test in PN specific Orai2 knockout (Orai2^{PKO}). These mice are the result of breeding a mouse line (Orai2^{Control}) in which part of the Orai2 gene is homozygously flanked with loxP sites (floxed) to a mouse line that expresses the Cre recombinase under the control of the promoter that drives the expression of the GluD2 receptor (Yamasaki et al. 2011) that is found almost exclusively in PNs. Because *orai2* is only deleted in PNs, any motor impairment seen in these mice can be attributed to defects in the PNs. The results of the elevated beam test with these mice are shown in Fig. 18. As expected, he difference between

Orai2^{PKO} and Orai2^{Control} mice was smaller compared to difference between Orai2$^{-/-}$ and wild type mice. However, Orai2^{PKO} mice (7 ± 1% of slips) score significantly worse than the control mice (4 ± 1 % of slips). These results were again independent of weight or gender (data not shown) and both groups showed equal motivation to walk the beam (Fig. 18, *right*). In conclusion, deletion of *Orai2* exclusively in PNs causes motor impairment and thus, Orai2 has an important role for cerebellar function.

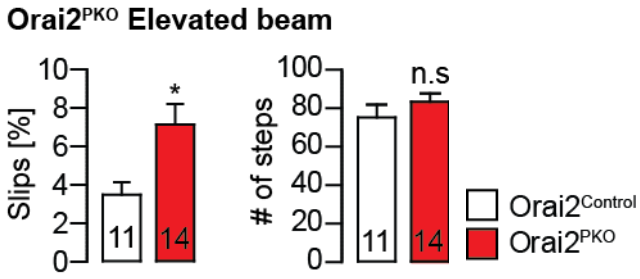

Figure 18 Orai2^{PKO} mice show impaired performance on an elevated beam. *Summary of the relative amount of paw slips (left) and number of steps (right) during an elevated beam test for Orai2^{Control} ('Control', white) and Orai2^{PKO} (red) mice.*

3.3.4 Normal fast synaptic signaling in PNs lacking Orai2

Next, I sought to characterize synaptic signaling in Orai2$^{-/-}$ and wild type mice. I started out with fast AMPAR-dependent synaptic transmission that is activated with single shock stimulation of parallel fibers. It was previously reported that motor problems can be caused by impaired fast synaptic signaling as well as mGluR1-mediated signaling (Ito, 2006). Paired-pulse facilitation (PPF) is a characteristic short term plasticity mechanism observed at parallel fiber synapses of PNs (Atluri et al. 1996). Paired activation of parallel fibers with different interpulse intervals (IPI) resulted in increased secondary responses. The enhancement of the second EPSC amplitudes declined with increasing length of IPIs and typically disappears at IPI > 500 ms (Fig. 19). The result shows that there is neither a difference between Orai2$^{-/-}$, Orai2^{PKO} and Orai2^{Control} mice. In short, Orai2-deficient mice show the same PPF as wild type mice. Because PPF at parallel fiber synapses is presynaptically regulated (Atluri et al. 1996) this is a strong indication for normal presynaptic glutamate release from parallel fiber terminals.

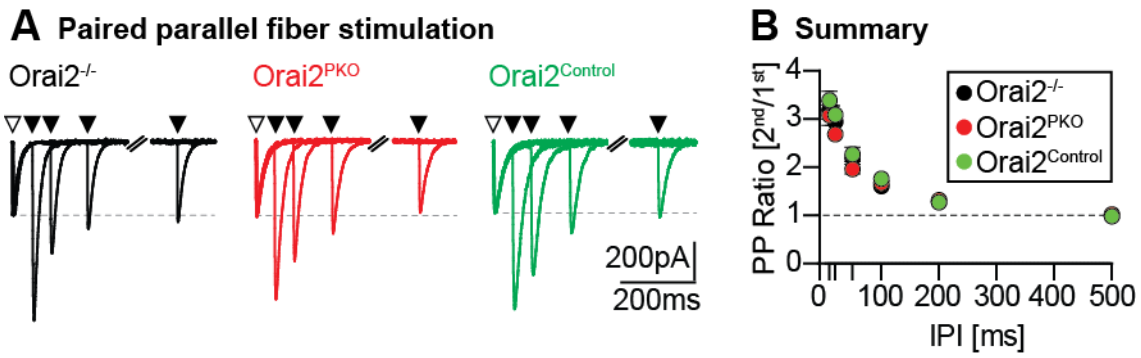

Figure 19 Normal paired pulse facilitation in Orai2-deficient mice. A *Whole-cell voltage-clamp recordings from PNs in cerebellar slices from Orai2$^{-/-}$ (black), Orai2^{PKO} (red) and Orai2^{Control} (green) mice. Overlay of five consecutive measurements with pairwise parallel fiber stimulation with increasing ISIs (white triangle = 1st EPSC, black = 2nd EPSC) in.* ***B*** *Summary: Mean paired-pulse ratio resulting from the division of the amplitudes of both EPSCs (2nd EPSC/1st EPSC) plotted against the IPI.*

I also looked into synaptic signaling between CF and PNs. Activation of the CF results in an all or nothing, large EPSC. The postsynaptic action potential that follows CF activation is called ‘complex spike’ because the initial spike is followed by a number of smaller spikelets. Activation of the CF opens voltage gated calcium channels, and can be seen by a fast calcium transient in almost the whole dendritic tree (Otsu et al. 2014). Indeed, stimulating the CF in cerebellar slices of wild type and Orai2$^{-/-}$ mice resulted in a calcium transient measured in the proximal part of the dendritic tree (Fig. 20A). Moreover, this calcium transient was accompanied with a typical complex spike, with its characteristic initial spike and following spikelets. The summary shows that both the dendritic calcium transient (WT 92 ± 10 %, KO 111 ± 17 %) as well as the number of spikelets (WT 4 ± 0.3, Orai2KO 4 ± 0.2) during the complex spike are unaltered in Orai2$^{-/-}$ mice compared to wild type mice. Taken together, this data suggests that the synaptic connection between CF to PN is intact despite the absence of Orai2.

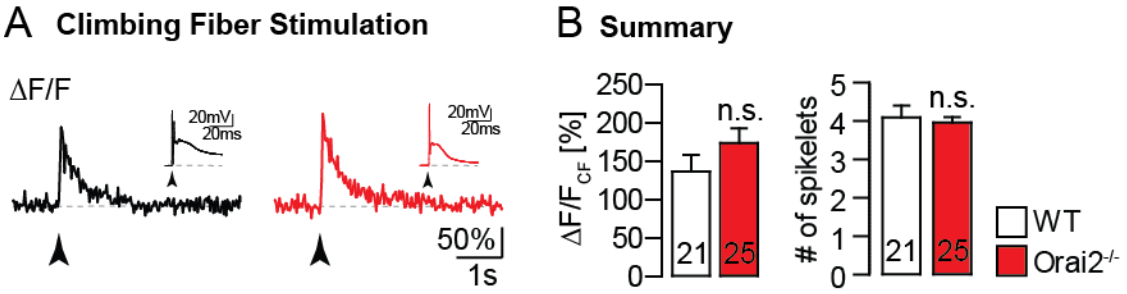

Figure 20 Climbing fiber responses are not altered in the absence of Orai2. ***A*** *OGB-1 fluorescence recording with the response to the activation of the CF. Inset: Whole-cell current-clamp recordings of complex spikes resulting from CF activation.* ***B*** *Summary: Mean calcium transient amplitudes (left) and mean number of spikelets in the complex spikes (right).*

3.3.5 Slow, mGluR1-mediated synaptic signaling is impaired in Orai2$^{-/-}$ mice

The experiment demonstrated in Fig. 20 shows data resulting from single parallel fiber stimulations. Parallel fibers *in vivo* can fire up to 1 kHz (Ito, 2006) and repetitive parallel fiber stimulation has been shown to activate postsynaptic mGluR1. I adopted a protocol from Hartmann (Hartmann et al. 2008) which allows me to see both fast and slow synaptic parallel fiber responses. More specifically, I used 200 Hz parallel fiber stimulation and partial AMRA receptor blockage with 10µM CNQX in the ACSF. The results are shown in Fig. 21. As described earlier (Hartmann et al. 2014) Repetitive (5 pulses) parallel fiber stimulation at 200Hz resulted in biphasic EPSCs. The AMPA receptor-mediated fast EPSCs (fEPSCs) are easily recognized by their immediate onset following stimulation. Opposed to this immediate response, the mGluR1-mediated slow EPSC (sEPSC) follows with a delay and peaks only a few hundred milliseconds after stimulation, indicating their dependence on intracellular pathways (Batchelor et al. 1993). In the confocal fluorescence recording performed concomitantly with 10V stimulation strength, delayed mGluR1-mediated calcium transient was observed (Fig. 21A, top) (144 ± 23 %). Stimulating the same dendritic region with 25V resulted in a pronounced slow current through TRPC3 (Fig. 21A, bottom) 114 ± 31 pA). In Orai2$^{-/-}$ mice however, the same stimulation resulted in strongly altered synaptic signals. No mGluR1-mediated calcium transient was observed

following repetitive 10V stimulation (Fig. 21B, top) (Orai2$^{-/-}$ 3 ± 3 %). In addition, the mGluR1-mediated sEPSC was fully abolished (Fig. 21B, bottom) (4 ± 4 pA). The quantification shows a highly significant difference between the TRPC3-mediated sEPSC in wild type and Orai2$^{-/-}$ mice (Fig. 21C, left). In Orai2^{PKO} and Orai2^{Control} mice, the same observation was made (Fig. 21D, E, F). In conclusion, these results indicate a strong defect in parallel fiber to PN synaptic signaling in the absence of Orai2, which appears to be highly specific to the mGluR1 pathway.

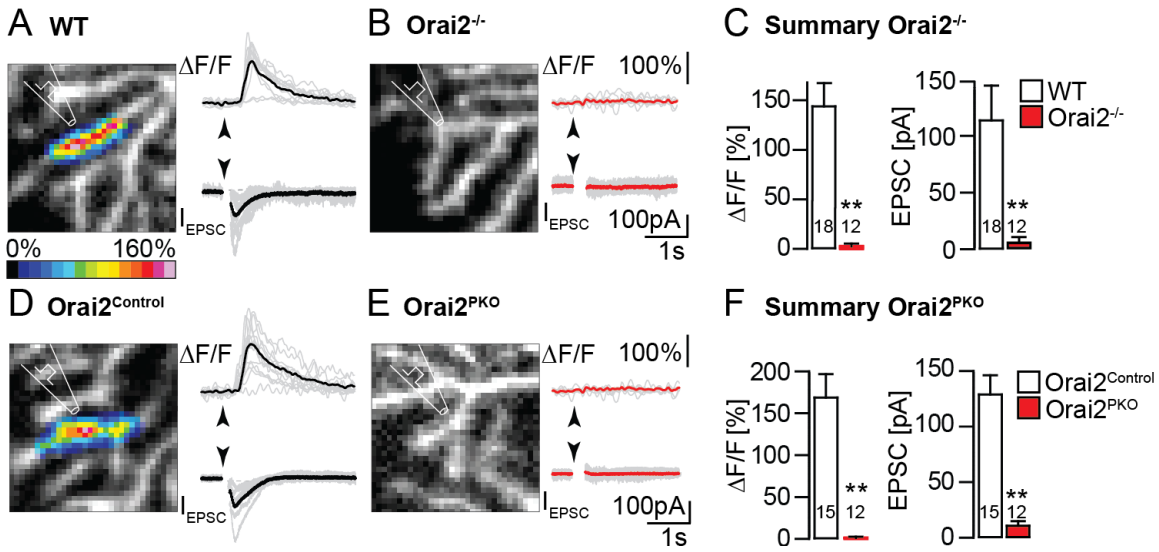

Figure 21 Synaptic signaling in the absence of Orai2. A *False color representation of a local calcium transient following 200Hz parallel fiber stimulation (5 pulses) in a dendritic subregion (left), time course of the Calcium signal (right, top) and the somatically recorded sEPSC (right, bottom). Time point of stimulation is indicated by the black arrowhead. Grey traces indicate individual trials; an averaged trace is overlaid in black.* ***B, D, E*** *Analogous experiments as in* ***A*** *for Orai2$^{-/-}$, Orai2^{Control} and Orai2^{PKO} respectively.* ***C*** *Bar graphs showing mean amplitudes of calcium transients following stimulation (left) and mean sEPSC amplitudes (right) for WT (white) and Orai2$^{-/-}$ (red) mice.* ***F*** *Analogous summary as in C for Orai2^{Control} (white) and Orai2^{PKO} (red) mice.*

In order to further investigate postsynaptic calcium signaling in PNs and its dependence of Orai channels I performed similar experiments in acute cerebellar slices with reduced frequency of repetitive parallel fiber stimulation. Earlier work

in our group had demonstrated that stimulating parallel fibers five times at a frequency of 50 Hz in the dendrites of PNs biphasic calcium signals consisting of an AMPAR and an mGluR1-mediated component (Takechi et al. 1998). Averaging multiple such responses from different cells resulted in a calcium trace with a sharp initial peak and a broad second peak. The first maximum reflects VGCC-mediated calcium influx while the second is IP_3-mediated calcium release from stores (Takechi et al. 1998; Fig. 22A, left). There is no contribution of calcium influx through TRPC3 because it is not activated under these conditions. On the other hand, Orai2$^{-/-}$ cells only show a sharp, AMPAR-mediated initial peak (Fig. 22A, middle). An overlay of the two reveals a noticeable difference in the time course of the signal (Fig. 22A, right) which can be quantified by measuring the half width of the calcium transient in both genotypes. The result indicates a significantly longer half width value for the wild type samples (0.30 ± 0.02 s) in comparison to Orai2$^{-/-}$ mice (0.20 ± 0.02), which can be explained by the lack of mGluR1-mediated calcium signal in the Orai2$^{-/-}$ (Fig. 22B). This experiment confirms the observation that Orai2$^{-/-}$ mice lack both types of mGluR1-mediated responses; the TRPC3-mediated sEPSC and the IP_3R-mediated calcium release from ER calcium stores.

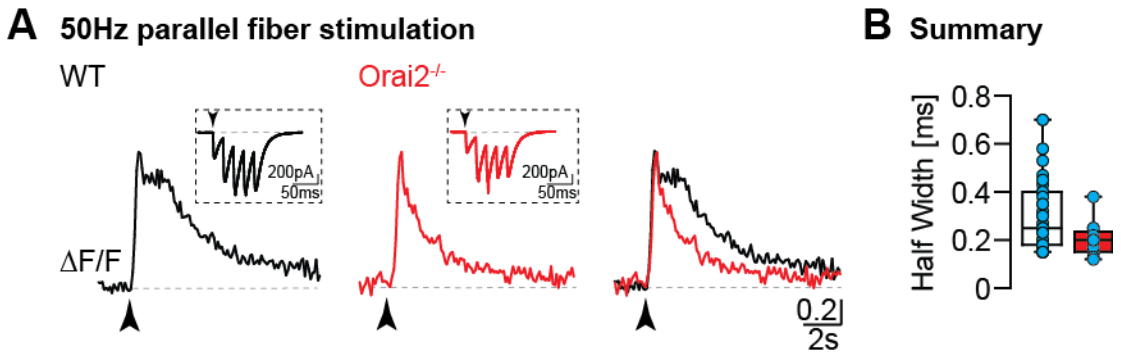

Figure 22 Lack of Orai2 causes failure to release calcium from stores. A *OGB-1 fluorescence recordings with 50Hz parallel fiber stimulation in WT (left), Orai2 (middle) and both traces superimposed (right). The inset shows the EPSC measured in the whole-cell voltage-clamp mode; the black triangle indicates the time point of the first stimulation.* ***B*** *Summary shows half widths of the calcium transients demonstrated in* ***A*** *for WT (white) and Orai2$^{-/-}$ (red). Blue dots correspond to individual measurements.*

3.3.6 Orai2$^{-/-}$ mice lack responsiveness to mGluR1 agonist application

The previous results indicated an obvious defect in parallel fiber-PN synaptic signaling in the absence of Orai2. This finding does not only appear to be specific for Orai2, but also for signaling downstream of mGluR1, since fast synaptic signaling remained unaltered. To substantiate this initial finding I chose to activate mGluR1 in PNs directly using local application of the group I mGluR-specific agonist (S)-3,5 Dihydroxyphenylglycine (DHPG). DHPG typically evokes both types of mGluR1-dependent response in PNs: IP_3-mediated calcium release and an inward current mediated by TRPC3 (Hartmann 2008). Puff application (200µM, 50 ms, 10 psi) of DHPG on PNs' dendrites in wild type mice produced such responses (Fig. 23A, left). The presence of this response proved to be highly reliable across different dendritic areas, slices and mice (Fig. 23B, top). Orai2$^{-/-}$ mice on the other hand mostly demonstrated unresponsiveness to the activation of mGluR1 (Fig. 23A, right). More precisely, only 25% of all dendritic regions tested showed responsiveness to DHPG (Fig. 23B, bottom). Comparison of mGluR1 responses between wild type and Orai2$^{-/-}$ mice showed highly significant differences for both calcium transients (mean ΔF/F amplitudes 147 ± 17 % in the wild type and 21 ± 6% in Orai2$^{-/-}$ mice) and TRPC3 activation (mean sEPSC amplitudes 129 ± 32pA in the wild type and 15 ± 4 pA in Orai2$^{-/-}$ mice) (Fig. 23C). However, this comparison was made by including both responsive and non-responsive Orai2$^{-/-}$ samples in one group. I defined responsiveness as a positive value for both calcium signal and inward current following DHPG application. When only responsive dendritic regions are included into the analysis it shows highly reduced mGluR-mediated responses in Orai2$^{-/-}$ mice (mean ΔF/F amplitudes WT 147 ± 17 %, Orai2$^{-/-}$ 21 ± 6 %, mean sEPSC amplitudes WT 129 ± 32 pA, Orai2$^{-/-}$ 15 ± 4 pA) (Fig. 23D). A similar experiment in Orai2^{PKO} mice shows similar results (Fig. 24A, B) albeit in a smaller sized sampling group. We did not observe any responses following mGluR1 activation in Orai2^{PKO} mice, while Orai2^{Control} mice showed normal mGluR1 activation (Calcium: Orai2^{Control} 263 ± 18 %, Orai2^{PKO} 1 ± 0.2 %; Current: Orai2^{Control} 237 ± 41 pA, Orai2^{PKO} 6 ± 5 pA). This nonetheless shows on the one hand the specificity of impairments of

the Orai2 deletion in PNs, and on the other hand the validity of both mouse models.

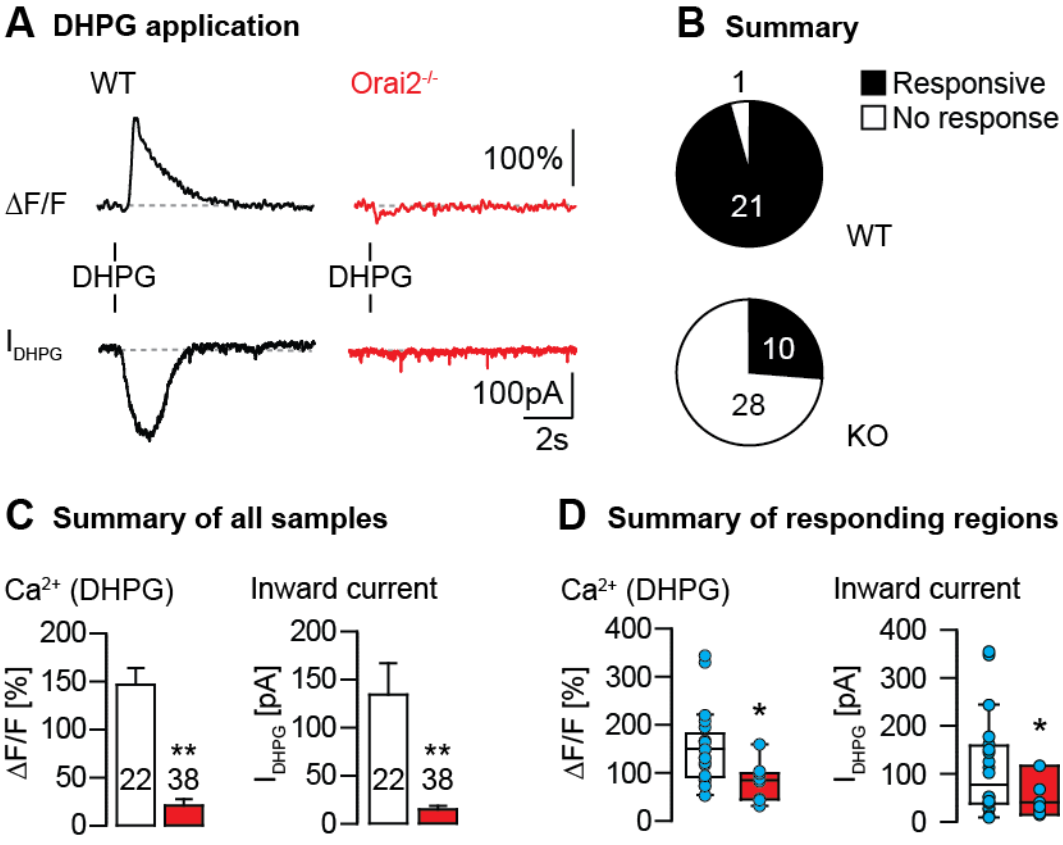

Figure 23 Disrupted mGluR1-dependent synaptic signaling in the absence of Orai2. ***A*** *Cytosolic calcium measurement (top) and whole cell current recording (bottom) during DHPG application in WT mice (left) and Orai2$^{-/-}$ mice (right).* ***B*** *Quantification of the share of DHPG responsive cells in WT (top) and Orai2$^{-/-}$ ('KO', bottom).* ***C*** *Summary: Mean calcium transient amplitudes (left) and maximum I_{DHPG} amplitudes (right) from all experiments as demonstrated in* ***A****.* ***D*** *Analogous summary for the responsive cells only (black areas in the pie chart of* ***B)****.*

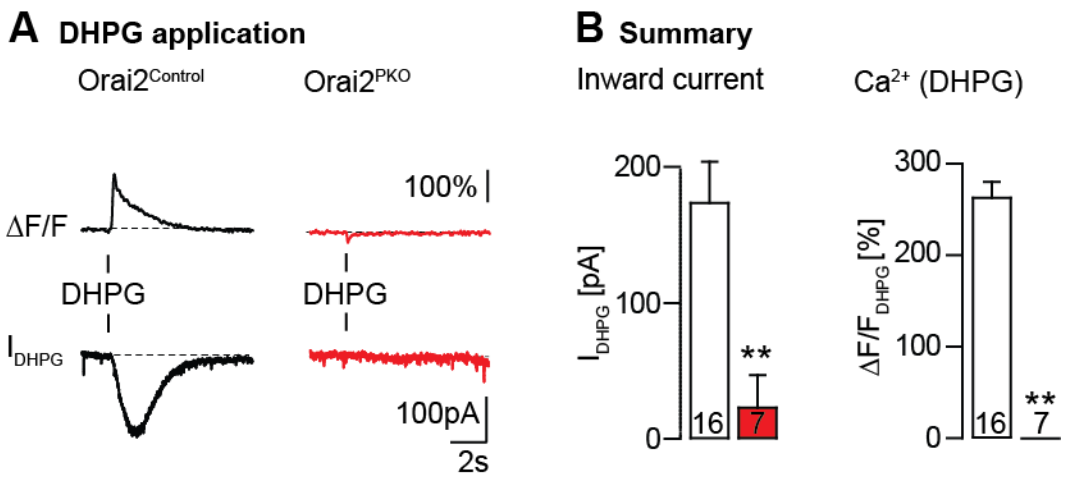

Figure 24 Disrupted mGluR1-dependent responses to agonist stimulation in Orai2^{PKO} mice A *Cytosolic calcium measurement (top) and whole-cell current recording (bottom) during DHPG application in Orai2^{Control} mice (left) and Orai2^{PKO} mice (right).* ***B*** *Summary: Mean I_{DHPG} amplitudes (left) and mean amplitudes of DHPG-evoked calcium transients (right) and for all experiments as in* ***A.***

3.3.7 Orai2$^{-/-}$ PNs show empty calcium stores under resting conditions

I decided to first take a look into the abolished calcium release signal in Orai2$^{-/-}$ mice following mGluR1 activation. There are two possible hypotheses that could explain this impairment. First, the ER calcium store could simply be empty due to abolished calcium homeostasis as was shown in the absence of Orais in other cell types (Robers-Thomson et al. 2010). Second, the deletion of Orai2 possibly causes a more fundamental defect in the signaling cascade downstream of mGluR1. In order to test the first hypothesis, I photo-uncaged NPE-caged IP_3 in wild type and Orai2$^{-/-}$ mice in an experimental setting analogous to those shown in Fig. 7 (Fig. 25). UV illumination was seen in the calcium trace as an out-of-range brightness artifact, and successful uncaging of IP_3 was demonstrated by a following calcium transient (Fig. 25A). IP_3 uncaging reliably evoked calcium release from ER calcium stores in wild type mice (Fig. 25, *left*), but not in Orai2$^{-/-}$ mice (Fig. 25A, B *right*). The summary of the experiments (Fig. 25, bar graphs) shows a highly significant decrease of calcium release in Orai2$^{-/-}$ mice (mean ΔF/F Orai2^{Control} 198 ± 31 %, Orai2^{PKO} 21 ± 11 %). To exclude the possibility that

deletion of Orai2 influenced the sensitivity of IP_3 receptors to IP_3, I challenged the store using an alternative method, namely via caffeine. Caffeine activates ryanodine receptors, which reportedly share a common calcium pool with IP_3 receptors (Khodakhah et al. 1997). The results are demonstrated in Fig. 25C. The summary indicates a large reduction in caffeine-induced calcium release, but different to the IP_3 sensitive calcium pool, there is still a residual response in about 30% of the dendritic regions tested. The mean amplitudes of caffeine-induced calcium transients were $Orai2^{Control}$ 38 ± 5 %, $Orai2^{PKO}$ 12 ± 2 %). (Fig. 25D, left) The remaining calcium signal could be explained by a number of reasons, for instance nonspecific effects of caffeine, or a unique calcium store that can only be addressed with caffeine. For the moment I decided to leave these questions unaddressed. Overall, based on these findings, I concluded that the calcium response to mGluR1 activation in $Orai2^{-/-}$ mice is absent because the ER store is empty.

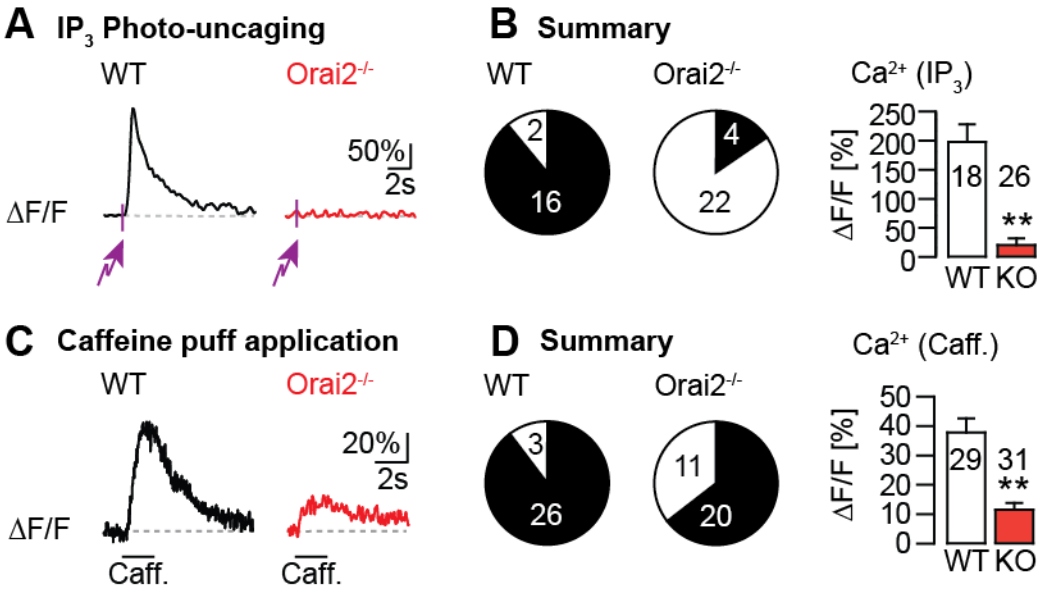

Figure 25 ER Calcium stores are empty at rest in Orai2$^{-/-}$ mice A *OGB-1 fluorescence recordings from dendritic regions with UV-flash uncaging of IP_3 (10ms, purple arrow) in WT (left, black) and Orai2$^{-/-}$ (right, red) mice.* ***B*** *Relative amount of responding cells (black) and unresponsive cells (white) from* ***A*** *for WT (left) and Orai2$^{-/-}$ (middle) and mean IP_3-evoked Calcium transient amplitudes (right).* ***C*** *Fluorescence recordings with caffeine puff application (80 mM, 2s) in WT (left, black) and Orai2$^{-/-}$ (right, red) mice.* ***D*** *Relative amount of responding cells (black) and unresponsive cells (white) from* ***A*** *for WT (left) and Orai2$^{-/-}$ (middle) and mean caffeine-induced Calcium transient amplitudes (right).*

3.3.8 mGluR1 responsiveness in Orai2$^{-/-}$ mice can be restored by transient depolarization

To test if signaling downstream of mGluR1 in Orai2$^{-/-}$ mice is still intact, I resorted to a method introduced by Hartmann (Hartmann et. al. 2014). This paper described a very similar impairment of calcium release signals and TRPC3 activation downstream of mGluR1 in STIM1 knockout mice. This defect however could be overcome by briefly depolarizing PNs, a finding that I was able to confirm in the same mouse line (Fig. 1). Because of the involvement of Orai2 and STIM1 in the same processes of calcium homeostasis and TRPC3 activability I applied the same method in Orai2$^{-/-}$ mice. The result is depicted in Fig. 26. As shown before, Orai2$^{-/-}$ PNs are unresponsive to DHPG under control conditions (Fig. 26A, left). I then applied a one-second depolarization to 0 mV and again applied DHPG (Fig. 26A, right) after 5s. The results demonstrated a division of cells into two groups; one showed a measurable inward current and elevation of cytosolic calcium in response to local DHPG application following depolarization, an effect from here on referred to as ‘rescue’ (Fig. 26A, right). The other group showed no rescue, e.g. an absence of an mGluR1-mediated response even after transient depolarization. Overall, about half of the cells tested showed rescue of the mGluR1 response (N=8) while the other half remained unresponsive (N=6) (Fig. 26B, left). This grouping does not include five cells because they showed either only a calcium or a current response. Taking all data into account, the depolarization induced overall a significant augmentation of the mGluR1 response (Fig. 26B, right) (Calcium Control 30 ± 13 %, dep 235 ± 30 %; Current

23 ± 10 pA, dep 90 ± 21 pA). Next, I repeated these experiments in Orai2^{PKO} mice. Control animals showed normal wild type-like mGluR1-dependent calcium and current responses (Fig. 28A). As expected, Orai2^{PKO} animals showed no DHPG responses under control conditions similarly to Orai2$^{-/-}$ mice (Fig. 28B, left, ①). The summary reveals a dramatic shows a dramatic reduction of overall responsiveness to DHPG activation (calcium Orai2^{Control} 263 ± 18 %, Orai2^{PKO} 0.2 ± 0.1 %; current Orai2^{Control} 237 ± 41 pA, Orai2^{PKO} 6 ± 6 pA (Fig. 28B) following deletion of Orai2 specifically in PNs. Indeed, all control neurons showed responsiveness to mGluR1 activation (Fig. 28C) while none of the Orai2PKO neurons did. I proceeded to depolarize Orai2^{PKO} neurons and tested mGluR1 responsiveness. Out of seven cells tested, 5 showed responsiveness to DHPG application after transient depolarization (Fig. 28C, right)

These findings suggest a number of things. First, depolarizing the cell restores the mGluR1-mediated calcium release from stores. The most likely underlying mechanism is that the store is charged via calcium influx of voltage gated calcium channels (Garaschuk et al. 1997). This means that the deletion of Orai2 does not lead to fundamental impairments in the mGluR1-IP_3 pathway, but rather suggests the calcium stores to be empty at resting membrane potentials. Secondly, activation of voltage gated calcium channels can restore the activation of TRPC3. This suggests that TRPC3 is not activated by direct interaction with Orai2, but by a calcium-dependent factor located near to orai2 channels. This conclusion is in line with the findings in PNs lacking STIM1.

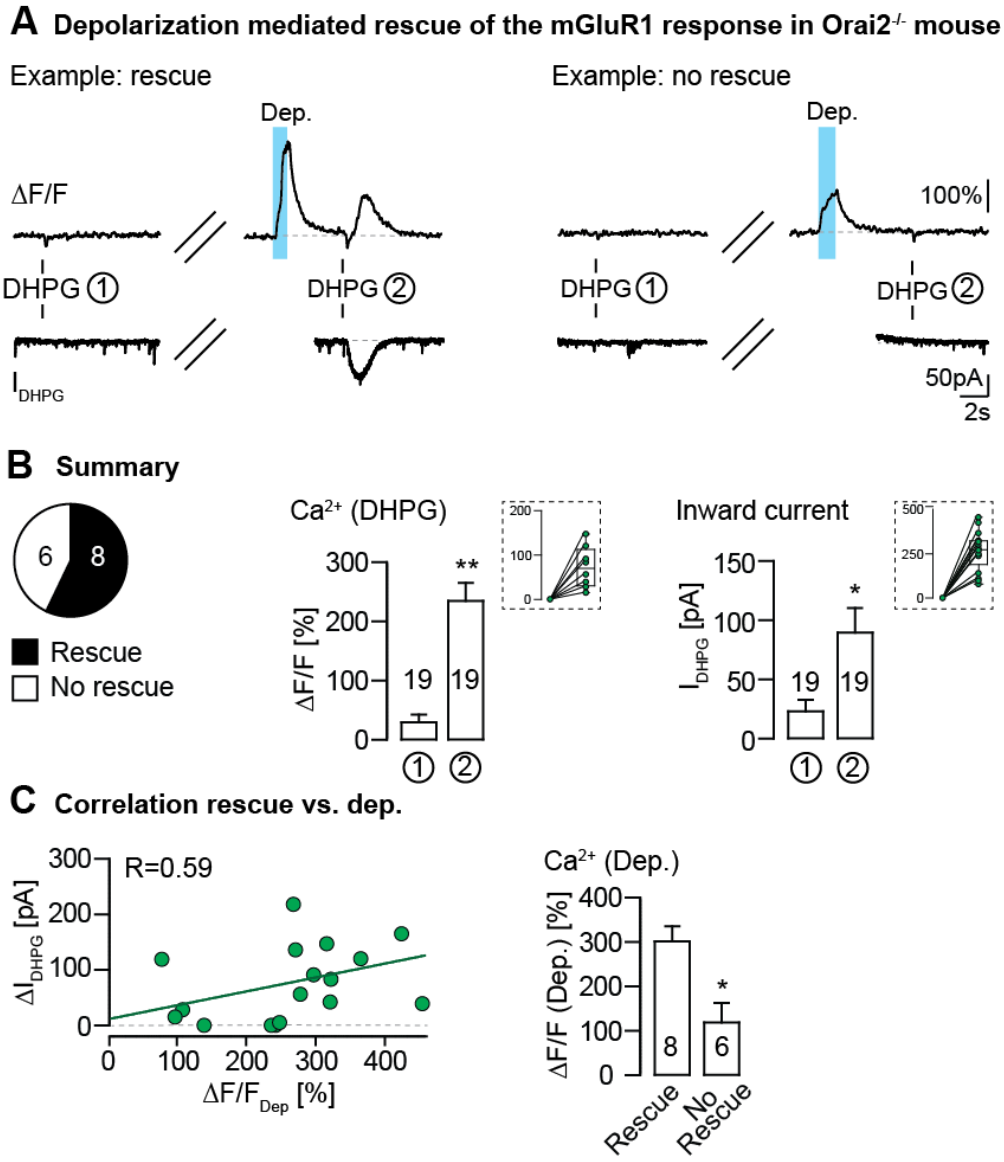

Figure 26 Depolarization-induced calcium influx rescues mGluR1 responses in Orai2$^{-/-}$ mice. A *DHPG application before and after transient depolarization. Depicted are representative traces of OGB-1 fluorescence fluorescence (top) and whole-cell voltage-clamp recordings (bottom) of a cell in which mGluR1-responses were rescued following the depolarization (left) and of a cell in which that did not happen (right).* ***B*** *Left Share of cell with and without rescue of the mGluR1-responsiveness. Middle DHPG-induced calcium response before and after depolarization; inset shows individual samples. Right DHPG-induced inward current before and after depolarization; inset shows individual samples.* ***C*** *Left Plot of the difference between I_{DHPG} amlitudes before and after depolarization (ΔI_{DHPG}) and the depolarization-induced calcium signal ($\Delta F/F_{Dep}$); green line indicates linear regression analysis. Right Depolarization-induced calcium signal for cells with and without rescue of mGluR1-dependent responses* ***B*** *(left).*

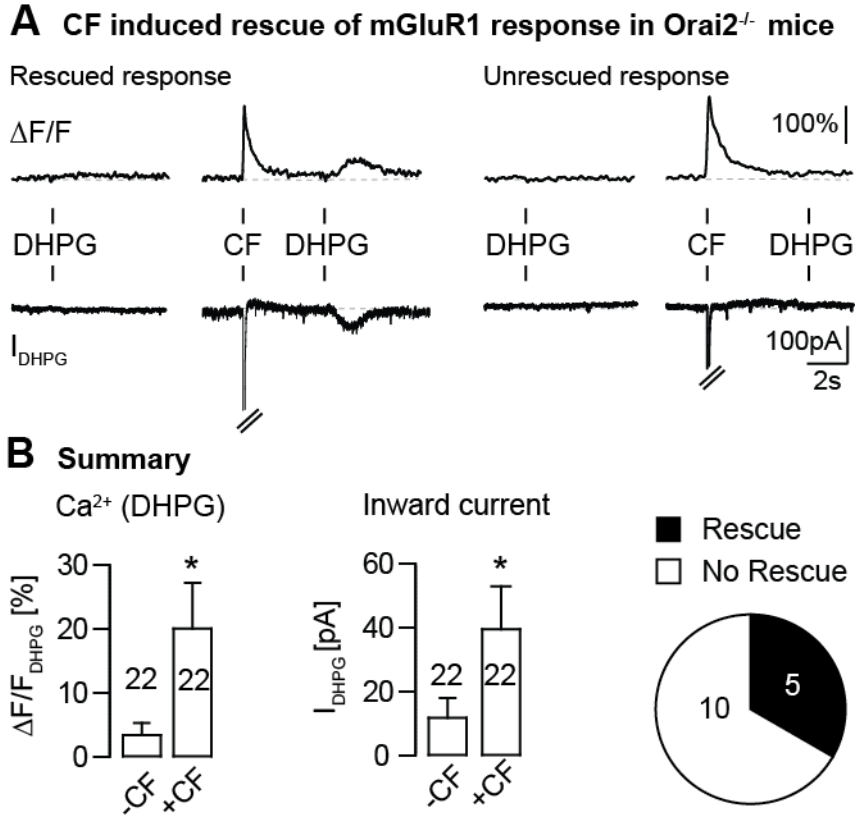

Figure 27 Climbing fiber activation rescues mGluR1-dependent responses in a subset of PNs. A *Example figures of a typical mGluR1 agonist application experiment where a subset of responses were successfully rescued after CF stimulation (left) and another subset did not (right).* ***B*** *Summary of the experiment shown in A. Left: calcium transients before (-CF) and after (+CF) CF stimulation. Middle: DHPG-mediated current before (-CF) and after (+CF) CF stimulation. Right: amount of 'rescued' responses.*

Interestingly, activation of the CF 5s prior to DHPG application can successfully rescue mGluR1 responses (Fig. 27A, left). As with the depolarization experiments demonstrated in Fig. 26 only a subset of cells was rescued while others were not (Fig. 27A, right). Meta-analysis shows a significant increase in both modalities of the mGluR1 response (Fig. 27B). The mean calcium signal amplitude increased from (control 3.4 ± 1.9 %, CF 20 ± 7 %), and mean I_{DHPG} amplitudes rose from (control 12 ± 6 pA, 40 ± 13 pA). The fraction of cells that are rescued is slightly lower compared to the depolarization-mediated rescue, namely about 30%. With this experiment I demonstrated it is possible to

reestablish mGluR1 responses in PNs with an Orai2 deletion via depolarization-induced calcium influx, as is the case with PNs lacking STIM1.

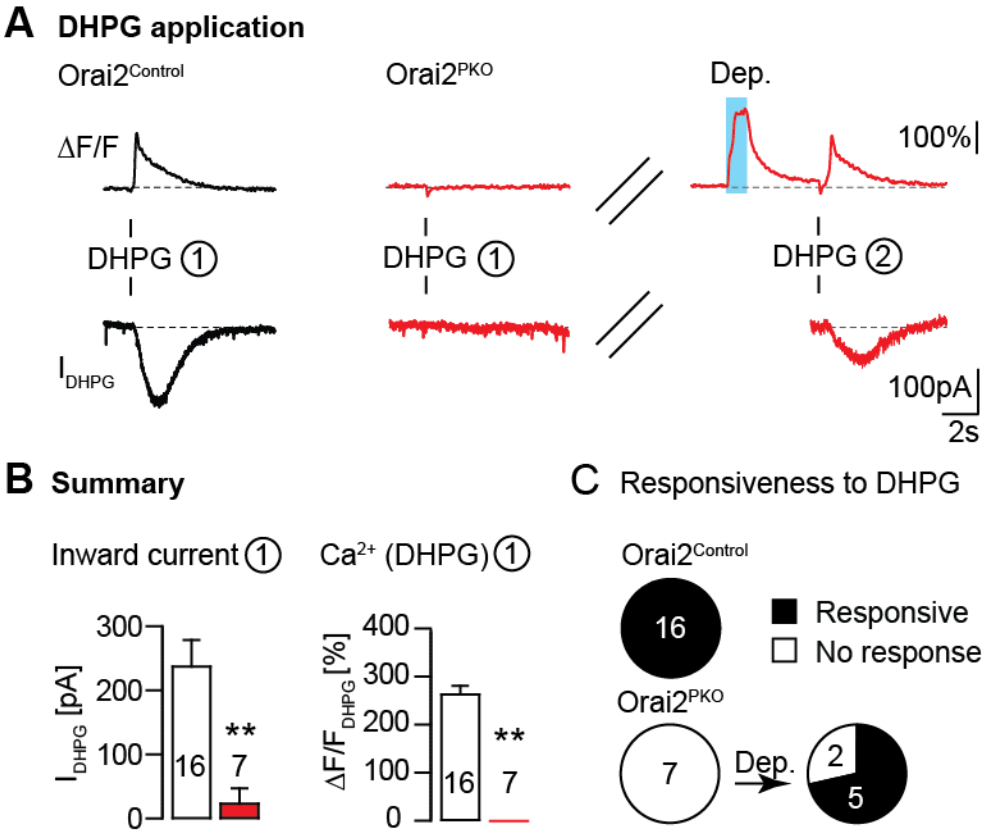

Figure 28 Depolarization-induced calcium influx rescues can return mGluR1-dependent signaling in PNs in Orai2^{PKO} mice. A *Left: OGB-1 fluorescence traces with DHPG application that is followed by a calcium transient (top) and an inward current in the somatic whole-cell recording (bottom) in a Orai2^{Control} mice. Middle: Analogous experiment in a Orai2^{PKO} mouse in which absent mGluR1-dependent responses were reactivated following a depolarization for 1s to 0 mV* ***B*** *Summary of the inward current (left) and calcium transients (right) following DHPG application.* ***C*** *Left: amount of DHPG responsive (black) and unresponsive (white) cells. Middle: DHPG responsiveness before and (right) after depolarization.*

3.3.9 Enhancing calcium influx during transient depolarization leads to improved return of mGluR1 responsiveness

Apart from the apparent similarity between the Orai2$^{-/-}$ and STIM1^{PKO} mice with regard to the effects of the mutations on mGluR1-dependent synaptic signaling, I observed a noticeable difference. During my experiments, the mGluR1 responses in STIM1^{PKO} mice were reliably rescued in almost all cells, an observation that was shared by colleagues that did similar experiments (personal communication, data not shown). As I demonstrated in Fig. 27 only half of the cells showed a successful restoration of mGluR1 responses following depolarization. I hypothesized about a possible underlying reason of this discrepancy. The experiments in STIM1^{PKO} mice described in 4.1.3 demonstrated a role for cytosolic calcium for the activation of TRPC3 (Fig.4).

When I compared the amplitudes of the calcium transients resulting from depolarization-evoked calcium influx upon transient depolarization between the group of cells in which TRPC3-mediated currents were rescued and those in which they were not I found a large difference (Fig. 27C). The amplitudes of the depolarization-induced calcium transients were plotted against the amplitude differences of TRPC3-mediated currents (before and after depolarization, ΔI_{DHPG}). The result is illustrated in Fig. 27C. It appears that a cell with a large calcium influx shows a larger TRPC3 current compared to cells with relatively small calcium transient. Statistical analysis shows a highly significant correlation between calcium influx and TRPC3 activation (Rescue: 301 ± 35 %, no Rescue 119 ± 44 %). This observation strengthens the finding that TRPC3 activation depends on cytosolic calcium. Overall, I conclude that TRPC3 gating depends on Orai2 during resting membrane potential; cellular activity in the form of membrane depolarizing events and consecutive calcium influx can overcome the absence of Orai2.

On the basis of the strong correlation between the depolarization-induced increase in the cytosolic calcium concentration and the extent of TRPC3-mediated current “rescue” it was predicted that by increasing the depolarization-

evoked calcium transients eventually in all PNs in Orai2$^{-/-}$ mice TRPC3 activation should be possible. To prove this assumption, I repeated the experiment from Fig. 26 in normal ACSF and in the presence of 4-Aminopyridine (4AP). 4AP is an antagonist of Kv1 potassium channels. Because of the increase in membrane resistance, the space clamp problem is reduced, increasing voltage control in more distal dendrites. Washing in 4AP often led to unwanted spontaneous activity; to counteract this, I simultaneously washed in 10 µM CNXQ. In control ACSF, in some cells the TRPC3-mediated was rescued, while in others TRPC3 remained unresponsive, in line with the previous experiment (Fig. 30A, Control; as example, a cell with a small rescue effect is shown). After waiting 10 minutes, DHPG responses went back to baseline (Fig. 29A, 4AP, ①); 4AP application did not alter the control responses to DHPG. With 4AP in the bath depolarization-induced calcium signals were dramatically augmented (Fig. 29B, *right*). The mean amplitude of depolarization-evoked calcium transients rose from 0 ± 0 %, (ΔF/F) in normal ACSF to 47 ± 25 %, and from 6.6 ± 4.5% in the presence of 100 mM 4AP to 177 ± 28%. It should also be noted that in the presence of 4AP the depolarization-induced calcium signals showed reduced variation across cells (Fig. 29B, *right*). The effect on mGluR1-mediated responses were equally dramatic, as all of the cells tested showed a return of the DHPG-responses so including those in which depolarization-induced rescue failed before 4AP application (Current Control① 7 ± 4 pA, ② 35 ± 12 pA; 4AP ① 14 ± 9 pA, ② 97 ± 18 pA). It seems that enhanced calcium influx increases the chance of TRPC3 reactivation, which is in line with the previous observation that TRPC3 activation depends on local cytosolic calcium levels close to the PM.

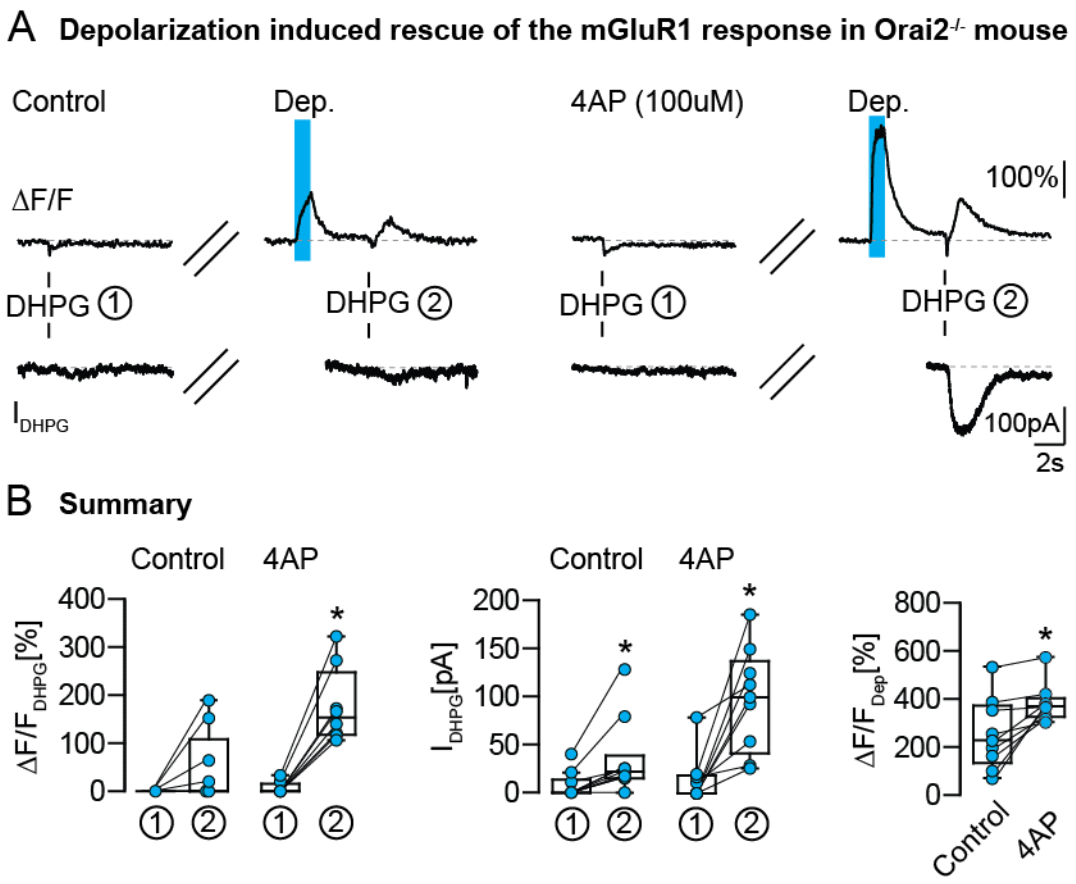

Figure 29 Reliable depolarization-dependent rescue of mGluR1-mediated signaling in Orai2-/- mice when Calcium influx is enhanced. A *DHPG application before and after depolarization (blue bar) in control ACSF (left) and in the presence of 4AP (right) in the same cell.* ***B*** *Left: Summary for the amplitudes of DHPG-evoked Calcium signals before and after depolarization under control and in the presence of 4AP Middle: Analogous summary for* I_{DHPG} *amplitudes Right: Analogous comparison of amplitudes of depolarization-induced Calcium transients in control ACSF and in the presence of 4AP.*

3.3.10 TRPC3 activation is regulated by local cytosolic calcium concentrations in STIM1$^{-/-}$ mice

This was further substantiated when analogous experiments were performed under conditions in which ER calcium stores are depleted in the presence of CPA in the extracellular solution. Again, 4AP was present in the bath, which dramatically increased the chance of TRPC3 activation rescue. The result indicates that TRPC3 can be activated even though the stores are empty, to

similar levels as without CPA (I_{DHPG} ① 19 ± 14 pA, ② 77 ± 30 pA, ③ 91 ± 22 pA. Calcium (① 11 ± 8 %, ② 49 ± 21 %,③ 41 ± 11 %) (Fig. 30A, B). Application of 4AP enhanced depolarization induced calcium signals but was unaltered by application of CPA (Dep. Ctr. 309 ± 34 %, CPA 338 ± 33 %) (Fig. 30B, right).

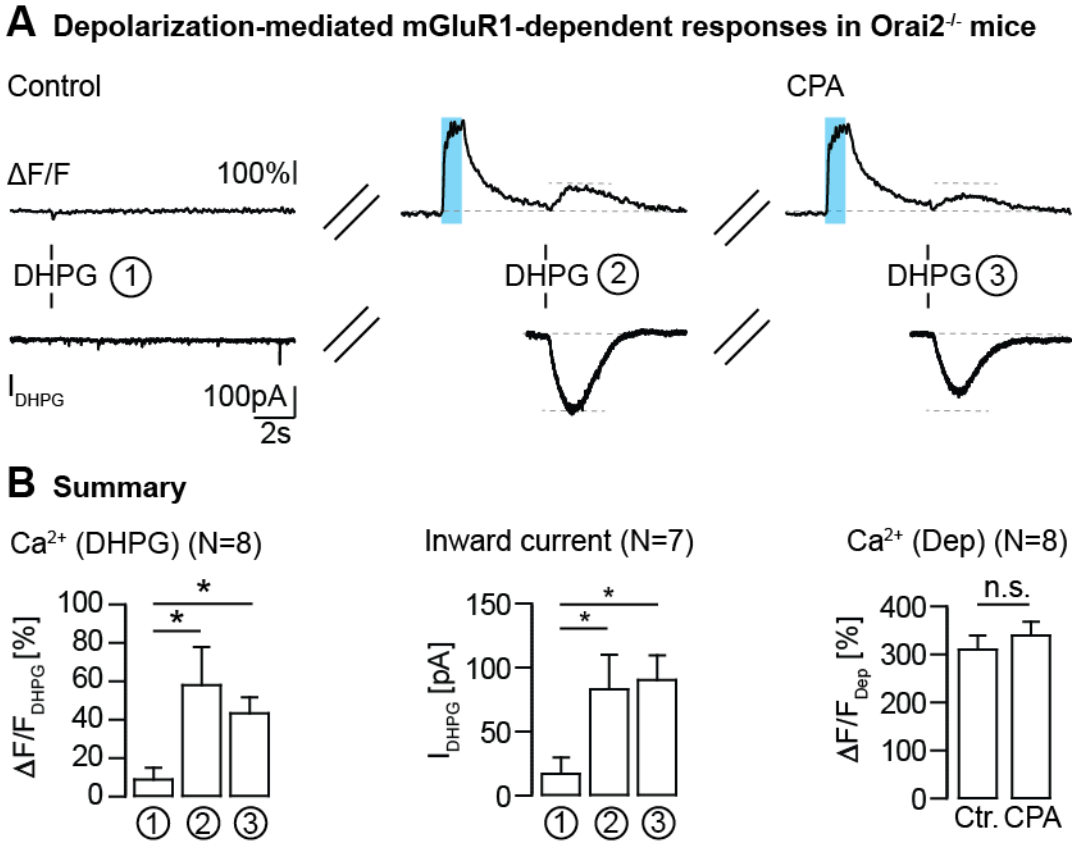

Figure 30 TRPC3 is activated under empty store conditions in Orai2$^{-/-}$ mice
A *Dendritic OGB-1 fluorescence recordings (top traces) and somatic voltage-clamp recordings (bottom traces) from a PN in an Orai2$^{-/-}$ mouse. 'Rescue' experiment in control (Control, left and middle) and in the presence of 30 µM CPA. Dotted horizontal lines indicate baseline amplitudes of responses to DHPG-application under control conditions.* ***B*** *Summary of* ***A****. Left: Mean amplitudes of calcium transients (ΔF/F) to DHPG. Middle: Mean I_{DHPG} amplitudes. Right: Comparison between the depolarization-induced calcium signal in control conditions and in the presence of CPA.*

Finally, to confirm the role of cytosolic calcium during TRPC3 activation across genotypes, I performed the rescue experiment while buffering intracellular calcium analogously to the experiments demonstrated in Fig. 32. The slow calcium buffer EGTA was unable to prevent TRPC3 reactivation, although it successfully blocked calcium influx following depolarization as well as any mGluR1-mediated calcium release from stores (Fig. 32A, top). The fast calcium buffer BAPTA however prevented any mGluR1-mediated signals, even after depolarization (Fig. 31A, bottom). The summary of the experiment shows that both EGTA and BAPTA buffered all calcium signals following DHPG application (Current CPA 90 ± 19 pA, BAPTA 0 ± 0 pA, EGTA 51 ± 16 pA; Calcium CPA 43 ± 8 %, BAPTA 0 ± 0 %, EGTA 1.5 ± 1.5 %) (Fig. 31B, top) but only fast buffering of cytosolic calcium by BAPTA could prevent TRPC3 opening in response to local DHPG-application. In short, this experiment demonstrates that TRPC3 activation depends on cytosolic calcium levels very near to the PM across genotypes.

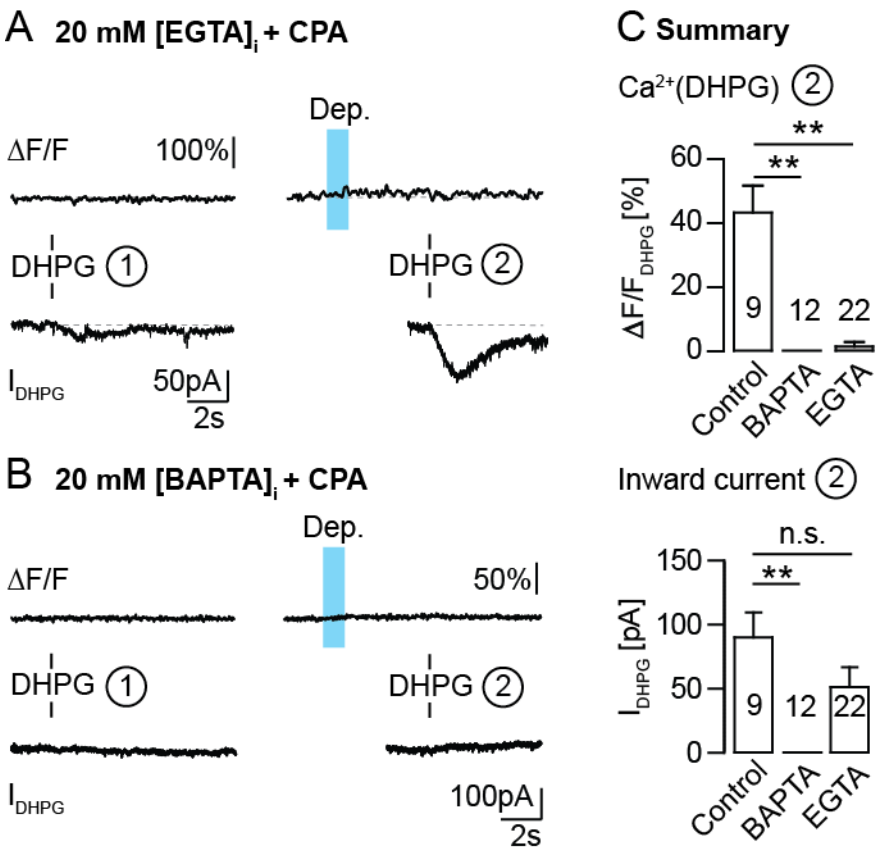

Figure 31 Fast calcium buffering prevents depolarization-induced rescue of TRPC3 activation in Orai2^{PKO} mice. A *OGB-1 fluorescence (top) and current recordings (bottom) with DHPG application before (left) and after (right) transient depolarization with 20 mM EGTA in the pipette solution intracellularly and in the extracellular presence of 30 µM CPA.* ***B*** *Analogous experiment as in A, but with 20mM BAPTA instead of EGTA.* ***C*** *Summary of the DHPG responses shown in* ***30A*** *(condition ③, CPA),* ***31A*** *(②) and* ***31B*** *(②): Mean inward current amplitudes (I_{DHPG}, top) and mean amplitudes of DHPG-evoked calcium transients ($\Delta F/F_{DHPG}$, bottom).*

3.3.11 Summary

The findings in this chapter have established a role for Orai2 in cerebellar PNs during mGluR1 signaling. More precisely, I describe:

- An ataxic phenotype for mice lacking Orai2 either ubiquitously or specifically in PNs;
- Orai2 has no role for fast synaptic signaling between PNs and presynaptic excitatory partners;
- Orai2 plays a crucial role for mGluR1-mediated postsynaptic signaling at test. Impairments in mGluR1-dependent signaling resemble STIM1 knockout mice;
- Orai2 does not directly activate TRPC3, but likely via an intermediate mechanism involving calcium influx through the PM;
- Impairment of mGluR1 caused by Orai2 deletion can be overcome by depolarization, either artificial or via physiological input.

Chapter 4 Discussion

In this thesis the properties of mGluR1-dependent TRPC3-mediated slow synaptic transmission and calcium signaling in cerebellar PNs with a special emphasis on the role of the calcium-permeable ion channel Orai2 were investigated. First, in whole-cell patch-clamp and confocal imaging experiments in acute cerebellar slices the rescue of the DHPG-evoked TRPC3-mediated inward current by calcium influx through VGCCs (Hartmann et al. 2014) was used as readout for the requirements for STIM1-independent activation of TRPC3 downstream of mGluR1. Based on tests with varying time intervals between depolarization and DHPG-application it was concluded that TRPC3 is not directly gated by binding of calcium ions to its subunits. In experiments with CPA in the external medium or calcium buffers in the pipette solution in STIM1^{pko}, wild type and TRPC3$^{-/-}$ mice it was shown that TRPC3 activability is not dependent on the filling state of the intracellular calcium stores but instead essentially requires permissive calcium levels in the cytosol. Moreover, a differential effect of the slow and fast calcium buffers EGTA and BAPTA, respectively, demonstrated that the unknown calcium-binding regulator of TRPC3 couples on a nanodomain scale to VGCCs. By activating mGluR1 in PNs both synaptically and pharmacologically in Orai2$^{-/-}$ and Orai2^{pko} mice it was established that at rest Orai2 is the STIM1-dependent calcium conductance that renders TRPC3 activable downstream of mGluR1. In addition, Orai2 also provides the calcium influx that is necessary for ER calcium store replenishment in cerebellar PNs. Orai2^{pko} mice exhibit an impaired motor coordination proving the importance of Orai2 expression in PNs for cerebellar function. This work thus identifies Orai2 as the calcium-permeable channel responsible for calcium homeostasis in PNs. Furthermore, this is the first demonstration of the crucial involvement of an Orai channel in glutamatergic synaptic transmission and thus extends the importance of Orai channels beyond the field of calcium store regulation.

4.1 Proposed model of mGluR1 signaling in PNs

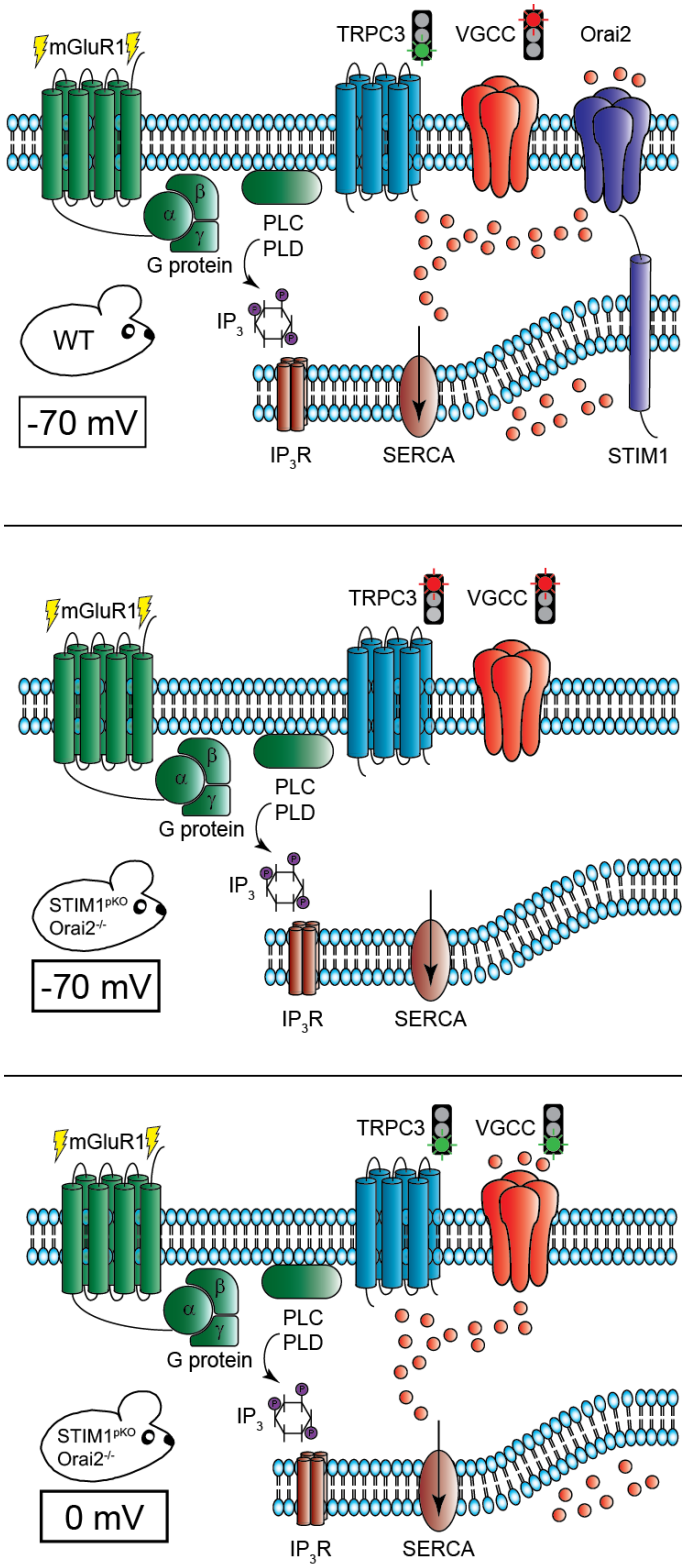

Figure 32 Schematic representation of synaptic signaling downstream of mGluR1 in cerebellar PNs ***Top*** *In the wild type at resting membrane potential cytosolic and ER calcium levels are maintained by constitutiveSTIM1 Orai2 activity, which allows for TRPC3 activation and calcium release upon mGluR1 activation.* ***Middle*** *In the absence of either STIM1 or Orai2 in the respective knockout mice at resting membrane potential ER calcium stores are empty of releasable calcium and TRPC3 is not activable because of the lack of Orai2-mediated calcium influx.* ***Bottom*** *Calcium influx through VGCCs during neuronal activity can substitute for the lack of STIM1 or Orai2 in STIM1pko and Orai2$^{-/-}$ mice, respectively and ensure both TRPC3 activation downstream of mGluR1 as well as replenishment of ER calcium stores.*

4.2 Cytosolic calcium and TRPC3 activation

Modulation of TRPC3 activity by cytosolic calcium levels have been reported before in TRPC3-transfected CHO cells (Zitt et al. 1997) and in HEK293 cells overexpressing TRPC3 (Lintschinger et al. 2000). These studies in expression systems reported a modulatory effect on TRPC3-mediated currents. In our group a similar observation was made in PNs from wild type mice that show slightly enhanced TRPC3-mediated currents following transient calcium influx through VGCCs. Our group provided the first demonstration that in a native system an impaired mGluR1/Gq-TRPC3 signaling cascade in the absence of STIM1 is "rescued" by a transient depolarization and the resulting calcium influx (Hartmann et al. 2014). My work for this thesis adds important new findings regarding the dependence of the activability of TRPC3 in PNs on intracellular calcium. First, the effect of the depolarization on TRPC3 activability in $STIM1^{pko}$ mice lasts for minutes (Fig. 1), thus, it is not based on direct binding of calcium ions to the channel subunits. Second, my experiments in the presence of CPA (Fig. 2) and with EGTA/BAPTA in the pipette (Fig. 4) clearly show that it is the cytosolic and not the luminal ER calcium concentration that determines TRPC3 function.

The hypothesis that TRPC3 is regulated by cytosolic calcium is strengthened by my observation that emptying calcium stores does not impair TRPC3 activation. *Vice versa*, calcium release from stores is normal in $TRPC3^{-/-}$ mice (Hartmann et al. 2008) (Fig. 3). This indicates that TRPC3 does not play a role in SOCE in cerebellar PNs, although TRPC channels have been described to be involved in SOCE in other cell types (Ambudkar et al. 2016). Our finding shows that TRPC3 in PNs is receptor-activated, rather than a SOCE channel. Third, my experiments with IP_3 uncaging and EGTA/BAPTA (Figs. 4) show that TRPC3 activation downstream of mGluR1 requires a calcium-binding regulator that is located near the mouths of VGCCs and Orai2 but not near the IP_3R channel. It is therefore likely that the TRPC3 activation mechanism is located near the PM, which is in our case the calcium entry site. An interesting possibility is that TRPC3 and Orai subunits form mixed channels that act as SOCE channels (Liao et al. 2007). However, I demonstrated that TRPC3 can be activated downstream

of mGluR1 in the absence of Orai2 (Fig. 27) and mGluR1/IP_3R-mediated calcium release is normal in TRPC3-deficient knockout mice (Hartmann et al. 2008). Therefore, the possibility that TRPC3 and Orai subunits together form SOCE channels can be discarded.

Based on the observations that TRPC3 requires cytosolic calcium and is not activated in $STIM1^{PKO}$ and $Orai2^{-/-}$ mice at resting membrane potential, I hypothesized that that cytosolic calcium levels in the latter two genotypes might be permanently lowered. However this idea was contested by recent experiments in an independently generated $STIM1^{pko}$ mouse line in which basal calcium levels at resting membrane potential, in PNs in acute cerebellar slices, were even slightly (but non-significantly) increased due to a reduced SERCA function in the absence of STIM1 (Ryu et al. 2017). This once more corroborates our own finding that not the bulk cytosolic calcium concentration is important for TRPC3 activability but the calcium concentration in a submembraneous shell.

4.3 TRPC3 regulation by phospholipase C/D

The molecular mechanism underlying direct activation of TRPC3 remains elusive. The dependence on cytosolic calcium and a membrane proximate mechanism strongly point towards the involvement of phospholipase C, which was reported to be calcium dependent (Lomasney et al. 1999) and membrane bound (Lemmon 2008). Experiments in transgenic PLCβ4 knock down mice demonstrated that TRPC3 activation in at least some regions of the cerebellum depend on this isoform, namely in the regions where PLCβ4 is the dominant one (Sugiyama et al. 1999). It was later reported that pharmacological blocking of PCLβ using U73122 did not inhibit TRPC3-mediated currents (Glitsch et al. 2010). In the latter study no clear reference to which cerebellar region was used is made, while Sugiyama and colleagues report that PLCβ deletion mainly affects the caudal region of the cerebellar vermis. Therefore, these two studies do not necessarily contradict each other, but rather point to a region specific regulation of TRPC3. Glitsch and her colleagues report in their study that not PLCβ, but phospholipase D (PLD) is responsible for TRPC3 activation via the small GTP-binding protein Rho. PLD is

found in multiple cellular locations but also on the PM (Bruntz et al. 2014) and at least two isoforms, PLD1 and PLD2, are expressed in human and rat brain (Meier et al. 1999). In addition, it was found that PKC activates PLD, with PKC activation depending on cytosolic calcium (Bruntz et al. 2014) (note however that Glitsch and colleagues reported that TRPC3 activation is independent from PKC (Nelson et al. 2012). Moreover, some PLD isoforms mainly found in plants require certain levels of calcium to be activated (Qin et al. 1997). In short, our data and the available literature points towards the possibility of phospholipases regulated TRPC3 activation, with regional specialization of isoforms within the cerebellum.

Still another possibility is the involvement of the phosphoinositide3 kinase (PI3K)/ mammalian target of rapamycin (mTOR) pathway. A very recent study demonstrated that in hippocampal slices, group I mGluR dependent LTD is impaired in mice lacking mTORC2 (Zhu et al. 2018). mTOR can be activated downstream of PI3K in neurons (Costa-Mattioli et al. 2013). Moreover, it has been shown that the nonselective current induced by brain derived neurotrophic factor (BDNF) is blocked by siRNA targeted against TRPC3 (Amaral et al. 2007). Thus, BDNF activates Pi3K and therefore, PI3K forms a molecular switch that can activate TRPC3. Additionally, Pi3K can be activated downstream of GPCRs and is located close to the PM (Gross et al. 2014). I have demonstrated that the latter is crucial for TRPC3 activation (Fig. 4). Finally, a study from 2003 demonstrated that BAPTA-mediated calcium buffering in a mouse osteoblast cell line prevents Pi3K phosphorylation, which indicates that Pi3K activation, to a certain extent, is regulated by cytosolic calcium (Danciu et al. 2003). Taken together, this makes Pi3K/mTOR pathway a possible candidate for the TRPC3-activating mechanism in cerebellar PNs. To elucidate this, however, is a matter of future research.

4.4 TRPC3 availability on the PM

Another possible mechanism underlying calcium-regulated TRPC3 activation was brought forth by Ambudkar's group (Singh et al. 2004). In short, Singh and colleagues reported that TRPC3 in HEK-293 cells is inserted into the membrane

by vesicle exocytosis and that this process is disrupted by the calcium chelator BAPTA. This causes less TRPC3 channels to be available on the PM. This observation is in line with my findings that intracellular BAPTA in PNs prevents TRPC3 activation. I tested if TRPC3 is available on the PM of several mice lines. Application of TRPC3 agonist GSK1702934A (Doleschal et al. 2015) led to reliable and reproducible inward currents in all genotypes except, as expected, in TRPC3 knockout mice. Interestingly, in comparison to wild type mice, we saw non-significant yet larger currents in STIM1^{pko} and Orai2^{pko} mice. The hypothesis that TRPC3 exocytosis underlies the calcium dependent rescue of inward currents in the absence of STIM1 and Orai2 therefore can be discarded As final remark it should be noted that calcium induced rescue of TRPC3 in my experiments takes place within hundreds of milliseconds (Fig. 1), whereas Singh and colleagues reported that after 40 seconds, only half of the original fluorescence is restored in a photo bleaching experiment involving fluorescently tagged TRPC3. It seems therefore unlikely that membrane insertion of TRPC3 is of significant consequence during my observations.

4.5 DAG/PKC

DAG has been long since established as an activator of TRPC3 and TRPC6 *in vitro* (Hofmann et al. 1999). However, direct experimental evidence of TRPC3 activation via DAG in PNs is lacking. Direct puff or bath application of OAG, a close DAG analogue, did not result in detectable slow inward currents in PNs in my own experiments in acute cerebellar slices (data not shown). In some experiments OAG at a concentration of 100 µM in the ACSF increased inward currents evoked by the concomitant presence of a low concentration of DHPG (30 µM). However, this result was not consistently reproducible. Interestingly, it was only observed in few cells that a membrane current was initiated by OAG-application. This was observed also in the experiments with photoactivated PhoDAG; PhoDAG was successfully photo-activated as verified by the stimulatory effect on PKC. However, a TRPC3-mediated inward current was never recorded in these experiments. The PhoDAG-evoked outward current can most likely be attributed

to the opening of PKC-activated BK channels (Widmer et al. 2003). The direct activation of TRPC3 by DAG, however, in PNs appears to be the exception rather than the rule. The reason underlying this discrepancy to other cell types remains to be elucidated.

4.6 IP_3/IP_3R effect on TRPC3

In my experiments with IP_3 uncaging I found that calcium released from stores does not modulate DHPG-evoked TRPC3-mediated inward currents in wild type mice (Fig. 6). Testing the rescue of TRPC3 activability by IP_3R-mediated calcium release is not possible in STIM1- or Orai2-deficient mice because ER calcium stores in their PNs are empty at rest. The facilitating effect of calcium influx through the PM on native TRPC3-mediated currents is not always present and is often small and therefore did not reach the significance level with n = 11 cells tested (Hartmann et al. 2014). The negative result in my experiments shown in Fig. 6 (IP_3 uncaging) provides therefore only weak evidence for an independence of TRPC3 activability on calcium ions released from stores compared to the strong undisputable evidence in favour of a dependence on calcium influx through the PM. Moreover, recent findings about the organization of IP_3-sensitive stores are suggestive for an interaction between the IP_3R and TRPC3. It was found that the population of IP_3Rs residing on the ER is not homologous (Thillaiappan et al. 2017). It appears that either receptor stimulation or IP_3 uncaging results in calcium signals that are mediated by relatively immobile IP_3Rs close to the PM. The mobile fraction IP_3Rs colocalizes with STIM1 in its inactive form, the immobile IP_3Rs do so with activated STIM1. Because active STIM1 binds to Orai1 in the PM (Derler et al. 2016), it is located close to the PM and is part of the ER-PM junction that brings together many proteins that are relevant for ER-associated calcium signaling (Roberts-Thomson et al. 2010). Thus, IP_3Rs could be part of the micro domain where activation of TRPC3 occurs. In line with this, a direct activation of TRPC3 by binding to activated IP_3Rs was reported in cell attached-mode HEK293 cells (Kiselyov et al. 1998). Our own data, however, do not suggest such a regulation of TRPC3 channels in cerebellar PNs. What the data

in Fig. 6, in contrast, clearly show, is the independence of TRPC3 activation of IP_3 or the activated IP_3R. The uncaged IP_3 did not alter TRPC3 currents, which makes it unlikely that TRPC3 is regulated by IP_3. In addition, the mGluR1-dependent sEPSC is insensitive to blockade of IP_3Rs with heparin (Tempia et al. 1998). Thus, although TRPC3 and IP_3Rs might be located in close proximity a gating of TRPC3 by IP_3Rs can be excluded.

4.7 Phenotype

So far our group and the group of Kim have been the only ones addressing behavioral deficits in mice lacking STIM1 in PNs (Ryu et al. 2017) (Hartmann et al. 2014). Ryu and his colleagues mention that the behavioral tests performed by our group (namely the elevated beam and rotarod test) lack cerebellar specificity since impairments in other brain regions also results in worsened test performance (Urakawa et al. 2007) (1). Here, I will address this criticism. First, the motor impairment observed in $STIM1^{PKO}$ animals (I repeated this experiment, data not shown) was tested in cell type specific mice. Deletion of $STIM1^{PKO}$ was specific to the point that signal in cerebellar granular neurons was maintained (Hartmann et. al. 2014). These knock down mice were compared with control mice expressing *Cre* from the same litter; control mice show much comparable results with unmodified wild type animals (own observations). In short, cerebellar specificity is not necessarily brought via the behavioral test but rather by the design of the transgenic mice.

Secondly, inquiries into the function of mGluR1 and its downstream targets in cerebellar PNs have a long history. It should be noted that motor deficits have been observed in mGluR1- (Aiba, 1994), IP_3R- (Matsumoto et al. 1996), $G\alpha_q$-, $G\alpha_{11}$- (Hartmann et al. 2004) and TRPC3- deficient (Hartmann et al. 2015) mice. In addition, I have shown that Orai2 cell type-specific knockout mice show the exact same impairment. All the components mentioned here cause cellular deficits downstream of mGluR1 when deleted. To summarize, the new findings presented in this thesis strengthen the notion that downstream targets of mGluR1 play a vital role in cerebellar function.

4.8 Climbing fiber-induced rescue of mGluR1-dependent signaling and motor impairments in Orai^{pko} mice

Hartmann and colleagues already showed that in STIM1^{pko} mice, TRPC3 activation can be restored by calcium influx through the PM (Hartmann et al. 2014). Not surprisingly, in view of the complementary roles of Orai2 and STIM1 in cerebellar PNs in calcium homeostasis, I was able to replicate this finding (with some variation) in Orai2$^{-/-}$ mice. Somatic depolarization by changing the holding potential in a voltage-clamp experiment is a rather artificial procedure. However, Fig. 22 in this thesis shows that a physiological stimulus, namely a single CF EPSC and the resulting Calcium signal is sufficient to rescue TRPC3 activability. CF activation onto PNs results in global depolarization and semiglobal calcium influx (Ito 2006). CFs *in vivo* fire at a frequency of 1 Hz (Ito, 2006). My own experiment depicted in Fig. 1 demonstrates that the restoration of mGluR1-dependent responses by depolarization-evoked calcium influx lasts for minutes. TRPC3-mediated sEPSCs and IP_3R-mediated calcium release in PNs lacking either STIM1 or Orai2 *in vivo* are most likely 'rescued' constantly. Taking this into consideration the question arises why the deletion of STIM1 or Orai2 exclusively in PNs resulted in behavioral deficits that are typical for disrupted mGluR1-dependent signaling (Hartmann et al. 2015) One possible explanation comes from observations of the group of Dieudonné (Otsu et al. 2014). They recorded CF-induced calcium transients in the whole PN dendritic tree. In distal dendrites these calcium transients are smaller compared to responses proximal dendrites in line with a predominant CF innervation of the proximal dendrite. I have found a strong correlation between the amount of calcium influx and the extent of rescue of the mGluR1 responses in Orai2$^{-/-}$ mice. Thus, CF input in distal dendrites *in vivo* might be insufficient to restore mGluR1 signaling.

In addition to that, a disturbed development of CF synapses could also underlie the observed motor discoordination in STIM1 and Orai2-deficient mice. During early postnatal development, a single PN is innervated by multiple CFs, of which all but one are removed (Ito 2006). For twenty years now it has been known that processes mediated by mGluR1 are crucial for this this CF elimina-

tion (Hirai, 2018). MGluR1-deficient knockout mice exhibit strong ataxia (Aiba et al. 1994) and rescue of mGluR1-expression results in normal CF development (Ichise et al. 2000). The remaining CF can be physiologically distinguished from the to-be-eliminated CFs by its larger EPSCs (Bosman et al. 2008), and it forms its synapses around the dendritic tree, while the retracted CFs innervate the PN soma until P15 (Hashimoto et al. 2009). Not only the presence of mGluR1 but also its downstream targets are important during development, such as Gαq, PKC and PLCβ4 (Hashimoto et al. 2001). Thus, since in STIM1- and Orai2-deficient mice mGluR1-dependent signaling is impaired, this possibly also affects the elimination of supernumerary CF synapses during development. Whether this is the case or not can be clarified in future experiments.

Finally, it has to be taken into account, that TRPC3 function itself is important for CF firing frequency. This was first assumed based on results from *in vivo* electrophysiological recordings from PNs in awake mice when the simple and complex spike firing frequencies between different modules were compared. Despite the seeming homogeneity of the cerebellar cortex there are molecular markers that subdivide the cerebellar cortex into bands that are oriented along the rostro-caudal axis (Brochu et al. 1990). The best known of these are the glycolytic enzyme aldolase C or zebrin II that is expressed in symmetric stripes perpendicular to the cerebellar folds (Brochu et al. 1990). It was found that simple and complex firing frequencies were significantly higher in zebrin II-negative than zebrin II-positive modules (Zhou et al. 2014). Interestingly, expression of TRPC3 is associated with zebrin II-negative PNs and pharmacological blockade of TRPC3 attenuated the difference in simple spike firing frequencies between both types of modules (Zhou et al. 2014). In our group it was shown earlier in mice with a PN-specific ablation of large-conductance voltage- and calcium-activated potassium (BK) channels that in these mice a reduction of simple spike frequency due to excessive depolarization leads to reduced CF activity. The reason for that is a malfunction in the tripartite olivocerebellar loop in which reduced simple spike firing in PNs results in less inhibition of the deep cerebella nuclei and thus in reduced disinhibition of the inferior olive and hence fewer complex spikes in

PNs (Chen et al. 2010). This could be the underlying mechanism of reduced complex spike firing in PNs located in zebrin II-positive modules (Zhou et al. 2014). This assumption is in line with the direct demonstration of reduced simple and complex spike firing frequencies in TRPC3^{pko} mice that lack TRPC3 exclusively in PNs by a former colleague in our group (Chen et al. unpublished). Thus, since in Orai2- and STIM1-deficient mice the TRPC3 function is reduced /abolished, it is to be expected that *in vivo* the CF fires with reduced frequency and thus there is only partial and/ or transient rescue of mGluR1-dependent calcium signaling and sEPSCs.

4.9 STIM1, Orai2 and SOCE in cerebellar PNs

Since STIM and Orai proteins are the crucial elements for SOCE in non-excitable cells (Hogan et al. 2015) the disrupted mGluR1-dependent calcium release due to empty calcium stores in the absence of either STIM1 (Hartmann et al. 2014) or Orai2 point towards a similar role also in cerebellar PNs. However, with regard to SOCE, neurons differ from non-excitable cells (Lu et al. 2016). SOCE was identified initially and is measured to date with the classical calcium readdition assay. For this, cells are first being perfused with a calcium-free solution with SERCA blockers such as thapsigargin or CPA. This causes a small calcium transient due to calcium leakage from the ER. Readdition of normal extracellular calcium then causes a large calcium influx that is characteristic of SOCE and that is absent when the STIM/Orai complex is not functioning (Hogan et al. 2015). In neurons, however, the calcium readdition assay is not applicable in the same way as in non-excitable cells in order to pinpoint SOCE. First, neurons are endowed with VGCCs, and a fraction of them is open even at resting membrane potential. Moreover, in contrast to non-excitable cells in which the ER calcium content is stable for many minutes in the absence of extracellular calcium, the ER calcium store in neurons immediately deplete under such conditions (Lu et al. 2016; Hartmann et al. 2014). The reason for that is the expression of various calcium leak channels in the membrane of the ER that appears to be higher in neurons than in non-excitable cells (examples are Sec61 (Erdmann et al. 2011), prese-

nilins (Tu et al. 2006) and the Ribosome translocon complex (van Coppenolle et al. 2004)). The depletion of the ER store with low extracellular calcium also affects cytosolic calcium levels. TRPC3 can no longer be activated downstream of mGluR1 (Hartmann et al. 2014), which as I describe depends on cytosolic calcium. Thus, the classic calcium readdition assay is not working in neurons in the same way as in non-excitable cells. My own experiments were in line with these observations. Reestablishing extracellular calcium in fresh slices that were bathed in a calcium-free, CPA containing solution did not result in a measurable cytosolic calcium transient in cerebellar PNs (data not shown). The existence of SOCE in PNs was, indirectly, concluded based on the observation that STIM and Orai proteins cluster after treatment with thapsigargin (Klejman et al. 2009). It should be noted that a more recent study successfully demonstrated SOCE in dorsal root ganglion neurons, albeit in a cell culture system (Wei et al. 2017).

PNs in wild type mice are unresponsive to mGluR1 activation similarly to PNs in Orai2 or STIM1-deficent knockout mice in a low extracellular calcium - containing solution. This strongly speaks in favor of a constitutively active STIM/Orai complex in neurons that has to constantly counteract calcium leakage from ER calcium stores. All in all, intracellular calcium regulation in neurons thus is much more dynamic than in non-excitable cells. Another factor that deserves consideration when investigating SOCE specifically in neurons is the interaction between STIM1 and VGCCs (Wang et al. 2010). This study showed that when STIM1 is active (that is, when the intraluminal ER calcium concentration is low) STIM1 inhibits L-Type VGCC activity. I demonstrated that the ER store in Orai2$^{-/-}$ PNs appears to be empty, which makes it likely that STIM1 is in its active conformation. The scenarios that in Orai2$^{-/-}$ PNs the voltage gated calcium channels are inhibited are therefore plausible. However, when I compared the calcium transient amplitude following depolarization or CF stimulation in Orai2$^{-/-}$ and wild type mice I found no difference (data not shown). The reason for that may be that PNs mainly express P/Q type VGCCs (Hartmann et al. 2005) while the initial report from Wang et al. only mentioned the inhibition of L-Type voltage gated calcium channels. In my own experiments I did not detect an alteration of depolariza-

tion-induced calcium influx by the presence of CPA in the extracellular medium. So far, it is not yet possible to explain why stronger depolarization and larger calcium influx is required in Orai2$^{-/-}$ mice compared to STIM1^{pko} mice for the rescue of mGluR1 responses.

How SOCE or the constitutive activity of STIM/Orai affects cellular and/or behavioral function is not well known. It was found that STIM2 is central for SOCE in cultured hippocampal neurons, and STIM2 knockdown neurons show significantly less calcium influx following ischemia (Berna-Erro et al. 2009). A mouse model of focal cerebral ischemia lacking STIM2 showed less cell death, indicating that STIM2 plays a critical role during neurological damage. STIM2 was also found to be involved in maintenance of mushroom spines and overexpression of STIM2 resulted in rescued spine loss as well as improved store operated calcium entry in a mouse model of Alzheimer's disease (Sun et al. 2014). A later study linked STIM1 to Alzheimer's disease via the gamma secretase pathway (Tong et al. 2016). References to the work of our group to STIM1 function in PNs have been made in the introduction of this work (Hartmann et al. 2014). In addition, it has been recently shown that deletion of STIM1 in PNs causes reduction of spontaneous firing and learning deficits during a vestibular ocular reflex paradigm (Ryu et al. 2017). STIM1 regulates SOCE in dopaminergic neurons via TRPC1, which upon activation inhibits L-Type voltage gated calcium channels via STIM1 causing cell death (Sun et al. 2017). Overexpression of STIM1 in excitatory neurons led to decreased anxiety behavior and improved contextual learning (Majewski et al. 2017).

Sparse data that point to a role of Orai2 in calcium homeostasis that is similar or complementary to Orai1 were mostly obtained in non-excitable cell lines. It was reported that co-expression of Orai1 and Orai2 with STIM increases the CRAC current (I_{crac}) that is needed for calcium store refilling (Hoth et al. 1992) in HEK293 cells (DeHaven et al. 2007; Lis et al. 2007; Mercer et al. 2006) and that silencing of *Orai2* attenuated SOCE in leukemia-relevant HL60 cells (Diez-Bello et al. 2017). Interestingly, in this cell line, the silencing of Orai2 reduced SOCE stronger than the knockdown of Orai1. This is different in human lung

mast cells in which only a minor reduction in SOCE was observed without functional Orai2 (Ashmole et al. 2013). However, both publications support the view of identical or complementary roles for Orai1 and Orai2. In contrast, in chondrocyte cells (Inayama et al. 2015) and dissociated T-cells silencing or deletion of *Orai2*, respectively, increases SOCE. It was suggested that Orai2 forms heteromeric channels with Orai1 and attenuates CRAC channel function (Vaeth et al. 2017). Moreover, deletion of Orai2 specifically in mast cells increases both receptor-activated calcium release as well as SOCE in high extracellular calcium (2mM) but reduces SOCE in low extracellular calcium (Tsvilovskyy et al. 2018). In bovine brain capillary endothelial cells, siRNA mediated knockdown of Orai2 did not reduced SOCE (Kito et al. 2015). In native cells, Orai2 is upregulated during the G2/M phase of the cell cycle to reduce SOCE. Thus, in non-excitable cells, the actions of Orai2 appear to be very diverse, depending on the cell type.

4.10 Orai as a crucial brain protein

My work presented in this thesis for the first time attributes a major role to Orai2 for the function of central neurons and for motor behavior in mice. Although SOCE in neurons was already described 17 years ago (Bouron 2000) the amount of inquiries into STIM and Orai in the brain has been limited. STIM- and Orai-mediated store operated calcium entry has by now been reported in multiple brain regions and cells (reviewed in Kraft, 2015; Bollimuntha et al. 2017).

My colleague Hsing-Jung Chen recently demonstrated in her thesis the crucial role of Orai2 for mGluR1-dependent calcium signaling in CA1 pyramidal neurons (Chen, TUM 2018). Most remarkably, Orai2-deficiency in Orai2$^{-/-}$ mice affected only IP_3R-mediated but not RyR-mediated calcium release. Using different approaches it was demonstrated that IP_3-sensitive and Ry-sensitive calcium stores constitute largely separate entities that share only 15-20% of their calcium pool. This situation is different in cerebellar PNs (Khodakhah et al. 1997) in which I found that IP_3R- and RyR-dependent calcium release are both impaired. However, similarly to STIM1^{pko} mice (Hartmann et al. 2014) the Orai2-deficient mice show a residual response to caffeine whereas IP_3R-dependent calcium release is

abolished. Khodakhah and Armstrong had suggested earlier that based on their results the existence of a small separate Ry-sensitive but IP_3-insensitive store cannot be excluded, and the small responses to caffeine in the absence of IP_3-responsivess in STIM1- and Orai2-deficient mice are in line with that. Most remarkably, in CA1 pyramidal neurons, in contrast to cerebellar PNs (Hartmann et al., 2014; this thesis) only Ry-sensitive not IP_3-sensitive stores could be refilled by calcium influx through VGCCs. These findings regarding the distinct entry pathways for Calcium ions that replenish IP_3- and Ry-sensitive Calcium stores suggest an arrangement of subcellular structures that places IP_3Rs, Orai2 channels and SERCAs close to one another in one type of signaling domain and RyRs, VGCCs and SERCAs in a different type of domain, without cytosolic diffusion of calcium ions between those signaling units. Such a possibility cannot be excluded for cerebellar PNs. One could speculate that the IP_3R-mediated calcium release could then be restored by VGCCs because the Ry-sensitive store shares its calcium pool with the IP_3-sensitive store. *Vice versa* calcium ions entering the cytosol through Orai2 channels at IP_3-sensitive domains are then shared with the Ry-sensitive store. For the STIM1/Orai1-dependent calcium store replenishment it is well established that it is organized at ER-PM junctions where the distance between ER and PMs does not exceed 10-20 nm (Chang et al. 2016. There, Orai subunits are organized in large supramolecular complexes that include IP_3Rs and SERCA, ensuring highly localized and specific calcium reuptake (Fernández-Busnadiego et al. 2015; Orci et al. 2009; Poteser et al. 2016). My experiments shown in Fig. 4 demonstrated that the calcium-sensitive TRPC3-regulator couples to Orai2 on a nanodomain scale and thus must be located at an ER-PM junction that contains STIM1, Orai2, IP3R1, SERCA and TRPC3.

Interestingly, in hippocampal CA1 pyramidal neurons, in contrast to cerebellar PNs (Hartmann et al. 2014), the expression of STIM2 is similar to that of STIM1 (Lein et al. 2007; Chen, TUM 2018). The *Stim1* and *Stim2* genes are largely homologous but STIM2 has a smaller affinity for calcium than STIM1 (Brandman et al. 2007). As a result, STIM2 has been shown to be activated by smaller changes in the intraluminal ER calcium concentration than STIM1. The

current view on both proteins is that STIM2 is responsible for sustaining a steady-state level of ER calcium while STIM1 is recruited by acute large drops in the ER calcium concentration (Brandman et al. 2007). In cerebellar PNs STIM2 has no discernible role for mGluR1-dependent postsynaptic signaling. This conclusion was drawn based on experiments in acute cerebellar slices from mice with a PN-specific deletion of the *Stim2* gene (STIM2^{pko} mice). The cellular phenotype of PNs in STIM2^{pko} mice with regard to glutamatergic synaptic transmission was indistinguishable from that of wild type mice. Moreover, STIM1/2 double knockout (STIM1/2^{pdko}) mice did not differ from STIM1^{pko} mice when mGluR1-dependent responses were tested in whole-cell patch-clamp and imaging experiments (Ryan Alexander, Master thesis). It can be clearly stated therefore that Orai2 must be mainly activated by STIM1. It is a matter of future research whether Orai2 can be activated also by STIM2, and CA1 pyramidal neurons are the appropriate system to test this.

4.11 Conclusion

The work presented in this thesis pinpoints for the first time the crucial role of an Orai protein for normal cerebellar output and cerebellar function. Moreover, with the demonstration that Orai2 is critical for synaptic transmission it assigns a novel, hitherto unknown, role to an Orai protein besides ER calcium store replenishment. Because of the wide distribution of mGluR1/5-dependent synaptic transmission throughout the mammalian brain (Yin et al. 2014) Orai2 may be a key regulator of calcium signaling and synaptic transmission in many other types of central neurons.

Acknowledgements

Science is often represented as the progress of a single brilliant mind, an isolated individual bent over his books or experiments. This image is obviously erroneous; day to day science is performed in teams, departments and communities. Almost all scientific inquiries are the result of scientists working together. The same holds true for the PhD project I am presenting in this thesis. Therefore, I would like to dedicate this section to the people who helped and guided me, both on a professional level as well as outside the lab.

Special thanks go to my mentors, Prof. Arthur Konnerth and Prof. Alexander Dietrich, who provided me with many useful tips and feedback on my experiments and thesis.

I also want to thank Dr. Jana Hartmann, who has been my direct supervisor and taught me on an almost daily basis. Without her enthusiasms and experience this project and thesis would have never become to what it is now.

I would like to thank all my colleagues with whom I worked together during my time in the Institute of Neurosciences. All of you are passion driven people with whom I would, without a doubt, work together again. Special thanks go to Hsing-Jung Chen for her advice on immunostainings, molecular biology and being my slice-partner in crime. Valerie Bonfardin and Zsuzsanna Varga helped with immunostainings and imaging and BeomJong Song gave many useful tips on electrophysiology. Technical problems were solved instantly by Christian Obermayer, Dietmar Beyer and Felix Bayer. Many thanks to our computer specialist and skiing teacher Andy Fohr. Rosa Maria Karl was essential during the PCR experiments and animal genotyping. I am equally grateful to Petra Apostolopoulos and Karin Kratz for the impeccable care of my mice. Many thanks to Helmut Adelsberger, who taught and helped me with all behavior experiments. A big thank-you

to Christine Karrer for helping me on a daily basis with experimental solutions and my German.

I would like to thank all my friends, both old and new, for being there during the past years and sharing so many wonderful moments (and beers) with me. Many thanks to André, Andrea and Orhan Dijke for continuously supporting me.

Finally I want to thank Hazal Salihoglu, who has been my life partner, best friend and inspiration during the last six years of my life, and hopefully for many years to come.

References

Ackermann, H. 2008. “Cerebellar Contributions to Speech Production and Speech Perception: Psycholinguistic and Neurobiological Perspectives.” *Trends Neuroscience* 31(6): 265-272

Aiba, A. 1994. “Deficient Cerebellar Long-Term Depression in and Impaired Motor Learning in mGluR1 Mutant Mice”. *Cell* 79: 377-388

Amaral, M. D. et al. 2007. “TRPC3 Channels Are Necessary for Brain-Derived Neurotrophic Factor to Activate a Nonselective Cationic Current and to Induce Dendritic Spine Formation.” *Journal of Neuroscience* 3(19): 5179–5189.

Ambudkar, I. S. 2016. “Calcium Signalling in Salivary Gland Physiology and Dysfunction.” *Journal of Physiology* 594(11): 2813–24.

Annis, D. S. et al. 2014. “Autism associated Neuroligin-3 Mutations Commonly Impair Striatal Circuits to Boost Repetitive Behaviors.” *Cell* 27(1): 198–212.

Armbrust, K. R. et al. 2014. “Mutant -III Spectrin Causes MGluR1 Mislocalization and Functional Deficits in a Mouse Model of Spinocerebellar Ataxia Type 5.” *Journal of Neuroscience* 34(30): 9891–9904.

Armstrong, D. M. et al. 2013. “Activity Patterns of Cerebellar Cortical.” (1979): 425–48.

Ashmole, I. et al. 2013. “The Contribution of Orai(CRACM)1 and Orai(CRACM)2 Channels in Store-Operated Ca2+ Entry and Mediator Release in Human Lung Mast Cells.” PLOS One 8(9):1-12

Atluri, P. P. et al. 1996. “Determinants of the Time Course of Facilitation at the Granule Cell to Purkinje Cell Synapse.” *The Journal of Neuroscience* 16(18): 5661–71.

Baba, Y. et al. 2008. “Essential Function for the Calcium Sensor STIM1 in Mast Cell Activation and Anaphylactic Responses.” *Nature Immunology* 9(1): 81–88.

Bachelor, A.M. et al. 1994. “Synaptic activation of metabotropic glutamate receptors in the parallel fibre-purkinje cell pathway in rat cerebellar slices.” *Neuroscience* 63 (4): 911-915

Baier, B, et al. 2009 “Anatomical Correlates of Ocular Motor Deficits in Cerebellar Lesions.” Brain 132: 2114-2124

Barboi, Alexandre C. 2000. “Cerebellar Ataxia.” *Movement Disorders* 7(2): 95–109.

Bastian, A. J. et al. 1996. “Cerebellar Ataxia: Abnormal Control of Interaction Torques Across Multiple Joints.” *Journal of Neurophyiology* 76: 492-509

Batchelor, A.M. et al 1993. “Novel Synaptic Potentials in Cerebellar Purkenje Cells: Probable Mediation by Metabotropic Glutamate Receptors.” *Neuropharmacology* 32(1): 11–20.

Batchelor, A.M. et al. 1997. “Pharmacological Characterization of Synaptic Transmission through mGluRs in Rat Cerebellar Slices” *Neuropharmacology* 36(3): 401-403

Becker, E. B. E. et al. 2009. “A Point Mutation in TRPC3 Causes Abnormal Purkinje Cell Development and Cerebellar Ataxia in Moonwalker Mice.” *Proceedings of the National Academy of Sciences* 106(16): 6706-6711

Berna-Erro, A. et al. 2009. “STIM2 Regulates Capacitive Calcium Entry in Neurons and Plays a Key Role in Hypoxic Neuronal Cell Death.” *Science Signaling* 2(93): ra67-ra67.

Bollimuntha S. et al, 2017. “Neurological and Motor Disorders: Neuronal Store-Operated Calcium Signaling: An Overview and Its Function.” *Adv Exp Med Biol.* 993: 535-556

Bosman, L. W. J. et al. 2008. “Homosynaptic Long-Term Synaptic Potentiation of the ‘Winner’ Climbing Fiber Synapse in Developing Purkinje Cells.” *Journal of Neuroscience* 28(4): 798–807.

Bouron, A. 2000. “Activation of a Capacitative Calcium Entry Pathway by Store Depletion in Cultured Hippocampal Neurones.” *FEBS Letters* 470(3): 269–72.

Brandman, O. et al. 2007. “STIM2 is a Feedback Regulator that Stabilizes Basal Cytosolic and Endoplasmic Reticulum Calcium Levels.”*Cell* 131(7): 1327–39.

Brochu, G. et al. 1990. “Zebrin II: A Polypeptide Antigen Expressed Selectively by Purkinje Cells Reveals Compartments in Rat and Fish Cerebellum.” *Journal of Comparative Neurology* 291(4): 538–52.

Bruntz, R. C. et al. 2014. “Phospholipase D Signaling Pathways and Phosphatidic Acid as Therapeutic Targets in Cancer.” *Pharmacological Reviews* 66(4): 1033–79.

Canepari, M. et al. 2001. “The Conductance Underlying the Parallel Fibre Slow EPSP in Rat Cerebellar Purkinje Neurones Studied with Photolytic Release of L-Glutamate.” *Journal of Physiology* 533(3): 765–72.

Chang, C. et al. 2016. “Homeostatic Regulation of the PI(4,5)P 2 –Calcium Signaling System at ER–PM Junctions.” *Biochimica et Biophysica Acta (BBA) - Molecular and Cell Biology of Lipids* 1861(8): 862–73.

Chen, X. et al. 2010. “Disruption of the olivo-cerebellar circuit by Purkinje neuron-specific ablation of BK channels.” *PNAS* 107(27) 12323-8

Clapham, D et al. 2001. “The TRP Ion Channel Family.” *Nature Reviews Neuroscience* 2(6): 387–96.

Conn, P J. et al. 1997. “Pharmacology and Functions of Metabotropic Glutamate Receptors.” *Annual Review of Pharmacology and Toxicology* 37(1): 205–37.

Costa-Mattioli, M. et al. 2013. “MTOR Complexes in Neurodevelopmental and Neuropsychiatric Disorders.” *Nature Neuroscience* 16(11): 1537–43

Danciu, T. E. et al. 2003. “Calcium Regulates the PI3K-Akt Pathway in Stretched Osteoblasts.” *FEBS Letters* 536(1–3): 193–97.

de Juan-Sanz, J. et al. 2017. Axonal Endoplasmic Reticulum Calcium Content Controls Release Probability in CNS Nerve Terminals. *Neuron* 93(4): 867-881

DeHaven, W.I. et al. 2008. “Complex Actions of 2-Aminoethyldiphenyl Borate on Store-Operated Calcium Entry.” *Journal of Biological Chemistry* 283(28): 19265–73.

Derler, I., et al. 2016. “The Molecular Mechanisms of STIM/Orai Communications. A Review in the Theme: STIM and Orai Proteins in Calcium Signaling.” *AJP Cell Physiology* 310: C643-C662

Diener H.-C. et al. 1992. “Pathophysiology of Cerebellar Ataxia” *Movement Disorders* 7(2): 95–109.

Diez-Bello, R. et al. 2017. “Orai1 and Orai2 mediate store-operated calcium entry that regulates HL60 cell migration and FAK phosphorylation.“ *Biochim Bhiophy Acta* 1864(6): 1064-1070

Doleschal, B. et al. 2015. “TRPC3 Contributes to Regulation of Cardiac Contractility and Arrhythmogenesis by Dynamic Interaction with NCX1.” *Cardiovascular Research* 106(1): 163–73.

Durand, G.M. et al. 2006. “Quantitative single-cell RT-PCR and Calcium imaging in brain slices.” *European Journal of Physiology* 451: 716-726

Dzubay, J. et al. 2002. “Climbing Fiber Activation of Metabotropic Glutamate Receptors on Cerebellar Purkinje Neurons.” *Neuron* 36(6): 1159–67.

Ebner, T. J. et al. 2012. “Parasagittal Zones in the Cerebellar Cortex Differ I Excitability, Information Processing, and Synaptic Plasticity”. *Cerebellum* 11(2)

Eccles, J. C. 1967. “Circuits in the Cerebellar Control of Movement.” *Phyiology*, 58: 336-343

Ekerot, C.F. et al. 1987. “Stimulation of Cat Cutaneous Nociceptive C Fibers Causing Tonic and Synchronous Activity in Climbing Fibres” *Journal of Physiology* 386: 539–46.

Erdmann, F. et al. 2011. “Interaction of Calmodulin with Sec61α Limits Calcium leakage from the Endoplasmic Reticulum.” *EMBO Journal* 30(1): 17–31.

Fellows, S J et al. 2001 “Precision Grip Deficits in Cerebellar Disorders in Man”. *Clinical Neurophysiology* 112: 1793-1802

Fernández-Busnadiego, R. et al. 2015. “Three-Dimensional Architecture of Extended Synaptotagmin-Mediated Endoplasmic Reticulum–plasma Membrane Contact Sites.” *Proceedings of the National Academy of Sciences* 112(16): E2004–13.

Feske, S. et al. 2006. “A Mutation in Orai1 Causes Immune Deficiency by Abrogating CRAC Channel Function.” *Nature* 441(7090): 179–85.

Finch, E A, et al. 1998. “Local Calcium Signalling by Inositol-1,4, 5-Trisphosphate in Purkinje Cell Dendrites.” *Nature* 396(6713): 753–56.

Frank, J. A. et al 2016. “Photoswitchable diacylglycerols enable optical control of protein kinase C.“ *Nat. Chem. Biol* 12(9): 755-62

Galvez, T. et al. 1999. “Mutagenesis and Modeling of the GABA(B) Receptor Extracellular Domain Support a Venus Flytrap Mechanism for Ligand Binding.” *Journal of Biological Chemistry* 274(19): 13362–69.

Garaschuk, O. et al. 1997. “Release and Sequestration of Calcium by Ryanodine-Sensitive Stores in Rat Hippocampal Neurones.” *Journal of Physiology* 502(1): 13–30.

Gemes, G. et al. 2011. “Store-Operated Calcium Entry in Sensory Neurons: Functional Role and the Effect of Painful Nerve Injury.” *Journal of Neuroscience* 31(10): 3536–49.

Glitsch, M. D. 2010. “Activation of Native TRPC3 Cation Channels by Phospholipase D.” *The FASEB journal : official publication of the Federation of American Societies for Experimental Biology* 24(1): 318–25.

Goodkin, H. P. et al 2018. “Preserved Simple and Impaired Compound Movement After Infarction in the Territory of the Superior Cerebellar Artery.” *Can. J. Neurol. Sci* 20: 93–104.

Gross, C. et al. 2014. “Neuron-Specific Regulation of Class I PI3K Catalytic Subunits and Their Dysfunction in Brain Disorders.” *Frontiers in Molecular Neuroscience* (7): 1–8.

Gruszczynska-Biegala, J. et al. 2013. “Native STIM2 and ORAI1 Proteins Form a Calcium-Sensitive and Thapsigargin-Insensitive Complex in Cortical Neurons.” *Journal of Neurochemistry* 126(6): 727–38.

Hartmann, J. et al. 2004. “Distinct Roles of G_q and G_{11} for Purkinje Cell Signaling and Motor Behavior.” *Journal of Neuroscience* 24(22): 5119–30.

Hartmann, J. et al 2005. “Determinants of Postsynaptic Calcium Signaling in Purkinje Neurons.” *Cell Calcium* 37(5): 459–66.

Hartmann, J. et al. 2008, “TRPC3 Channels Are Required for Synaptic Transmission and Motor Coordination.” *Neuron* 59(3): 392–98.

Hartmann, J. et al. 2011 “mGluR1/TRPC3-Mediated Synaptic Transmission and Calcium Signaling in Mammalian Central Neurons.” *Cold Spring Harbor Perspectives in Biology* 3(4)

Hartmann, J. et al. 2014. “STIM1 Controls Neuronal Calcium Signaling, mGluR1-Dependent Synaptic Transmission, and Cerebellar Motor Behavior.” *Neuron* 82(3): 635–44.

Hartmann, J. et al. 2015. “TRPC3-dependent Synaptic Transmission in Central Mammalian Neurons.” *Journal of Molecular Medicine* 93(9): 983–89.

Hashimoto, K. et al. 2001. “Roles of Phospholipase Cβ4 in Synapse Elimination and Plasticity in Developing and Mature Cerebellum.” *Molecular Neurobiology* 23(1): 69–82.

Hashimoto, K. et al. 2009. “Translocation of a ‘Winner’ Climbing Fiber to the Purkinje Cell Dendrite and Subsequent Elimination of ‘Losers’ from the Soma in Developing Cerebellum.” *Neuron* 63(1): 106–18.

Hayashi, T. 1952. “A physiological study of epileptic seizures following cortical stimulation in animals and its application to human clinics.” *Jpn J Physiol* 3: 46–64

Henry L. P. 2009. “The Spinocerebellar Ataxias.” *J Neuroophthalmol* 29(3): 227–37.

Hermans, E. et al. 2001. “Glutamate Receptors : Prototypic Family C G-Protein-Coupled Receptors.” *Society* 484: 465–84.

Hille, B et al. 2016. “Phosphoinositides regulate ion channels.” *Biochim Biophys Acta*. 1851(6): 844–56.

Hinds, H. L. et al. 2003. “Essential Function of Alpha-Calcium/Calmodulin-Dependent Protein Kinase II in Neurotransmitter Release at a Glutamatergic Central Synapse.” *Proceedings of the National Academy of Sciences of the United States of America* 100(7): 4275–80.

Hirai, H. 2018. “Protein Kinase C in the Cerebellum: Its Significance and Remaining Conundrums.” *Cerebellum* 17(1): 23–27.

Hirono, M, et al. 1998. “Phospholipase C-Independent Group I Metabotropic Glutamate Receptor-Mediated Inward Current in Mouse Purkinje Cells.” *Biochemical and biophysical research communications* 251(3): 753–58.

Hofmann, T. et al.1999. “Direct Activation of Human TRPC6and TRPC3 Channels by Diacylglycerol.” *Nature* 397(January): 259–63.

Hogan, P.G. et al 2015. “Store-Operated Calcium Entry: Mechanisms and Modulation.” *Biochemical and Biophysical Research Communications* 460(1): 40–49

Hoth, M. et al. 1992. “Depletion of intracellular calcium stores activates a calcium current in mast cells”. *Nature* 355: 353–356.

Hoth, M. et al. 1993. “Calcium Release Activated Calcium Current in Rat Mast Cells. Journal of Physiology 465: 359-386

Hoth, M. et al. 2013. “ The Neglected CRAC Proteins: Orai2, Orai3 and STIM2”. *Current Topics in Membranes* 71: 237-271

Hou, Peng Fei et al. 2015. “Knockdown of STIM1 Improves Neuronal Survival After Traumatic Neuronal Injury Through Regulating MGluR1-Dependent Calcium Signaling in Mouse Cortical Neurons.” *Cellular and Molecular Neurobiology* 35(2): 283–92.

Huang W.-C et al 2007 “Changes in TRPC channel expression during postnatal development of cerebellar neurons”. *Cell Calcium* 42(1) 1-10

Ichise, T et al. 2000. “MGluR1 in Cerebellar Purkinje Cells Essential for Long-Term Depression, Synapse Elimination, and Motor Coordination.” *Science* 288(5472): 1832–35.

Imai, Y et al. 2012. “A Self-Limiting Regulation of Vasoconstrictor-Activated TRPC3/C6/C7 Channels Coupled to PI(4,5)P_2 -Diacylglycerol Signalling.” *The Journal of Physiology* 590(5): 1101–19.

Inayama, M. et al. (2015). “Orai1-Orai2 complex is involved in store-operated calcium entry in chondrocyte cell lines.” *Cell Calcium* 57, 337-347

Ito, M. 2006. “Cerebellar Circuitry as a Neuronal Machine.” *Progress in Neurobiology* 78(3–5): 272–303.

Kano, M. et al. 1997. “Persistent Multiple Climbing Fiber Innervationof Cerebellar Purkinje Cells in Mice Lacking mGluR1.” *Neuron* 18(1): 71–79.

Kano, M. et al. 1998. “Phospholipase C 4 Is Specifically Involved in Climbing Fiber Synapse Elimination in the Developing Cerebellum.” *Proceedings of the National Academy of Sciences* 95(26): 15724–29.

Kano, M. et al. 2008. “Type-1 Metabotropic Glutamate Receptor in Cerebellar Purkinje Cells: A Key Molecule Responsible for Long-Term Depression, En-

docannabinoid Signalling and Synapse Elimination." *Philosophical Transactions of the Royal Society B: Biological Sciences* 363(1500): 2173–86.

Khodakhah, K. et al. 1997. "Inositol Trisphosphate and Ryanodine Receptors Share a Common Functional Calcium Pool in Cerebellar Purkinje Neurons." *Biophysical Journal* 73(December): 3349–57.

Kim, S.J. et al. 2003. "Activation of the TRPC1 cation channel by metabotropic glutamate receptor mGluR1." *Nature* 426(20): 285–91.

Kiselyov, K et al. 1998. "Functional Interaction between InsP3 Receptors and Store-Operated Htrp3 Channels." *Nature* 396(6710): 478–82.

Kito, H.et al. 2015. "Regulation of store operated Ca2+ entry activity by cell cycle dependent up-regulation of Orai2 in brain capillary endothelial cells". *Biochemical and Biophysical Research Communications* 459(3) 457-462

Klejman, M. E. et al. 2009. "Expression of STIM1 in Brain and Puncta-like Co-Localization of STIM1 and ORAI1 upon Depletion of Calcium Store in Neurons." *Neurochemistry International* 54(1): 49–55.

Klose, A. et al 2008. "1-[6-[[(17β)-3-Methoxyestra-1,3,5(10)-trien-17-yl]amino]hexyl]-1H-pyrrole-2,5-dione (U73122) Selectively Inhibits Kir3 And BK Channels in a Phospholipase C-Independent Fashion." *Molecular Pharmacology* 74(5): 1203–14.

Konnerth, A. et al.1990. "Synaptic Currents in cerebellar Purkinje cells." *Neurobiology* 87: 2662–65.

Konno, A. et al. 2014. "Mutant Ataxin-3 with an Abnormally Expanded Polyglutamine Chain Disrupts Dendritic Development and Metabotropic Glutamate Receptor Signaling in Mouse Cerebellar Purkinje Cells." *Cerebellum* 13(1): 29–41.

Kraft, R. 2015. "STIM and ORAI Proteins in the Nervous System." *Channels* 9(5): 244–52.

Lalonde J. et al. 2015. "Store-Operated Calcium Entry Regulates Transcription Factor Sp4 in Resting Neurons." *Sci Signal* 7(328): 1–26.

Lein, E. S. et al. 2007. "Genome-Wide Atlas of Gene Expression in the Adult Mouse Brain." *Nature* 445(7124): 168–76.

Leinders-Zufall, T. et al. 2018 “PhoDAGs Enable Optical Control of Diacylglycerol-Sensitive Transient Receptor Potential Channels“. *Cell Chemical Biology* 25(2) 215-223

Lemmon, M. A. 2008. “Membrane Recognition by Phospholipid-Binding Domains.” *Nature Reviews Molecular Cell Biology* 9(2): 99–111.

Liao, Y. et al. 2007. “Orai Proteins Interact with TRPC Channels and Confer Responsiveness to Store Depletion.” *Proceedings of the National Academy of Sciences of the United States of America* 104(11): 4682–87.

Lintschinger, B. et al. 2000. “Coassembly of Trp1 and Trp3 Channels Generates Diacylglycerol and Calcium- Sensitive Cation Channels.” *Journal of Biological Chemistry* 275(36): 27799–805.

Liou, J. et al. 2005. “STIM Is a Calcium Sensor Essential for Calcium -Store-Depletion- Triggered Calcium Influx.” *Current Biology* 15(13): 1235–41.

Lis, A. et al. 2007. “CRACM1, CRACM2, and CRACM3 are store operated Ca^{2+} channels with distinct functional properties.” *Current Biology* 17(9) 794-800

Llano, I. et al. 1991. “Intradentic Release of Calcium Induced by Glutamate in Cerebellar Purkinje Cells.” *Neuron* 7: 577–83.

Llano, I. et al. 1991. “Synaptic- and Agonist- induced Excitatory Current of Purkinje Cells in Rat Cerebellar Slices”. *Journal of Physiology* 434: 183–213.

Lomasney, J. W. et al. 1999. “Activation of Phospholipase C Delta 1 through C2 Domain by a Calcium-Enzyme-Phosphatidylserine Ternary Complex.” *Journal of Biological Chemistry* 274(31): 21995–1.

Lu, B. et al. 2016. “Neuronal SOCE : Myth or Reality?” 26(12): 890–93.

Mailleux, P et al. 1992. “Immunohistochemical Distribution of Neurons Containing the G-Proteins G_qa/G_{11}a in the Adult Rat Brain.” *Neuroscience* 51(2): 311–16.

Majewski, Ł. et al. 2017. “Overexpression of STIM1 in Neurons in Mouse Brain Improves Contextual Learning and Impairs Long-Term Depression.” *Biochimica et Biophysica Acta - Molecular Cell Research* 1864(6): 1071–87.

Maltecca, F. et al. 2015. “Purkinje Neuron Calcium Influx Reduction Rescues Ataxia in SCA28 Model.” *Journal of Clinical Investigation* 125(1): 263–74.

Manto, M et al. 2012. “Roles of the Cerebellum in Motor Control- The diversity of Ideas on Cerebellar Involvement in Movement.” *Cerebellum* 11(2): 457–87.

Manto, M. et al. 2009. “Cerebellar Ataxias.” *Current Opinion in Neurology* 22(4): 419–29.

Masu M. et al. 1991. “Sequence and expression of a metabotropic glutamate receptor.” *Nature* 349: 760–765.

Matsumoto, M et al. 1996. “Ataxia and Epileptic Seizures in Mice Lacking Type 1 Inositol 1,4,5- Trisphosphate Receptor.” *Nature* 379: 168–71.

Meera, P. et al. 2017. “A Positive Feedback Loop Linking Enhanced MGluR Function and Basal Calcium in Spinocerebellar Ataxia Type 2.” *eLife* 6: 1–14.

Meier, K. E. et al. 1999. “Expression of Phospholipase D Isoforms in Mammalian Cells.” *Biochimica et Biophysica Acta - Molecular and Cell Biology of Lipids* 1439(2): 199–213.

Mercer, J. C. et al. 2006. “Large Store Operated Calcium Selective Currents Due To Co-Expression of Orai1 or Orai2 With The Intracellular Calcium Sensor, STIM1.” *J Biol Chem* 281(34): 24979–90.

Minke B. et al. 1977 “Drosophila mutant with a transducer defect”. *Biophys Struct Mech*, 3:59-64.

Mitchell, C.B. et al. 2012. “STIM1 Is Necessary for Store-Operated Calcium Entry in Turning Growth Cones.” *Journal of Neurochemistry* 122(6): 1155–66.

Moran, M. M. et al. 2004. “TRP Ion Channels in the Nervous System.” *Current Opinion in Neurobiology* 14(3): 362–69.

Muik, M. et al. 2008. “Dynamic Coupling of the Putative Coiled-Coil Domain of ORAI1 with STIM1 Mediates ORAI1 Channel Activation.” *Journal of Biological Chemistry* 283(12): 8014–22.

Nakao, H. et al. 2007. “Metabotropic Glutamate Receptor Subtype-1 Is Essential for Motor Coordination in the Adult Cerebellum.” *Neuroscience Research* 57(4): 538–43.

Naraghi, M. et al. 1997. “Linearized Buffered Calcium Diffusion in Microdomains and Its Implications for Calculation of [Calcium] at the Mouth of a Calcium Channel.” *Journal of Neuroscience* 17(18): 6961–73.

Nelson, C. 2012. “Lack of Kinase Regulation of Canonical Transient Receptor Potential 3 (TRPC3) Channel-Dependent Currents in Cerebellar Purkinje Cells.” *Journal of Biological Chemistry* 287(9): 6326–35.

Ng, A. N. et al. 2011. “Dendritic EGFP-STIM1 Activation after Type I Metabotropic Glutamate and Muscarinic Acetylcholine Receptor Stimulation in Hippocampal Neuron.” *Journal of Neuroscience Research* 89(8): 1235–44.

Nusser, Z. et al. 1994. “Subsynaptic Segregation of Metabotropic And Ionotropic Glutamate Receptors as Revealed by Immunogold Localization.” *Neuroscience* 61(3) 421-427.

O’Hara, P J et al. 1993. “The Ligand-Binding Domain in Metabotropic Glutamate Receptors Is Related to Bacterial Periplasmatic Binding Proteins.” *Neuron* 11: 41–52.

Ohtani, Y. et al. 2014. “The Synaptic Targeting of MGluR1 by Its Carboxyl-Terminal Domain Is Crucial for Cerebellar Function”. *Journal of Neuroscience* 34(7): 2702–12.

Okubo, Y. et al. 2015. “Visualization of Calcium Filling Mechanisms upon Synaptic Inputs in the Endoplasmic Reticulum of Cerebellar Purkinje Cells.” *Journal of Neuroscience* 35(48): 15837–46

Orci, L. et al. 2009. “STIM1-Induced Precortical and Cortical Subdomains of the Endoplasmic Reticulum.” *Proceedings of the National Academy of Sciences* 106(46): 19358–62

Otsu, Y. et al. 2014. “Activity-Dependent Gating of Calcium Spikes by A-Type K+ Channels Controls Climbing Fiber Signaling in Purkinje cell Dendrites.” *Neuron* 84(1): 137–51.

Park C. et al. 2010. “The CRAC Channel Activator STIM1 Binds and Inhibits L-Type Voltage-Gated Calcium Channels.” *Science* 330: 101–6.

Parker, N J et al. 1997. “Molecular Cloning of a Novel Human Gene (D11S4896E) at Chromosomal Region 11p15.5.” *Genomics* 37(2): 253–56.

Paulson, H. L. 2009. “The Spinocerebellar Ataxias.” *J Neuroophthalmol* 29(3): 227–37.

Pin J.-P et al. 1994. “Domains involved in the specificity of G protein activation in phospholipase C-coupled metabotropic glutamate receptors.” *The EMBO Journal* 13(2): 342–48.

Popugaeva, E. et al. 2015. “STIM2 Protects Hippocampal Mushroom Spines from Amyloid Synaptotoxicity.” *Molecular Neurodegeneration* 10(1): 1–13.

Poteser, M. et al. 2016. “Live-Cell Imaging of ER-PM Contact Architecture by a Novel TIRFM Approach Reveals Extension of Junctions in Response to Store-Operated Calcium-Entry.” *Scientific Reports* 6(October): 1–13

Power, E. M. et al. 2016. “Prolonged Type 1 Metabotropic Glutamate Receptor Dependent Synaptic Signaling Contributes to Spino-Cerebellar Ataxia Type 1.” *The Journal of neuroscience* 36(18): 4910–16.

Putney, J.W. 1986. “A Model for Receptor-Regulated Calcium Entry” *Cell Calcium* 7:1-12.

Qin, W. et al. 1997. “Molecular Heterogeneity of Phospholipase D (PLD).” *Biochemistry* 272(45): 28267–73.

Ribeiro, F. M. et al. 2017. “Metabotropic Glutamate Receptors and Neurodegenerative Diseases.” *Pharmacological Research* 115: 179–91.

Riecker, A et al. 2005 “FMRI Reveals Two Distinct Cerebral Networks Subserving Speech Motor Control.” *Neurology* 64: 700-706.

Roberts-Thomson, S.J. et al. (2010). ORAI-mediated calcium entry: Mechanism and roles, diseases and pharmacology. *Pharmacol Therapeut* 127, 121-130.

Roos, J. et al. 2005. “STIM1, an Essential and Conserved Component of Store-Operated Calcium Channel Function.” *Journal of Cell Biology* 169(3): 435–45.

Ryazantseva, M. et al. 2017. “Presenilin-1 Delta E9 Mutant Induces STIM1-Driven Store-Operated Calcium Channel Hyperactivation in Hippocampal Neurons.” *Molecular Neurobiology*: 1–14.

Ryu, C. et al. 2017. “STIM1 Regulates Somatic Calcium Signals and Intrinsic Firing Properties of Cerebellar Purkinje Neurons.” *The Journal of Neuroscience* 37(37): 3973–16.

Samtleben, S. et al. 2013. “Direct Imaging of ER Calcium with Targeted-Esterase Induced Dye Loading (TED).” *Journal of Visualized Experiments* (75): 1–17.

Sharp, A. H. et al. 1999. “Differential Cellular Expression of Receptors in Neurons and Glia in Brain.” *The Journal of Comparative Neurology* 220(May 1998): 207–20.

Shi, J. et al. 2004. “Multiple Regulation by Calcium of Murine Homologues of Transient Receptor Potential Proteins TRPC6 and TRPC7 Expressed in HEK293 Cells.” *The Journal of Physiology* 561(2): 415–32.

Shi, J. et al. 2013. “Molecular Determinants for Cardiovascular TRPC6 Channel Regulation by Calcium/Calmodulin-Dependent Kinase II.” *The Journal of physiology* 2851-66

Shim, S. et al. 2013. “A Critical Role for STIM1 in Filopodial Calcium Entry and Axon Guidance.” *Molecular Brain* 6(1): 51 .

Shin, J. H. et al. 2005. “An NMDA Receptor/Nitric Oxide Cascade Is Involved in Cerebellar LTD But Is Not Localized to the Parallel Fiber Terminal.” *Journal of Neurophysiology* 94(6): 4281–89.

Shuvaev, A. N. et al. 2017. “Progressive Impairment of Cerebellar mGluR Signaling and Its Therapeutic Potential for Cerebellar Ataxia in Spinocerebellar Ataxia Type 1 Model Mice.” *Journal of Physiology* 595(1): 141–64.

Singh, B. B. et al. 2004. “VAMP2-Dependent Exocytosis Regulates Plasma Membrane Insertion of TRPC3 Channels and Contributes to Agonist-Stimulated Calcium Influx.” *Molecular Cell* 15(4): 635–46.

Sladeczek, F. et al. 1985. “Glutamate stimulates inositol phosphate formation in striatal neurons” *Nature* 317: 717–719.

Sillevis Smitt, P. et al. 2000. “Paraneoplastic Cerebellar Ataxia Due to Autoantibodies against a Glutamate Receptor.” *The New England Journal of Medicine* 342(1): 22–27.

Somasundaram, A. et al. 2014. “Store-Operated CRAC Channels Regulate Gene Expression and Proliferation in Neural Progenitor Cells.” *Journal of Neuroscience* 34(27): 9107–23.

Steinbeck, J. et al. 2011. “Store-Operated Calcium Entry Modulates Neuronal Network Activity in a Model of Chronic Epilepsy.” *Experimental Neurology* 232(2): 185–94 .

Strick, P. L. et al. 2009. “Cerebellum and Nonmotor Function.” *Annual Review of Neuroscience* 32(1): 413–34.

Stroh, O. et al 2012. “NMDA-receptor dependent synaptic activation of TRPC channels in olfactory bulb granule cells.” *Journal of Neuroscience* 32(17): 5737–5746.

Sugiyama, T et al. 1999. “Localization of Phospholipase Cbeta Isozymes in the Mouse Cerebellum.” *Biochemical and biophysical research communications* 265(2): 473–78.

Sun, S. et al 2014. “Reduced synaptic STIM2 expression and impaired store-operated calcium entry cause destabilization of mature spines in mutant presenilin mice”. *Neuron* 82(1): 79-93

Sun, Y. et al. 2017. “Inhibition of L-Type Ca $^{2+}$ Channels by TRPC1-STIM1 Complex Is Essential for the Protection of Dopaminergic Neurons.” *The Journal of Neuroscience* 37(12): 3364–77.

Takechi, H. et al. 1998. “A New Class of Synaptic Response Involving Calcium Release in Dendritic Spines.” *Nature* 396(6713): 757–60.

Tanaka, J et al. 2000. “Gq Protein Alpha Subunits Galphaq and Galpha11 Are Localized at Postsynaptic Extra-Junctional Membrane of Cerebellar Purkinje Cells and Hippocampal Pyramidal Cells.” *The European journal of neuroscience* 12(3): 781–92.

Tempia, F. et al. 1998. “Postsynaptic Current Mediated by Metabotropic Glutamate Receptors in Cerebellar Purkinje Cells.” *Journal of neurophysiology* 80(2): 520–28.

Thillaiappan, N. B. et al. 2017. “Calcium signals Initiate at Immobile IP3receptors Adjacent to ER-Plasma Membrane Junctions.” *Nature Communications* 8(1):1505.

Thomas H. et al. 1999. “Direct Activation of Human TRPC6and TRPC3 Channels by Diacylglycerol.” *Nature* 397: 259–63.

Thorn, K. 2010. “Methods in Enzymology Spinning-Disk Confocal Microscopy of Yeast” *Methods in Enzymology* 470: 581-602

Tong, B. C. et al. 2016. “Familial Alzheimer’s disease–associated presenilin 1 mutants promote γ-secretase cleavage of STIM1 to impair store-operated Calcium entry” *Science Signaling* 9(444): 1–26.

Trebak, M. et al. 2003. “Signaling Mechanism for Receptor-Activated Canonical Transient Receptor Potential 3 (TRPC3) Channels.” *Journal of Biological Chemistry* 278(18): 16244–52.

Tsutsumi, S. et al. 2015. “Structure-Function Relationships between Aldolase C/Zebrin II Expression and Complex Spike Synchrony in the Cerebellum.” *Journal of Neuroscience* 35(2): 843–52.

Tsvilovskyy V. et al. 2018. “Deletion of Orai2 augments endogenous CRAC currents and dedranulation in mast cells leading to enhanced anaphylaxis.” *Cell Calcium* 71: 24-33

Tu, H. et al. 2006. “Presenilins Form ER Calcium Leak Channels, a Function Disrupted by Familial Alzheimer's Disease-Linked Mutations” *Cell* 126(5): 981–93.

Urakawa, S. et al. 2007. “Environmental Enrichment Brings a Beneficial Effect on Beam Walking and Enhances the Migration of Doublecortin-Positive Cells Following Striatal Lesions in Rats.” *Neuroscience* 144(3): 920–33.

Vaeth, M. et al. 2017. “ORAI2 Modulates Store-Operated Calcium Entry and T Cell-Mediated Immunity.” *Nature Communications* 8: 1–17.

Van Coppenolle, F. 2004. “Ribosome-Translocon Complex Mediates Calcium Leakage from Endoplasmic Reticulum Stores.” *Journal of Cell Science* 117(18): 4135–42.

Venkatachalam, K. 2003. “Regulation of Canonical Transient Receptor Potential (TRPC) Channel Function by Diacylglycerol and Protein Kinase C.” *Journal of Biological Chemistry* 278(31): 29031–40.

Venkiteswaran, G et al. 2009. “Intracellular Calcium signaling and store-operated Calcium entry are required in Drosophila Neurons for flight.” *Proceedings of the National Academy of Sciences of the United States of America* 106(25) 10326-10331.

Vig, M. et al. 2006. “CRACM1 Multimers Form the Ion-Selective Pore of the CRAC Channel”. *Current Biology* 16(20): 2073–79.

Vigont, V. et al. 2015. “Both Orai1 and TRPC1 Are Involved in Excessive Store-Operated Calcium Entry in Striatal Neurons Expressing Mutant Huntingtin Exon 1.” *Frontiers in Physiology* 6: 1–9.

Voogd, J et al. 1998. “Anatomy of the Cerebellum.” *Trends Neuroscience* 21(9): 370–5.

Wagner, M. J. et al. 2017. “Cerebellar Granule Cells Encode the Expectation of Reward.” *Nature* 544(7648): 96–100.

Wagner, M. J. et al. 2017. “Cerebellar Granule Cells Encode the Expectation of Reward.” *Nature* 544(7648): 96–100.

Wang, Y. et al. 2010. “The calcium store sensor, STIM1, reciprocally controls Orai and CaV1.2 channels.” Science 330(6000): 105-9

Wei, D. et al. 2017. “Orai1 and Orai3 Mediate Store-Operated Calcium Entry Contributing to Neuronal Excitability in Dorsal Root Ganglion Neurons.” *Frontiers in Cellular Neuroscience* 11: 1-15.

Widmer, H. A. et al. 2003. “Conditional Protein Phosphorylation Regulates BK Channel Activity in Rat Cerebellar Purkinje Neurons.” *The Journal of physiology* 552(Pt 2): 379–91.

Wilkie, T. M. et al. 1991. “Characterization of G-Protein Alpha Subunits in the Gq Class: Expression in Murine Tissues and in Stromal and Hematopoietic Cell Lines.” *Proceedings of the National Academy of Sciences of the United States of America* 88(22): 10049–53.

Williams, R. T. et al. 2001. “Identification and Characterization of the STIM (Stromal Interaction Molecule) Gene Family: Coding for a Novel Class of Transmembrane Proteins.” *Biochemical Journal* 357(3): 673.

Wissenbach, U. et al. 2007. “Primary structure, chromosomal localization and expression in immune cells of the murine ORAI and STIM genes”. *Cell Calcium* 42(4-5): 439-446.

Xia, J. et al. 2014. “Native Store-Operated Calcium Channels Are Functionally Expressed in Mouse Spinal Cord Dorsal Horn Neurons and Regulate Resting Calcium Homeostasis.” *The Journal of Physiology* 592(16): 3443–61.

Yamasaki, M. et al. 2011. “Glutamate Receptor Δ2 Is Essential for Input Pathway-Dependent Regulation of Synaptic AMPAR Contents in Cerebellar Purkinje Cells.” *The Journal of neuroscience* 31(9): 3362–74.

Yin, S. et al. 2014. “Progress towards advanced understanding of metabotropic glutamate receptors: structure, signalling and therapeutic indications.” *Cell Signal* 26(10): 2284-2297

Zeng, W. et al. 2009. “STIM1 gates TRPC channels but not Orai1 by electrostatic interaction.” 32(3): 439–48.

Zhang, M. et al. 2014. “Suppression of STIM1 in the Early Stage after Global Ischemia Attenuates the Injury of Delayed Neuronal Death by Inhibiting Store-Operated Calcium Entry-Induced Apoptosis in Rats.” *Neuroreport* 25(7) 507-513.

Zhang, S. L et al. 2006. “Genome-Wide RNAi Screen of Calcium Influx Identifies Genes That Regulate Calcium Release-Activated Calcium Channel Activity.” *Proceedings of the National Academy of Sciences of the United States of America* 103: 9357–62.

Zhang, X. Y. et al. 2016. “Cerebellar Fastigial Nucleus: From Anatomic Construction to Physiological Functions.” *Cerebellum & Ataxias* 3(1): 9.

Zheng, L. et al. 2011. “Auto-Inhibitory Role of the EF-SAM Domain of STIM Proteins in Store-Operated Calcium Entry.” *Proceedings of the National Academy of Sciences* 108(4): 1337–42.

Zhou, H. et al. 2014. “Cerebellar modules operate at different frequencies.” *Elife* e02536

Zhu, P. J. et al. 2018. “MTORC2, but Not MTORC1, Is Required for Hippocampal MGluR-LTD and Associated Behaviors.” *Nature Neuroscience* 21(6): 799–802.

Zitt, C et al. 1997. “Expression of TRPC3 in Chinese Hamster Ovary Cells Result in Calcium-Activated Cation Currents Not Related to Store Depletion.” *J Biol Chem* 138(6): 1333–41.